FREEZING AND MELTING OF HELIUM

C. LE PAIR

INSTITUUT-LORENTZ
voor theoretische natuurkunde
Nieuwsteeg 18-Leiden-Nederland

FREEZING AND MELTING OF HELIUM

FREEZING AND MELTING OF HELIUM

PROEFSCHRIFT

TER VERKRIJGING VAN DE GRAAD VAN DOCTOR
IN DE WISKUNDE EN NATUURWETENSCHAPPEN AAN DE
RIJKSUNIVERSITEIT TE LEIDEN,
OP GEZAG VAN DE RECTOR MAGNIFICUS
DR D. J. KUENEN, HOOGLERAAR
IN DE FACULTEIT DER WISKUNDE EN NATUURWETENSCHAPPEN,
TEN OVERSTAAN VAN EEN COMMISSIE UIT DE SENAAT
TE VERDEDIGEN OP DINSDAG 29 JUNI 1965 TE 15.00 UUR

DOOR

CORNELIS LE PAIR

GEBOREN TE LEIDEN IN 1936

KONINKLIJKE DRUKKERIJ VAN DE GARDE N.V.
ZALTBOMMEL

Promotor: Prof. Dr K. W. Taconis

Aan mijn grootouders
Aan mijn ouders
Aan Riek, Djamila en Noortje

CONTENTS

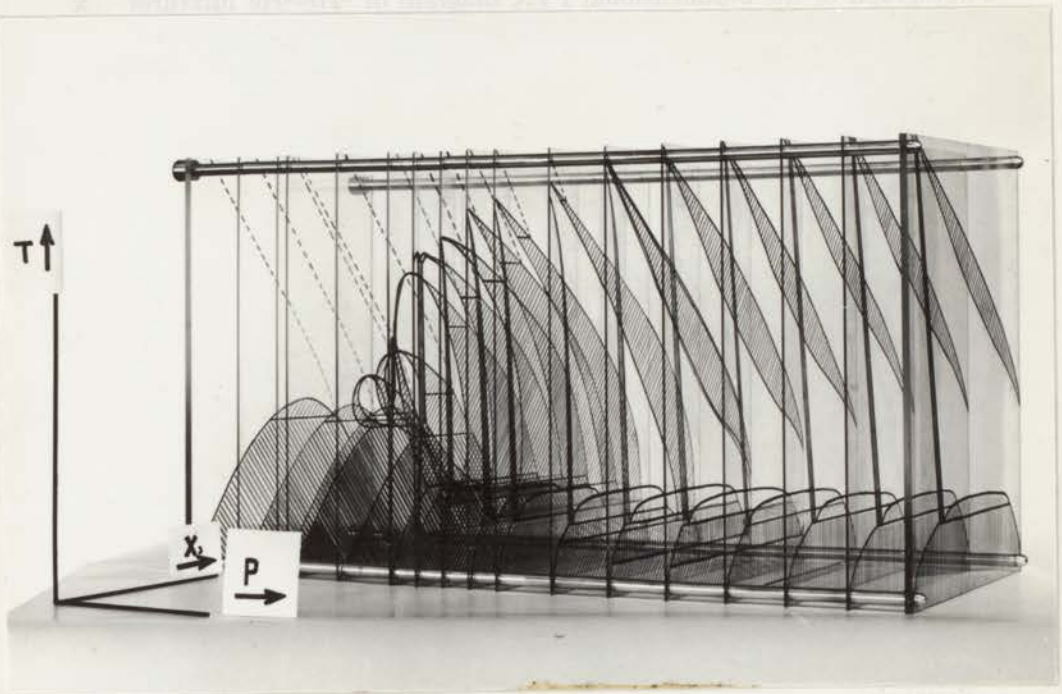

Photograph of the 3-dimensional PTX diagram of ^{3}He–^{4}He mixtures.
Pressure range: $21 \leqslant P \leqslant 34$ atm; temperature range: $0 \leqslant T \leqslant 2.0$ °K.
Inhomogeneous regions between equilibrium lines are indicated by hatched areas.
The λ-transition is indicated by dashed lines.

INTRODUCTION

Helium – ^{3}He, ^{4}He as well as their mixtures – is the only substance that remains liquid down to absolute zero of temperature. This has been ascribed to the small attractive forces between the atoms together with the large zero point energy, which acts as an extra repulsive force. To solidify the substance, an external pressure has to be applied, amounting to 25 to 30 atm at 0°K. Fluid mixtures are unstable at low temperatures. They separate into two phases, one with a low and one with a high concentration in ^{3}He. The same happens in solid mixtures. To explain these phenomena a cell model, involving the difference in zero point energy originating from the mass difference between the ^{3}He and the ^{4}He atoms, has been successful. Explanations using the statistical mechanics of a mixture of Fermions and Bosons have been given also. Both ^{3}He and ^{4}He are known in three solid forms, body centered cubic, hexagonal close-packed and face centered cubic.

^{3}He shows no sign of any superfluidity at $T > 0.01$°K, whereas superfluidity is still found in mixtures containing about 64% ^{3}He. Furthermore ^{3}He is known to have a minimum in its melting curve, which was unique at the time we started our investigations.

This thesis deals with some properties of helium at pressures higher than the saturated vapour pressure. In part I A we describe a number of experiments on solidification and melting of mixtures and of ^{4}He. In this part also measurements of the λ-transition of fluid mixtures are presented. The freezing and melting lines of the mixtures have minima in the PT-plane, similar to ^{3}He. If the freezing pressure is written $P = XP_3^0 + (1 - X)P_4^0 + P^E(T, X)$, the excess term $P^E(T, X)$ is negative and may reach a value of —9 atm. X denotes the molar fraction ^{3}He, P_3^0 the freezing pressure of pure ^{3}He and P_4^0 the freezing pressure of pure ^{4}He. We ascribe these properties to the degeneration of the entropy of mixing, which sets in at higher temperatures in the fluid than it does in the solid. The degeneration of the entropy of mixing is an outstanding example of the validity of Nernst's heat theorem. With the aid of the results obtained by us and several other workers, we

constructed a phase diagram, which is presented in part I B. Because of the many phases involved it is rather complicated. One of the most striking properties shown in the diagram is the existence of a closed solid region at pressures where neither ^{3}He nor ^{4}He can be solidified. The λ-phenomenon does not complicate the picture very much, as it does not contribute a new phase to the system. He I and He II have the same space configuration, as was known before. At the junction of the λ-line with a first order transition line, a kink occurs in the latter. In general the concentrations of the fluid and the solid phases in equilibrium are different. Under certain conditions they can be the same; in that case the sample is called azeotropic.

The energy related to the fluid-solid transition of helium was discussed by London. In part II we reanalysed London's considerations. Therefore we used a "random close-packed" geometrical model of the fluid. The random close-packing of hard spheres is being studied by various investigators. The results fit within the experimental accuracy to the known structural data obtained from X-ray and neutron diffraction of liquids of simple substances. It seems that the stability of the fluid phase at low temperatures must be attributed to a difference in zero point energy between fluid and solid, which was absent in London's theory. In this section we present also experimental evidence for the existence of a melting pressure minimum of ^{4}He. The occurrence of this poorly pronounced minimum is due to the phonon energy spectrum of the ^{4}He fluid. In the solid the number of degrees of freedom of wave propagation exceeds that of the fluid. Therefore, provided the sound velocity in the solid is not much larger than that of the fluid, the entropy difference between fluid and solid may become negative.

PART I

THE PHASE DIAGRAM OF ^{3}He-^{4}He MIXTURES AT PRESSURES LARGER THAN THE SATURATED VAPOUR PRESSURE

Synopsis

Part A. A full report is given of measurements of the onset of solidification, the onset of melting and the λ-transition of mixtures of ^{3}He and ^{4}He at pressures larger than the saturated vapour pressure. The measurements cover the complete concentration range: 0%; 0.99%; 2.77%; 8.9%; 22.8%; 50.5%; 64.5% and 80.1% ^{3}He. The apparatus and measuring techniques are described. The temperature range is 0.5–2.17°K. The pressure range is 0–48.4 atm. At low temperatures the freezing pressure of the mixtures is much lower than the weighted average of the freezing pressures of the pure substances. The difference can be as much as 9 atm. By entropy considerations this can qualitatively be explained. The freezing lines of the mixtures show steep minima, which can be understood by the same considerations. Some preliminary results of the temperature at which the volume minimum exists are given. Solidification is detected either by the blocked capillary technique, by observing kinks in pressure-temperature diagrams of constant amounts of fluid, or by watching the pressure as a function of temperature of a solidifying mixture in a flexible "Bourdon" vessel. The melting curves are detected by a special technique, which enables us to follow the solidification of a mixture at constant temperature.

Part B. From the measurements reported in the previous part a set of TX diagrams of ^{3}He–^{4}He mixtures at constant pressure have been constructed. Peculiar properties such as: Azeotropy, phase stratification of the fluid and the solid, a polymorph phase transition in the solid and the λ-transition have been taken into account. One, or perhaps two closed solid regions exist at pressures below 25 atm. The results are compared with those of several authors.

A. PRESSURE-TEMPERATURE MEASUREMENTS INCLUDING FREEZING AND MELTING.

1. *Introduction.* Helium is the only substance that remains liquid, when cooled under its own vapour pressure down to 0°K. It solidifies only when a rather large external pressure is exerted (large, in comparison with the saturated vapour pressure). This peculiar property can be ascribed to small

attractive forces between the helium atoms and the influence of the large quantum mechanical zero point energy*).

A lot of work on the isotopic mixtures of ^{3}He and ^{4}He has been carried out. The number of publications on ^{3}He and ^{3}He–^{4}He mixtures increases, steeply. It amounted to about 190 last year. For a survey of this literature, the reader is referred to the review article by Taconis and De Bruyn Ouboter, which appeared in 1964[1]). The majority of the available data are related to properties in the saturated vapour pressure region. This paper confines itself to properties at higher pressures of which little is known still. There are for instance no volumetric data and only very few

TABLE I

A survey of the literature of ^{3}He–^{4}He mixtures at pressures higher than the saturated vapour pressure

property	author	
specific Heat solid, C_v	Edwards, McWilliams, Daunt [2])	exp. $T = 0.06$–1.0°K
	Zimmerman [3])	exp. at several pressures
heat of mixing solid, H^E	Edwards, McWilliams, Daunt [2])	calculations from specific heat experiment
	Klemens, De Bruyn Ouboter, Le Pair [4])	theor. model, agreement with Edwards e.a.
volume of contraction V^E	Klemens, Maradudin [5]),	theor.
	Klemens, De Bruyn Ouboter, Le Pair [4])	theor.
phase separation fluid	Zinov'eva [6])	exp.
phase separation solid	Edwards, Mc Williams, Daunt [2])	exp.
	Klemens, De Bruyn Ouboter, Le Pair [4])	theor.
velocity of sound	Vignos, Fairbank [7])	exp.
freezing curve	Esel'son, Lazarev [8])	exp. $T = 1.4$–4.2°K
	Le Pair, Taconis, De Bruyn Ouboter, Das [9]) [10]) [11])	exp. $T = 0.45$–2.2°K $P < 48$ atm
	Le Pair, Taconis, De Bruyn Ouboter, De Jong, Pit [12])	exp.
	Weinstock, Lipschultz, Kellers, Lee [13])	exp. $T = 0.3$–1.3°K
	Lee, Lipschultz, Tedrow [14])	exp.
	Tedrow, Lee [15]) [16])	exp.
	Lipschultz, Tedrow, Lee [17])	exp.
	Berezniak, Bogoyavlenskii	exp.
	Esel'son [18]) [19]) [20])	exp.
	Zinov'eva [6])	exp.
	Lifshitz, Sanikidze [21])	theor.
	Vignos, Fairbank [7])	exp.

*) A detailed discussion on the solidification of the pure isotopes in connection with fluid and solid structure will be given in Part II.

TABLE I (*continued*)

property	author	
melting curve	Lifschitz, Sanikidze [21])	theor.
	Berezniak, Bogoyavlenskii, Esel'son [19])	exp. T = 1.4–4.2°K
	Le Pair, Taconis, De Bruyn Ouboter, De Jong, Pit [12])	T = 0.5 — 1.3 °K
	Zimmerman [22])	exp.
	Tedrow, Lee [16])	exp.
heat conductivity solid mixtures	Walker, Fairbank [23])	exp. X = 0.0138
	Sheard, Ziman [24])	theor.
	Klemens, Maradudin [5])	theor.
	Callaway [25])	theor.
	Bertman, White, Fairbank [26])	exp.
	Berman, Rogers [27])	exp.
hcp–bcc transition	Vignos, Fairbank [7])	exp.
	Berman, Rogers [27])	exp.
	Berezniak, Bogoyavlenskii, Esel'son [19]) [20])	exp.
nuclear relaxation	Garwin, Reich [28])	exp. dilute solutions
λ-lines	Le Pair, Taconis, De Bruyn Ouboter, Das [9]) [10]) [11])	exp.
phase-diagrams	Lifshitz, Sanikidze [21])	theor.
	Le Pair, Taconis, Das, De Bruyn Ouboter [11]) [12])	exp.
	Zinov'eva [6])	exp.
	Berezniak, Bogoyavlenskii, Esel'son [19]) [20])	exp. T = 1.4–4.2°K
	Tedrow, Lee [15]) [16])	exp.
	Lipschultz, Tedrow, Lee [17])	exp.
	Le Pair, Taconis, De Bruyn Ouboter, De Jong, Pit [12])	exp.

heat data available. In table I we have summed up all present literature in the field as far as it is known to us. The present theoretical considerations deal mainly with properties at saturated vapour pressure. Helium is a highly compressible fluid, its molar volume (saturated vapour pressure) $\approx$ 27.4 cm^3 mol^{-1} against 23.25 at 25 atm*), the work done on the fluid by external pressure becomes of the same order of magnitude as the thermal energy thus providing appreciable changes in the chemical potentials etc. This puts serious limitations to the possibility of extrapolation of the known low pressure data. Theoretical considerations on mixtures of hard spheres by Lebowitz and Rowlinson[29]) predict a negative excess volume of mixing. This is expected also by Prigogine c.s. for ^{3}He–^{4}He mixtures[74]). This has been observed at saturated vapour pressure by Kerr[30]) [31]) and remains true probably at higher pressures.

When we started the experiments reported in this paper we did not know

*) ^{3}He and mixtures are even more compressible than ^{4}He.

whether our earlier observations at saturated vapour pressure on the vanishing entropy of mixing[32]) would remain valid at higher pressures or not. If so it should cause an interesting behaviour of the solidification properties as will be shown.

Both pure ^{4}He and pure ^{3}He show a minimum in their melting curves. In the case of ^{4}He this is caused by the peculiar energy spectrum of the fluid, with phonons as the only excitations in the low temperature region. For ^{3}He, where the minimum is much deeper, it is caused by the spin contribution to the entropy (see first note, page 2).

The earliest measurements on the solidification of ^{3}He–^{4}He mixtures were published in 1954 by Esel'son and Lasarev[8]). They were carried out at temperatures above 1.4°K and performed by so-called blocked capillary measurements. Doing so freezing lines had been measured in a temperature region where no striking peculiarities happen. We extended this work down to lower temperatures. Therefore we had to develop some experimental equipment, which will be described here.

2. *Apparatus.* In order to carry out experiments to get the desired information about the fluid-solid equilibrium of both pure components and mixtures of ^{3}He–^{4}He, we built a number of apparatus. In the construction of these, two main difficulties had to be overcome:

1. The scarcity and the price of ^{3}He forced us to build a foolproof closed circuit in which the sample can be pressurized and from which it can be removed, all without losses.
2. The apparatus ought to have the possibility of pressure-measurement on the spot, i.e. in the low temperature region itself.

The need for an apparatus with this property was pointed out by Sydoriak[33]) criticising the freezing point measurements of ^{3}He. The core of the problem consists of the following: When retrograde melting occurs, that is when the melting curve of a substance in the PT diagram shows a minimum at some temperature T_M, then no pressure, higher than this minimum pressure, can be measured if the sample under consideration and the manometer are on both sides of the temperature of the minimum on the temperature scale; because in that case a blockage in the connecting tubes prevents pressure readings. We shall discuss this in more detail when we describe the measuring techniques.

Without the pretention to be complete, we shall sum up briefly the different kinds of apparatus which have been used by various experimentalists in order to overcome this problem and which are important in relation to the helium case:

1. The spring loaded bellows, used by Grilly, Sydoriak and Mills[39]). With this apparatus very accurate volumetric experiments have been

carried out on the pure components. It permits volume changes of the sample and so has one degree of freedom more than type 2.

2. The thin-walled cylinder provided with a strain gauge. This type is used by Edwards, Baum, Brewer and Daunt[40]) and many other groups.

3. The wide capillary. In this type the tubing is so wide that although solid blocks are formed, the pressure can still be transmitted. Solid helium has a rather loose structure, it can be deformed easily. So one can pressurize through the minimum pressure region at least to some extent. This type is used for instance in connection with sound measurements by Vignos and Fairbank[41]) and by Zinov'eva[29]) who looked into the sample vessel.

4. The Bourdon tube used by us, which also permits a volume change at low temperatures and which will be described below.

Experimental equipment. To pressurize the fluid samples we use a stainless steel "toepler" system as drawn in figure 1.

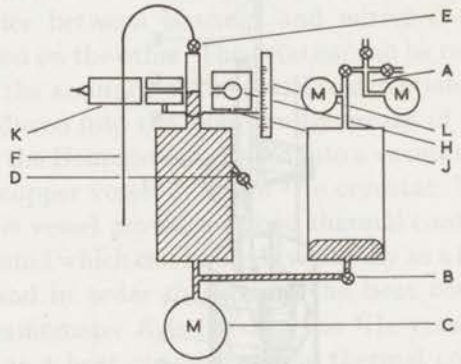

Fig. 1. High pressure toepler system. Explanation in the text.

The sample is introduced into the evacuated left steel vessel via valve *D*, when the mercury level is at the bottom of the container. With compressed air introduced via the air admittance valve system *A*, the mercury in the cylinder on the right can be put under pressure. Manometer *C* indicates the pressure of the sample. Its value is corrected for the height of the mercury which can be "seen" with aid of a γ-ray "telescope". *K* is a Geiger-Müller counter tube behind a diaphragm and *H* is a lead chamber containing a piece of radioactive cobalt. *E* is a valve with a dead-volume less than 3 mm³. *F* is the capillary leading to the apparatus in the cryostat (inner diameter 0.18 mm). Manometer *C* represents a Heise manometer. Its Bourdon tube is filled with mercury. Pressures can be measured from 0 till 242 atm. The accuracy is about 0.2 atm. This manometer, calibrated by the manufacturer, is used as a standard throughout the measurements. Some times it was replaced by another one with a pressure range: 0–40 atm giving a higher accuracy especially for the measurements on the melting

lines. Top and bottom of the cylinders as well as all other connections were sealed with O-rings. Valve B proved to be very effective to apply slight pressure variations*).

In the cryostat we used four different apparatus. The first two differ only slightly. The first one can be cooled by a ^{4}He-bath only. No experiments below 1°K were done with it. Results of measurements with this apparatus were published in 1962[9]). To extend the measurements to lower temperatures, the second apparatus was built. It is equiped with a ^{3}He cryostat, which permits so-called blocked capillary measurements below 1°K.

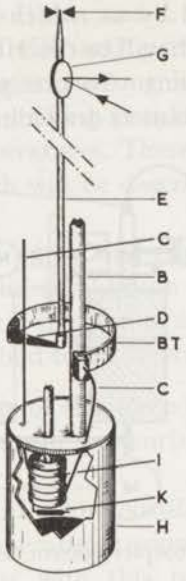

Fig. 2. Second apparatus for the measurement of freezing and λ-curves of ^{3}He–^{4}He mixtures.

BT – Bourdon tube	F – bearings
B – pumping line to H	G – mirror
C – capillary	H – vacuum jacket
D – leverage	I – ^{3}He cryostat
E – glass rod	K – carbon resistor

Results with this apparatus were described at the 8th Conference on Low Temperature Physics (LT8) in 1962[10]). The apparatus is shown in figure 2. The lowest temperature obtained with this equipment was about 0.45°K. The ^{3}He is pumped by a small double stage rotary pump (Balzer type DUO 1, ~16 l/min) into a ^{3}He gas container of a volume of about 1 l.

*) Finally we used a still more accurate Heise manometer, which permits readings ±0.01 atm. The pressure range is 0–50 atm. The accuracy is necessary to investigate the fluid-solid equilibrium of mixtures with low concentrations of ^{3}He and to check the measurements on the melting curve minimum of ^{4}He.

Connections are made with a flexible stainless steel tube, Edwards O-ring connections and Edwards-Saunders valves of $\frac{1}{2}''$ size. The ^{3}He container is mounted on the pump. The equipment is very simple to replace and to use in other experiments. Connecting it and setting it into operation takes one or two minutes. In figure 2 the most important part is the Bourdon tube: *BT*. It is an ordinary Bourdon tube taken from a commercial manometer (0–30 atm). It is made from a Cu–Ni–Zn alloy*). The volume of *BT* is about 900 mm^3. *BT* is soldered to a fixed supporting stainless steel tube *B*. This tube serves also as a pumping line to evacuate the vacuum jacket *H*. The free end of the Bourdon tube carries a leverage *D* to which a glass rod *E* is fixed. The glass rod ends in the top of the cryostat, where it is drawn into a fine needle point, thus producing a low friction bearing *F*. The capillary *C* connects this apparatus with the gas handling system (fig. 1). When the Bourdon tube is pressurized, the free end of the tube translates and rotates a little. The translation does not influence the readings because of the large difference in distance between bearings and mirror *G* on one hand and bearings and Bourdon on the other. The rotation can be read by means of the mirror. In this way the accuracy of the pressure detection is about 0.05 atm. The sample is introduced into the Bourdon by means of capillary *C*, which before entering into the Bourdon tube, is led into a vacuum jacket and wound tightly around the copper vessel *I*, of the ^{3}He cryostat. The screwthread in the outer wall of this vessel provides a good thermal contact. Around this a resistance wire is wound which can be used eventually as a heater. "Lock-tite" is used as a glue and in order to increase the heat conductivity. A "De Vroomen" type thermometer *K* is fixed to the ^{3}He vessel. Lock-tite seems to serve very well as a heat conductor. The thermal contact between the heater and the thermometer via lock-tite and copper vessel turns out to be greater by an order of magnitude than the contact between the ^{3}He liquid in the vessel and the thermometer. The whole apparatus is immersed in a ^{4}He bath, which can be cooled down to 1°K. As we knew before[10]) this apparatus did not permit us to measure a possible minimum in the freezing curves below 1°K.

In order to do this, we modified the second apparatus in such a way that the *BT* itself can be cooled also by the ^{3}He cryostat. This arrangement is pictured in figure 3 and called third apparatus. The *BT* is soldered onto the ^{3}He vessel. No mirror is used for detection. Instead a piece of ferroxcube *F* is attached to a "pointer" *P* fixed to the free end of the *BT*. The position of this piece of ferroxcube is measured within a superconducting coil *L*. The inductance of the coil *L* is measured with an Anderson A. C. bridge[34])[35]), figure 4, operated at 331 Hz. The advantages of this bridge method have been described by various authors (e.g. ref. 36) and can be summarized as

*) See appendix.

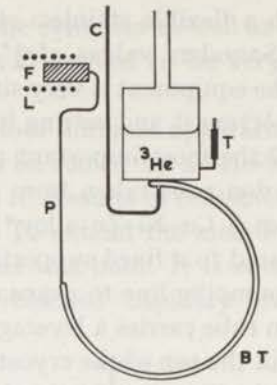

Fig. 3. Third apparatus for the measurement of freezing curves and λ-curves of ^{4}He and of ^{3}He–^{4}He mixtures at temperatures below 1°K and below the temperature at which a minimum in the freezing curve occurs. The picture shows only the part of the apparatus inside the vacuum jacket.

BT – Bourdon tube
F – piece of ferroxcube
T – carbon resistor
L – coil
P – pointer
C – capillary

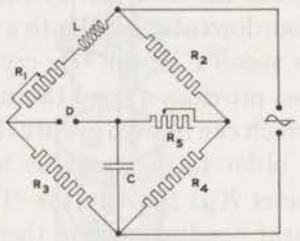

Fig. 4. Anderson A.C. bridge

follows:

1. Application of a constant capacitor, which provides:
2. A high degree of reproducibility.
3. Only one resistance R_5 needs to be read in order to calculate the self-inductance L of the coil, although a second one R_1 has to be adjusted at the same time to compensate the small effect caused by the hysteresis of the ferroxcube core and of course for the small variation of the resistance of the leads to the coil in the cryostat.

The detection D consists of a selective amplifier together with a Philips oscilloscope. On the horizontal declination of this instrument the same signal is put as on the A.C. bridge. In this way a quick registration of the pressure inside the Bourdon tube is possible. The inductance of the coil without core amounts to ca 17 mH. It is wound in five sections in order to decrease its capacity. In operation, with the core situated within the coil, the self-inductance at low temperatures is of the order of 45 mH. At low

temperatures the Bourdon tube is used up to 48 atm. This causes a displacement of the core of about 6 mm. Pressures can be read with an accuracy of 0.003 atm. The magnetic permeability of ferroxcube seems to vary linearly with T at these low temperatures. When the experiment is performed at different temperatures a correction for this effect has to be applied. As the magnitude of this correction itself is dependent on the position of the core within the coil, this cannot be done with very high precision and in the most extreme case we lose a factor 10 in accuracy.

Measurements of the melting line of ^{3}He–^{4}He mixtures have been done in the fourth apparatus, which permits us to change the volume of the sample. The apparatus is shown in figure 5. Only the part within the vacuum jacket is drawn. The Bourdon tube BT here, is no longer a com-

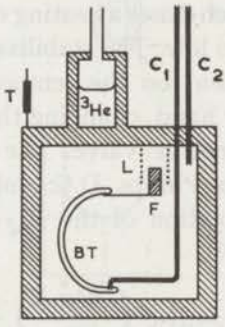

Fig. 5. Fourth apparatus for the measurement of melting lines of ^{3}He–^{4}He mixtures

C_1 – capillary for sample supply
C_2 – capillary to pressure chamber
BT – Bourdon tube
L – coil
F – core (ferroxcube)
T – carbon resistor

mercial one. It is made in the laboratory from a stainless steel tube, 2.67 mm i.d., which is machined on a lathe to a wall thickness of about 25 μ. Afterwards it is flattened by hammering it, until the two flat walls touch. Then it is wound up until it has the required shape. At room temperature the volume of this Bourdon tube increased about thirty percent, when the pressure was changed from 0–30 atm. When during the experiment the Bourdon was filled with fluid helium at freezing pressure, we could introduce ^{4}He in the surrounding high-pressure chamber and in this way decrease the volume of the Bourdon tube. In this way an isothermal isobaric phase transition of the sample under consideration can be produced. The volume of the Bourdon tube at 30 atm at low temperature is about 30 mm^3. Pressure measurements now require two readings: The reading of the position of the ferroxcube core, which gives the pressure exerted on the sample by the walls of the Bourdon tube, and the pressure of the surrounding ^{4}He which must be added to the latter to obtain the effective pressure on

the sample. Of course here the same difficulties arise as are described in connection with the third apparatus. In the actual apparatus the free space in the high pressure chamber is reduced as much as possible in order to avoid large mass transports of ^{4}He if a volume change is wanted. Such a mass transport should involve a large heat supply which had to be avoided as our helium-three cryostat operating with about 1 cm^3 liquid ^{3}He was not able to extract large quantities of heat.

Temperature measurement and units. For measurement and control of temperature we used a De Vroomen-type carbon resistor. It is calibrated each time during each measuring day against the vapour pressure of ^{3}He (1962 scale) and ^{4}He (1958 scale). The resistance is measured with a Wheatstone D.C. bridge. The temperature of the ^{4}He bath is stabilised using a Philips PR 2210 A 21 "recorder" as a zero current indicator. The recorder operates a switch which closes a heating current circuit, if the temperature of the bath becomes too low. The stabilisation thus obtained is better than $\Delta T = 0.002$°K, dependent on the temperature. The temperature of the ^{3}He bath is monitored by hand, changing the pumping speed of the ^{3}He pump through a lab-made needle valve. The zero current meter of the ^{3}He-thermometer-circuit is a Philips D.C. voltmeter: G.M. 6010 ($\Delta T \approx$ ≈ 0.002°K). For the interpolation of the $R \leftrightarrow T$ calibration the formula of Clement and Quinnell[37])

$$^{10}\log R = A\sqrt{\left(\frac{^{10}\log R}{T}\right)} + B$$

for carbon resistors proved to be very helpful, although for these thermometers "$^{10}\log R$ versus the square root" curves are not exact straight lines.

Throughout this paper we use the physical atmosphere (atm) as a pressure unit, in contrast to earlier publications in which we used the kg cm^{-2}, the latter being a unit which is about 1.033 times smaller than the present one. In calculations we replace [atm] by 0.1013 [Joule cm^{-3}]. In this work X denotes the molar fraction ^{3}He: $n_3/(n_3 + n_4)$.

3. *Freezing pressures.* Experimental procedure. The easiest method to measure freezing pressures is the so-called "blocked capillary method" of Kamerlingh Onnes and Van Gulik[38]). In this method two manometers are connected with each other by means of a narrow capillary C. See figure 6. The lower part of the capillary is immersed in a thermostated cooling liquid. Through the needle valve the gas is slowly admitted into the manometer system and the two manometers indicate the same increasing pressure. At a certain moment the freezing pressure is reached. A solid block is formed in the capillary. M_1 stops. It indicates the freezing pressure, while M_2 remains indicating a steadily increasing pressure. This method is used by many experimentalists. It is usually referred to as Keesom's method.

Keesom applied it, when doing the first experiments on the solidification of helium.

The apparatus described in the preceding section give the opportunity to practise the blocked capillary method. Results, obtained in this way are listed in table II. They are in good agreement with measurements reported by other authors.

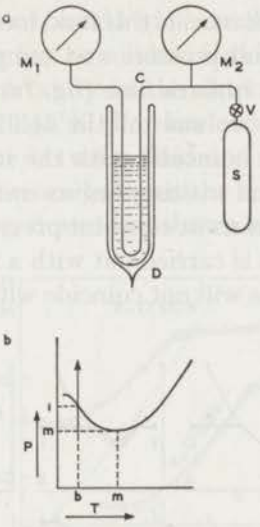

Fig. 6. *a*. Principle of the blocked capillary method by Kamerlingh Onnes and Van Gulik.

M_1 and M_2 – manometers
C – capillary
D – dewar vessel with cryogenic liquid
S – storage cylinder with compressed gas sample
V – needle valve.

b. Impracticability of the blocked capillary method when the freezing curve has a minimum; pressure-temperature diagram.

A serious disadvantage of the blocked capillary technique was mentioned before. If the freezing curve of a certain substance shows a minimum in the $P(T)$ graph, the blocked capillary method does not give correct results below the temperature T_M at which the minimum occurs. Imagine one has a freezing curve as drawn in figure 6*b*. The capillary is kept at constant temperature T_b somewhere below room-temperature. As the capillary itself has a finite heat conductivity the temperature of the capillary changes continuously from room-temperature to T_b. Somewhere the temperature of the capillary will be T_M. If one carries out the blocked capillary process, the capillary will block at $P = P_M$. This will not take place down in the capillary, but somewhere above the level of the cooling liquid. For the observer the outcome is the same. Hence for $T < T_M$ one will find P_M

instead of P_1. With flexible vessels in which the pressure can be measured at low temperatures, this difficulty can be overcome.

Initially there existed no knowledge about the hardness of solid mixtures of ^{3}He–^{4}He. I.e. it was not certain whether the blocked capillary technique should give reliable results or not. The manometer at the low temperature spot enables us to detect onset of freezing in a different way. The pressure is followed, when a constant amount of fluid is cooling. Consider a homogeneous fluid of a pure substance. If this fluid has a zero expansion coefficient and we start from an initial pressure and temperature indicated by *i*, the cooling curve is a straight isobaric line (fig. 7*a*). When freezing sets in, the pressure decreases, as the volume of the solid is smaller than the liquid volume. The cooling curve coincides with the freezing curve. At the lowest point the freezing stops and melting begins until all solid has disappeared. Then the cooling line continues at constant pressure till the final temperature *f* is reached. If this process is carried out with a mixture of two components, in general the cooling curve will not coincide with the freezing curve (fig. 7*b*)

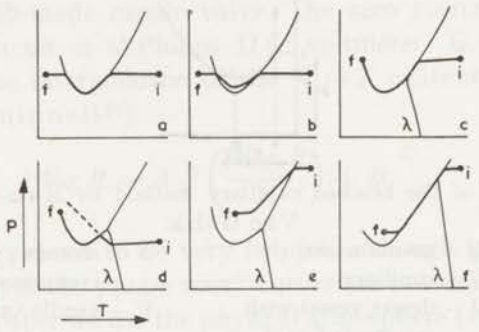

Fig. 7. Pressure-temperature diagrams. Solid lines represent various cooling curves. Thin lines represent real freezing curves of the sample.

as the concentrations of the solid and the liquid in equilibrium will differ and after some solid has been formed the concentration of the liquid has been changed. If not too much solid is formed this change is of little importance. The kink in the diagram, however, indicates sharply the onset of freezing. We never succeeded in obtaining a temperature low enough to leave the solid region. As a consequence we find fig. 7*c*. This is due to the non-zero expansion coefficient of our samples. In fact when the temperature is below the λ-temperature of the mixtures the expansion coefficient has a large negative value causing a cooling curve as indicated in figure 7*d*. The slope of the curve in the homogeneous fluid region is equal to α_P/β_T, α_P being the expansion coefficient and β_T the compressibility of the fluid. Here we neglect the volume change of the Bourdon tube and the influence of the

dead volume in the capillary and the valve (fig. 1, E) outside the cryostat. In figure 7*d* the dotted line indicates the probable cooling curve if no solid were formed. From this picture it is immediately clear why we never succeeded in getting a homogeneous fluid again at low temperatures. When the mixture has a high concentration of ^{3}He and one starts at a high initial pressure, say 45 atm, the cooling curve has the shape of fig. 7*e*. A kink indicates onset of freezing i.e. a point of the freezing curve of this mixture. In the ideal case a second kink would indicate the termination of freezing, giving a point of the melting line or solidus. Unfortunately the second kink is smeared out and the uncertainty in the determination of the solidus in this way amounts to about 0.15°K. For low concentrations, for instance a 8.9% mixture, the difference between fluid and solid is small. As a consequence we did not see a difference between the actual cooling curve and the freezing curve (fig. 7*f*). In fig. 8 we have shown a few typical runs from our

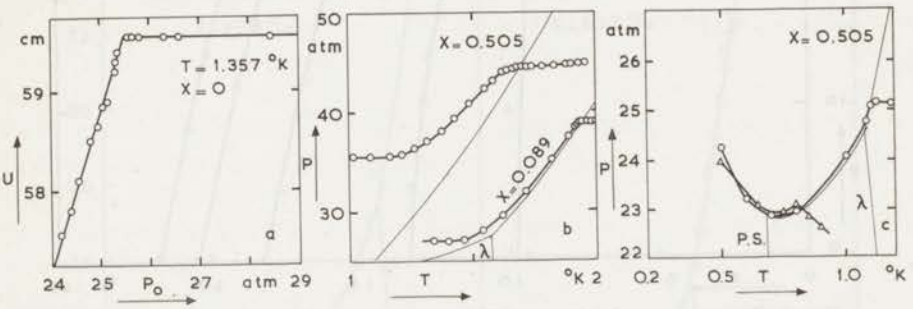

Fig. 8. Typical runs for the determination of the freezing points of ^{3}He–^{4}He mixtures.
a. blocked capillary measurement; mirror readings versus outside pressure.
b. cooling curves at high pressures of 50.5% and 8.9% mixture, thin lines indicate the freezing and λ-lines.
c. cooling curves at lower pressures of 50.5% mixtures at different initial pressures. The thin line indicates the freezing line.
λ – λ-line; P.S. – phase-separation of the fluid.

set of freezing line determinations. Figure 8*a* represents the measurement of a freezing point by means of the blocked capillary method. This particular measurement was carried out with the second apparatus (fig. 2), at $T =$ $= 1.357$°K and $X = 0$. As can be seen, 1 atm corresponds to 1.5 cm on the scale. At 25.45 atm the capillary is blocked; a further increase of the pressure outside the cryostat does not affect the pressure within the bourdon tube. In figure 8*b* two cooling curves are given. One of a fluid mixture with initial pressure 45 atm and initial molar fraction ^{3}He $X = 0.505$. The other has an initial pressure of 39 atm and a molar fraction of ^{3}He equal to 0.089. Obviously the cooling curves cannot be called isopycnes ($\rho =$ constant) as the volume of the Bourdon depends upon the pressure. At high concentrations a large difference exists between freezing and melting. This causes a large

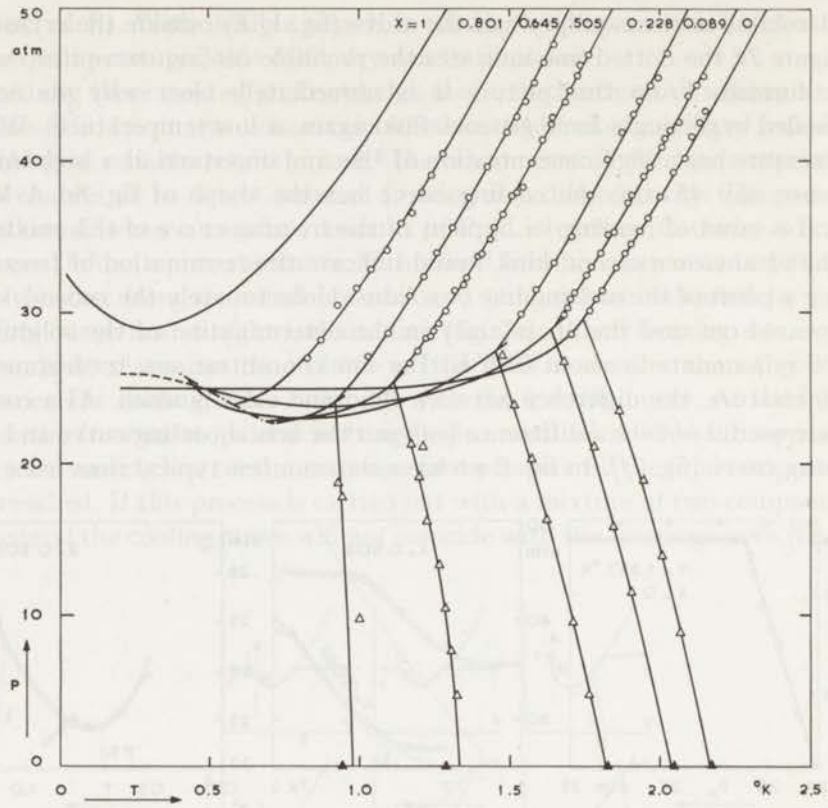

Fig. 9. Freezing- and λ-lines of ^{3}He, mixtures of ^{3}He–^{4}He and of ^{4}He.
○ denote freezing pressures
△ denote λ-pressures
▲ denote λ-temperatures at saturated vapour pressure from Roberts and Sydoriak [43])
—·—·— three phase equilibrium between two fluids and the solid
– – – – – – probable curve at lower temperatures (see for instance Lee[16]) [17])).
The drawn line for ^{3}He is taken from the measurements of Grilly, Mills and Sydoriak [44])[45]), extrapolated according to Goldstein [46]).

change of the concentration of the fluid when some solid has been formed. At low concentrations the difference is much smaller and the cooling curve coincides nearly with the freezing curve. Figure 8*c* shows cooling curves at low pressures. No appreciable difference has been found here between the cooling curves as can be seen from the two cooling curves starting from different initial pressures. This is due partly to the fact that only a little solid is formed which causes only a slight change in the fluid concentration. The second reason is that the freezing curves for different concentrations do not differ too much here, which means that slight variations of the concentration do not give very different results.

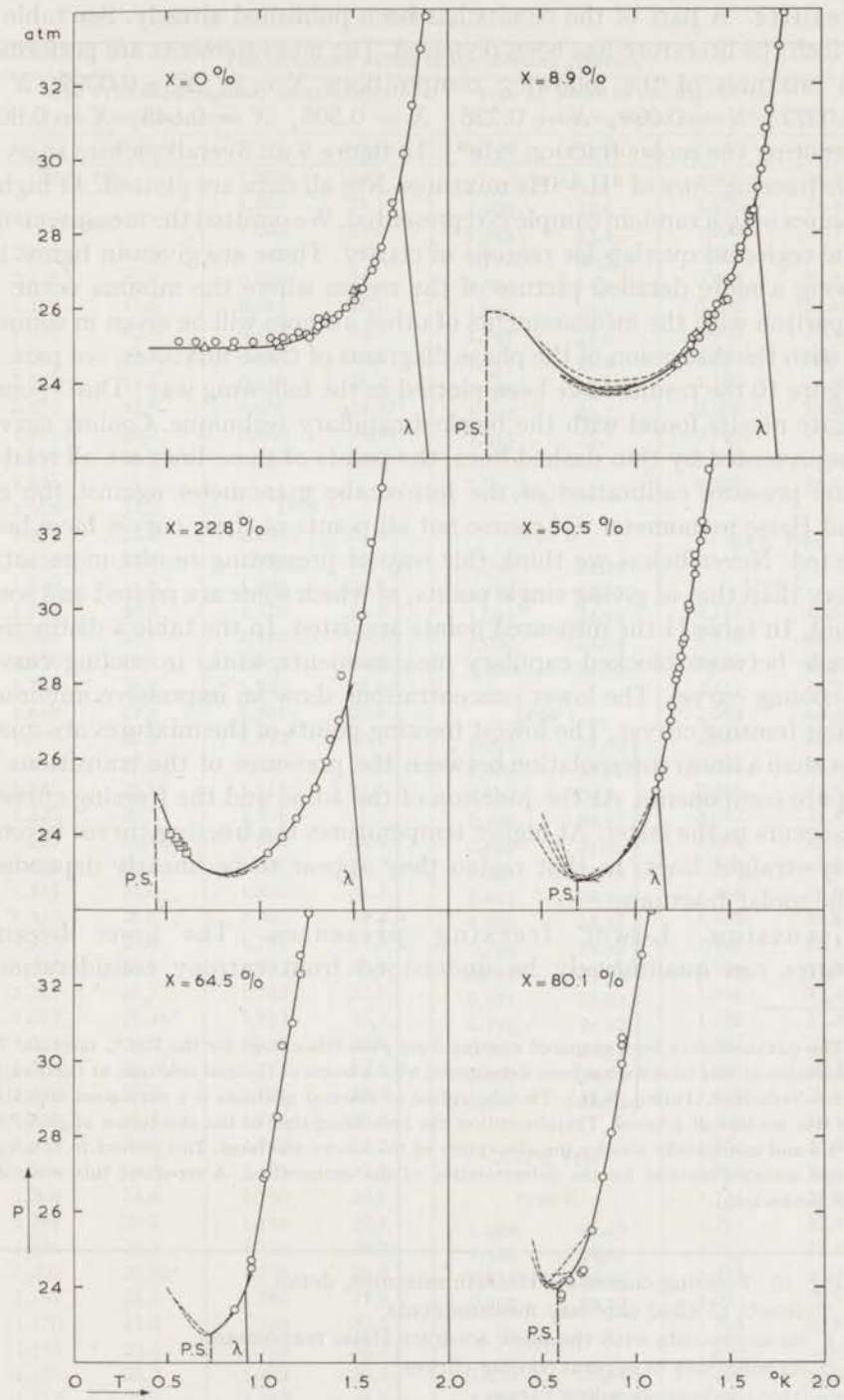
atm
X = 0 %
X = 8.9 %
X = 22.8 %
X = 50.5 %
X = 64.5 %
X = 80.1 %
P.S.
λ
P
T
°K

Results. A part of the results has been published already. See table I, in which the literature has been reviewed. The measurements are performed with mixtures of the following compositions $X = 0$; $X = 0.0099$; $X = 0.0277$; $X = 0.089$; $X = 0.228$; $X = 0.505$; $X = 0.645$; $X = 0.801$, X denoting the molar fraction ^{3}He*). In figure 9 an overall picture is given of the freezing lines of ^{3}He–^{4}He mixtures. Not all data are plotted. At higher pressures only a random sample is represented. We omitted the measurements in the region of overlap for reasons of clarity. These are given in figure 10, showing a more detailed picture of the region where the minima occur. A comparison with the measurements of other authors will be given in connection with the discussion of the phase diagrams of these mixtures, see part B. In figure 10 the results have been plotted in the following way: The 0-points indicate results found with the blocked capillary technique. Cooling curves are represented by thin dashed lines, the points of these lines are all related to one pressure calibration of the ferroxcube manometer against the external Heise manometer. Of course not all points of these curves have been detected. Nevertheless we think this way of presenting results more satisfactory than that of giving single points, of which some are related and some are not. In table II the measured points are listed. In the table a distinction is made between blocked capillary measurements, kinks in cooling curves and cooling curves. The lower concentrations show an impressive minimum in their freezing curves. The lowest freezing points of the mixtures are much lower than a linear interpolation between the pressures of the transitions of the pure components. At the junction of the λ-line and the freezing curve a kink occurs in the latter. At higher temperatures the freezing curves become nearly straight lines. In that region they appear to be linearly dependent on the molar fractions.

Discussion. Lower freezing pressures. The lower freezing pressures can qualitatively be understood from entropy considerations.

*) The mixtures have been prepared starting from pure ^{3}He except for the 50.5% mixture. The concentration of this mixture has been determined with a beam of thermal neutrons at the Reactor Centrum Nederland (Petten, N.H.). The absorption of thermal neutrons is a very good indication of the ^{3}He content of a vessel. The absorption has been compared to the absorption of pure ^{3}He, pure ^{4}He and incidentally also by the absorption of the known mixtures. This proved to be a very easy and accurate method for the determination of the composition. A report of this work will appear before long.

Fig. 10. Freezing curves of ^{3}He–^{4}He mixtures, detail.
○ denote blocked capillary measurements
△ measurements with the more accurate Heise manometer
□ terminations of several cooling curves
– – – (thin) indicates cooling curves
- - - (solid) indicates extrapolation to lower temperatures
——— (solid) onset of phase stratification according to Zenov'eva [6]).

TABLE II

The measured values of the freezing pressure

type 0 blocked capillary measurements
type I cooling curves
type II kinks in cooling curves } belonging to one calibration

T(°K)	P(atm)	T(°K)	P(atm)	T(°K)	P(atm)	T(°K)	P(atm)
0% ^{3}He		1.089	25.2	type II		1.200	24.95
		1.080	25.1	1.905	34.6	1.100	24.81
type 0		1.053	25.2	1.845	33.4	1.023	24.77
2.155	43.2	1.045	25.1	1.772	30.2	0.900	24.74
2.135	42.4	0.958	25.1	1.765	29.9	0.800	24.76
2.109	41.5	0.859	25.1	1.750	29.4	0.700	24.85
2.088	40.7	0.752	25.1	1.747	27.8	0.600	24.95
2.047	39.2	0.650	25.1	1.717	28.8	0.500	25.11
2.042	39.1	0.559	25.1	1.646	27.6	1.100	24.85
2.000	37.6	1.000	24.97†	1.532	26.7	0.800	24.80
1.961	36.2	0.850	24.96†	1.515	25.7	0.700	24.87
1.957	36.2	0.700	24.96†			0.600	24.98
1.931	35.3			0.99% ^{3}He		0.500	25.16
1.905	34.5	type I					
1.883	33.8	2.040	37.4	type 0		8.9% ^{3}He	
1.855	32.9	1.998	37.0	1.265	25.26		
1.810	31.4	1.988	36.8	1.172	25.10	type 0	
1.788	30.8	1.978	36.5	1.087	24.99	2.145	45.5
1.766	30.1	1.970	36.2	1.000	24.94	2.142	46.3
1.705	28.5	1.959	36.0	0.900	24.93	2.124	44.9
1.702	28.8	1.950	35.6			2.117	44.7
1.647	27.6	1.941	35.4	type I		2.094	44.2
1.607	27.2	1.892	34.1	1.000	24.96	2.061	42.5
1.593	27.0	1.885	33.8	0.900	24.92	2.052	42.9
1.545	26.5	1.815	31.9	0.792	24.91	2.035	41.9
1.523	26.5	1.805	31.7	0.700	24.93	2.017	41.4
1.500	26.47†	1.810	31.4	0.600	24.95	2.004	40.8
1.500	26.2	1.815	31.7	0.536	24.98	1.994	41.0
1.455	26.0	1.805	31.3	0.980	24.96	1.965	39.5
1.448	26.0	1.803	31.2	0.900	24.93	1.959	39.4
1.413	25.8	1.798	31.0	0.792	24.90	1.948	38.9
1.400	25.9	1.792	30.9	0.998	24.93	1.906	37.7
1.381	25.7	1.788	30.8	0.901	24.93	1.896	37.4
1.357	25.45†	1.783	30.7	0.792	24.92	1.892	37.3
1.354	25.6	1.779	30.6	0.700	24.93	1.891	37.2
1.350	25.76†	1.774	30.5	0.600	24.95	1.846	35.2
1.320	25.2	1.770	30.4	0.535	25.00	1.831	35.1
1.302	25.7	1.766	30.3			1.828	35.1
1.302	25.5	1.762	30.2	2.77% ^{3}He		1.800	33.9
1.296	25.4	1.755	29.8			1.797	33.9
1.266	25.4	1.750	29.6	type 0		1.771	33.0
1.258	25.2	1.744	29.4	1.284	25.23	1.761	32.9
1.246	25.3	1.736	29.3	1.150	24.88	1.755	32.4
1.200	25.35†	1.755	29.8	1.017	24.73	1.717	31.3
1.197	25.3	1.760	29.8	0.900	24.73	1.714	30.9
1.170	25.2	1.765	30.0			1.704	30.8
1.155	25.3	1.768	30.2	type I		1.698	30.8
1.155	25.2	1.772	30.3	1.350	25.44	1.695	30.3
1.115	25.2	1.762	29.9	1.300	25.23	1.689	30.2

† measured with the more accurate gauge

TABLE II (*continued*)

T(°K)	P(atm)	T(°K)	P(atm)	T(°K)	P(atm)	T(°K)	P(atm)
1.677	29.8	1.027	23.7	0.913	23.7	1.536	29.8
1.675	29.7	1.021	24.0	0.792	23.8	1.427	28.2
1.667	29.7	1.005	24.1	0.688	23.9	1.416	27.0
1.667	29.6	0.991	24.0	0.603	24.2	1.350	25.9
1.656	29.2	1.325	25.4	0.530	24.8	1.291	25.2
1.646	29.0	1.248	24.9	0.981	23.9	1.237	24.9
1.638	28.6	1.182	24.6	0.849	23.8	1.188	24.4
1.637	29.2	1.121	24.3	0.738	23.9	1.102	23.9
1.628	28.6	1.066	24.1	0.643	24.1	1.037	23.5
1.618	28.3	0.992	23.8	0.603	24.2	1.370	26.5
1.617	28.3	1.325	25.2	0.623	24.2	1.285	25.6
1.611	28.4	1.248	24.7	0.643	24.1	1.212	24.9
1.607	28.0	1.121	24.3	0.849	23.8	1.147	24.4
1.566	27.5	1.220	24.5	0.913	23.8	1.088	24.1
1.564	27.6	1.136	24.3	0.947	23.8	1.010	23.7
1.559	27.3	1.055	24.1	0.981	23.8	1.295	25.4
1.554	27.8	0.981	24.0	1.017	23.9	1.215	24.8
1.518	26.8	0.912	24.0			1.115	24.1
1.517	26.9	1.179	24.4	type II		1.010	23.5
1.498	26.7	1.136	24.2	2.205	48.7	0.925	23.1
1.494	26.2	1.055	24.1	2.140	45.7	0.832	23.0
1.482	26.3	0.981	24.0	2.082	43.7	1.000	23.4
1.472	26.2	1.121	24.3	2.063	43.3	0.943	23.3
1.438	26.1	1.066	24.2	1.965	39.5	0.980	23.2
1.430	25.8	0.992	24.0	1.930	38.5		
1.429	25.8	0.932	23.9	1.928	38.7	type I	
1.411	25.5	1.066	24.2	1.860	36.6		
1.390	25.6	1.015	24.2	1.830	35.4	1.007	23.3
1.387	25.5	0.950	24.1	1.785	33.5	0.990	23.2
1.369	25.6	0.892	24.0	1.761	33.1	0.973	23.2
1.341	25.2	0.975	24.1	1.760	33.3	0.905	23.0
1.329	25.3	0.912	24.0	1.697	31.0	0.786	23.0
1.315	24.8	0.950	24.2	1.675	30.0	0.686	23.1
1.307	25.2	0.892	24.1	1.645	28.8	0.686	23.1
1.296	25.0	0.811	24.1	1.630	28.9	0.602	23.5
1.282	24.9			1.601	28.4	0.565	23.7
1.273	25.0	type I		1.518	26.9	0.530	23.8
1.255	24.6			1.466	26.2	0.498	24.0
1.253	24.6	1.312	25.3	1.443	26.0	0.547	23.9
1.252	24.9	1.266	25.0			0.530	23.9
1.250	24.7	1.241	24.8	22.8% ^{3}He		0.565	23.7
1.223	24.5	1.165	24.4			0.574	23.7
1.214	24.5	1.055	24.2	type 0		0.558	23.8
1.181	24.4	0.981	24.1	2.026	47.0	0.547	23.8
1.177	24.2	0.913	24.1	1.997	45.4	0.513	24.0
1.155	24.5	0.849	24.1	1.970	44.9	0.923	23.0
1.150	24.3	0.792	24.1	1.933	43.9	0.905	22.9
1.135	24.1	0.738	24.2	1.911	43.0	0.843	22.9
1.117	24.2	0.643	24.4	1.873	41.8	0.735	23.0
1.096	24.0	0.565	24.8	1.823	40.0	0.643	23.2
1.089	24.2	0.495	25.1	1.769	37.7	0.603	23.2
1.065	24.3	1.241	24.5	1.703	35.0	0.602	23.5
1.061	23.8	1.178	24.1	1.644	33.2	0.565	23.7
1.053	24.0	1.055	23.9	1.588	31.5	0.530	23.9

TABLE II (*continued*)

T(°K)	P(atm)	T(°K)	P(atm)	T(°K)	P(atm)	T(°K)	P(atm)
50.5% ^{3}He		1.051	24.2	1.687	43.6	0.750	22.8
		1.051	24.1	1.668	44.8	0.650*	22.9
type 0		1.021	23.7	1.651	44.7	0.550*	23.6
1.763	46.9	1.013	23.7	1.580	40.3		
1.752	46.8	0.962	23.6	1.575	38.6		
1.731	46.2	1.282	30.3	1.495	35.7	80.1% ^{3}He	
1.724	45.5	1.226	29.5	1.419	33.4		
1.701	44.6	1.210	29.0	1.294	31.0	type 0	
1.700	44.8	1.149	26.9	1.271	28.7		
1.687	43.8	1.092	25.2			1.272	40.4
1.685	44.4	1.181	27.5			1.238	39.0
1.670	43.7	1.118	25.3	64.5% ^{3}He		1.206	37.8
1.643	42.8	1.063	24.6			1.174	36.5
1.630	42.3	0.990	23.7	type 0		1.144	35.8
1.610	41.3	0.928	23.7	1.645	47.6	1.086	34.0
1.606	41.1			1.610	46.4	1.035	32.8
1.505	41.2	type I		1.580	45.1	0.987	31.5
1.571	39.8	1.000	24.0	1.550	43.8	0.925	30.4
1.546	38.2	0.950	23.6	1.520	42.8	0.925	30.6
1.522	37.9	0.850	23.1	1.488	41.8	0.869	28.1
1.521	37.8	0.747	22.8	1.421	39.5	0.822	26.9
1.509	37.6	0.650*	23.0	1.361	37.5	0.764	25.5
1.475	36.4	0.550*	23.9	1.308	35.5	0.702	24.4
1.472	35.5	0.500*	24.6	1.255	33.9	0.648	24.2
1.445	35.5	0.600*	23.2	1.212	32.3	0.598	23.8
1.432	34.8	0.800	22.9	1.167	31.0	0.522*	23.9
1.405	33.8	1.100	25.1	1.091	28.5	0.987	31.6
1.405	35.1	1.075	24.8	1.026	27.0	0.925	29.9
1.390	33.7	1.000	24.1	1.284	35.3	0.702	24.4
1.378	32.1	0.800	22.9	1.210	32.8	0.598	23.7
1.353	32.3	0.700	22.8	1.145	31.5		
1.344	31.8	0.600*	23.2	1.087	29.2	type I	
1.318	31.4	0.500*	24.2	0.988	26.5		
1.318	31.2	0.900	23.2	0.988	26.8	0.750	25.4
1.318	30.9	0.850	23.1	1.115	30.4	0.700	25.2
1.286	30.0	0.600*	23.2	1.011	26.9	0.605	24.8
1.283	30.1	0.550*	23.6	0.947	24.5	0.600	24.5
1.261	29.2	0.500*	23.8	0.947	24.7	0.550*	24.2
1.251	29.1	0.460*	24.4	0.842	23.4	0.500*	24.2
1.241	28.7	0.800	22.8	0.967	24.2	0.460*	25.0
1.235	28.4	0.750	22.8	0.947	24.1	0.600	24.0
1.221	28.3	0.650*	22.9	0.858	23.4	0.500*	24.3
1.211	28.1	0.550*	23.3			0.650	24.4
1.192	27.4	0.460*	24.0			0.600	24.4
1.189	27.0	0.800	23.1	type I		0.550*	24.3
1.165	26.6	0.750	22.9	0.850	23.4	0.600	24.2
1.147	25.7	0.650*	23.0	0.800	23.0	0.550*	24.0
1.123	25.5	0.500*	23.9	0.700*	22.8	0.500*	24.1
1.123	24.8			0.650*	22.9	0.450*	24.7
1.108	25.1	type II		0.600*	23.1	0.600	24.1
1.086	24.6	1.869	50.9	0.550*	23.6	0.550*	24.1
1.072	24.4	1.772	46.8	0.500*	24.0	0.500*	24.1

* three-phase equilibrium

Consider an amount of pure ^{4}He at $T = 0.7°$K at the fluid-solid equilibrium. The Clausius-Clapeyron equation:

$$dP/dT = \underset{1}{\Delta S}/\underset{1}{\Delta V}$$

holds. dP/dT is the slope of the equilibrium curve. $\underset{1}{\Delta S} = S_{fl} - S_{sol}$, $\underset{1}{\Delta V} = V_{fl} - V_{sol}$. At this temperature $dP/dT \approx 0$; $\underset{1}{\Delta V} \neq 0$. Hence $\underset{1}{\Delta S} \approx 0$. If one introduces a certain amount of ^{3}He into the fluid and the solid, for low concentrations a qualitative picture of the new equilibrium conditions can be obtained from the change of the Gibbs function. From the heat capacity measurements on liquid mixtures[32]) we know that the entropy of mixing is not ideal. At $T = 0.7°$K a negative excess entropy, $S^E = -0.0775$ Joule mol^{-1} °K^{-1} (% ^{3}He)$^{-1}$ occurs. This is in agreement with Nernst's heat theorem, which states that at absolute zero of temperature the entropy should be zero. In classical thermodynamics this is not the case for a mixture, as the ideal entropy of mixing: $-R\{X \ln X + (1 - X) \ln (1 - X)\}$, a positive quantity, is independent of temperature. In quantum statistics this difficulty does not arise, as here this term goes to zero with decreasing temperature (because of the degeneracy). This was recognised by Keesom as early as 1913[47]), when he treated the mixing of ideal gases at low temperatures, using the results of the early quantum mechanics by Planck etc. More recently Heer and Daunt[73]) have discussed this phenomenon with respect to the mixtures with which we are dealing here. Obviously when one tries to describe the properties in classical terms with a constant ideal entropy of mixing one will find a negative excess entropy. In the solid the same should happen. Measurements of the specific heat of solid mixtures ^{3}He–^{4}He however show that degeneration takes place at lower temperatures[2]). The entropy of mixing of the solid at 0.7°K is still ideal. Thus the entropy of the fluid decreases more rapidly than the entropy of the solid when some ^{3}He is added. In comparison with the Gibbs function of pure ^{4}He the equilibrium pressure may decrease in such a way that:

$$\Delta P \cdot V \approx TS^E$$

yielding: $\Delta P = -0.05$ atm (% ^{3}He)$^{-1}$. This is roughly in agreement with our results. A more rigorous treatment cannot be given at this moment because the necessary data for the calculation of the partial thermodynamic potentials (μ_i) are still lacking. More accurate estimations can possibly be made from these measurements if combined with the measurements on the melting curves. We have not yet carried out these calculations.

Minima. The same kind of reasoning can be held about the temperature dependency of the freezing curves. This yields a gradual increase of the entropy term TS of the Gibbs function, which implies the negative slope

of the freezing curves. In both considerations the differences between solidification of pure substances and mixtures have been overlooked. The slope of the freezing curve of a mixture is determined by:

$$\left(\frac{\mathrm{d}P}{\mathrm{d}T}\right)_{X_n} = \frac{X_{\mathrm{sol}}(S_{3,\mathrm{fl}} - S_{3,\mathrm{sol}}) + (1 - X_{\mathrm{sol}})(S_{4,\mathrm{fl}} - S_{4,\mathrm{sol}})}{X_{\mathrm{sol}}(V_{3,\mathrm{fl}} - V_{3,\mathrm{sol}}) + (1 - X_{\mathrm{sol}})(V_{4,\mathrm{fl}} - V_{4,\mathrm{sol}})}.$$

S_i denoting the partial molar entropy; V_i denoting the partial molar volume. Thus the behaviour of the slope of the freezing curve is not as simply dependent of the total entropy as in a one-component system. But it is not so much different that an explanation of the minima is likely to be from other origins than from entropy degeneration.

Kinks. The slope of the freezing curve of a pure substance is determined by the Clausius-Clapeyron equation. As De Bruyn Ouboter and Beenakker pointed out[48]), in mixtures a kink exists in the first order phase transition line at the junction with a second order transition line. Let us consider first the case of pure ^{4}He: $\underset{1}{\Delta}S$ and $\underset{1}{\Delta}V$, being the differences in entropy and volume at both sides of the first order transition line, vary continuously, as the λ-transition is a phase transition of the second order i.e.

$$\underset{2}{\Delta}(\mathrm{d}P/\mathrm{d}T)_{\mathrm{freezing}} = 0.$$

$\underset{2}{\Delta}$ means the difference of a quantity between both sides of a second order transition line. The second derivatives of the Gibbs free energy however do not change continuously. This gives rise to an abrupt change of the curvature of the freezing line:

$$\underset{2}{\Delta}\left(\frac{\mathrm{d}^2P}{\mathrm{d}T^2}\right)_{\mathrm{fr}} = \frac{-2\dfrac{\underset{1}{\Delta}S}{\underset{1}{\Delta}V}\cdot V\cdot\underset{2}{\Delta}\alpha_P + \dfrac{1}{T}\cdot\underset{2}{\Delta}C_P - \left(\dfrac{\underset{1}{\Delta}S}{\underset{1}{\Delta}V}\right)^2\cdot V\cdot\underset{2}{\Delta}\beta_T}{\underset{1}{\Delta}V}.$$

α_P = the isobaric expansion coefficient; β_T = the isothermal compressibility. In binary mixtures the situation is different because $\underset{2}{\Delta}(\mathrm{d}P/\mathrm{d}T)_{\mathrm{fr}}$ does not vanish. As De Bruyn Ouboter and Beenakker showed:

$$\underset{2}{\Delta}\left(\frac{\mathrm{d}P}{\mathrm{d}T}\right)_{X_n,\mathrm{fr}} = \frac{V_{\mathrm{fl}}\left(\dfrac{\mathrm{d}P}{\mathrm{d}T}\right)_{X_n,\mathrm{fr}}\cdot\underset{2}{\Delta}\beta_T - \dfrac{\underset{2}{\Delta}C_{P,\mathrm{fl}}}{T}}{\dfrac{\partial V_{\mathrm{fl}}}{\partial X_{\mathrm{fl}}} - \dfrac{\underset{1}{\Delta}V}{\underset{1}{\Delta}X} - V_{\mathrm{fl}}\left(\dfrac{\mathrm{d}T}{\mathrm{d}X_{\mathrm{fl}}}\right)_{\lambda}\cdot\underset{2}{\Delta}\beta_T}\cdot\left(\frac{\mathrm{d}T}{\mathrm{d}X_{\mathrm{fl}}}\right)_{\lambda}.$$

fl denotes the fluid phase and fr the freezing curve. $C_{P,\mathrm{fl}}$ is the specific heat

at constant pressure of the fluid phase. The discontinuity is due to the fact that $\underset{1}{\Delta} X \neq 0$ at the fluid-solid transition. If the λ-surface should join in some point the azeotropic line (i.e. the line through the azeotropic points) the discontinuity would vanish. However, as far as our measurements indicate, the λ-line and the azeotropic line do not coincide.

Straight lines. In the case of an assembly of hard spheres, according to Uhlenbeck[49]) one could expect a linear dependence of the transition pressure on T. Unfortunately helium certainly does not consist of a number of hard spheres (see Part II). Such a simple explanation cannot be given therefore. As the molecules of both isotopes differ only energetically as to their zero point energies, which add up to the kinetic energy, one may expect a kind of linear interpolation between the curves of the pure isotopes, because this extra zero point "kinetic energy" enlarges the classical kinetic energy linearly with the molar fraction ^{3}He.

4. *Melting curves.* Experimental procedure. Measurements are performed with the fourth apparatus (fig. 5). The mixture is compressed to its freezing pressure or to the minimum freezing pressure where the capillary is blocked, when the temperature of the Bourdon tube is below T_M. Then we increase the pressure in the vessel around the Bourdon tube by admitting ^{4}He gas to this space. In doing so the Bourdon tube alters its shape just as if the pressure within decreases. Actually a Bourdon-manometer indicates only the pressure difference between the pressure inside and outside the Bourdon. If the fluid within the Bourdon is a pure substance, then we see that at first the rise of the outside pressure equals the fall of the "Bourdon" pressure. As the total pressure on the sample is equal to the sum of the pressure of the walls of the Bourdon tube and the outside pressure, this involves the pressure of the sample to remain constant. A solidification at constant pressure and temperature takes place until the solidification is complete. Of course the heat of melting has to be extracted by the ^{3}He cryostat. From that moment a further increase of the outside pressure causes an increase of the pressure of the sample, because of the small compressibility of the solid. If instead of a pure substance a mixture of ^{3}He–^{4}He is investigated, in general the process differs a little from the one described here. When some solid has been formed, the concentration of the fluid has been changed. The freezing pressure of the remaining fluid is somewhat higher than the freezing pressure of the initial mixture. During the proces of solidification we notice a pressure increase. When all fluid has disappeared the increase becomes steeper. This change of slope in the graph of total pressure versus outside pressure is rather sharp and indicates the termination of freezing called the melting point. Sometimes there is no difference in concentration between fluid and solid in equilibrium. A mixture

under these specific TPX conditions is called azeotropic. If an azeotropic mixture solidifies, the behaviour is essentially the same as that of a pure substance. In figure 11 two typical runs are shown. Part *a*) shows the solidification of a mixture containing 8.9% ^{3}He. The solidification is azeotropic.

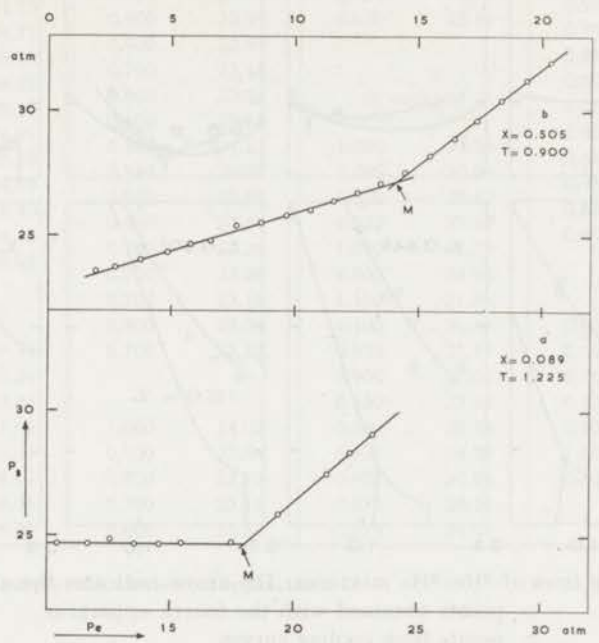

Fig. 11. Solidification of two mixtures at constant temperature by volume decrease. The pressure of the sample P_s plotted against the external ^{4}He-pressure P_e of the chamber around the Bourdon. The volume of the Bourdon is a continuous monotonous function of $P_s - P_e$. M indicates the melting point.

a. solidification of a 8.9% mixture under azeotropic conditions.

b. solidification of a 50.5% mixture.

From the diagram of the freezing curves at different concentrations, it is already obvious that azeotropy would occur. We shall return to this at the discussion of the phase diagram. In figure 11*b* the solidification of a 50.5% mixture is shown. The molar fraction of ^{3}He in the fluid changes during the process of solidification. The equilibrium pressure at constant temperature increases, indicating this change.

Results. Measurements have been done on mixtures of the following composition: $X = 0.089$, $X = 0.228$, $X = 0.351$, $X = 0.505$, $X = 0.645$, $X = 0.801$. The results of the measurements which have been presented to the Ninth Conference on Low Temperature Physics[12]) are listed in table III and shown in figure 12. The measurements show a larger error than the freezing point measurements. This is due to the obstruction against free movements of the Bourdon tube caused by the pieces of solid inside.

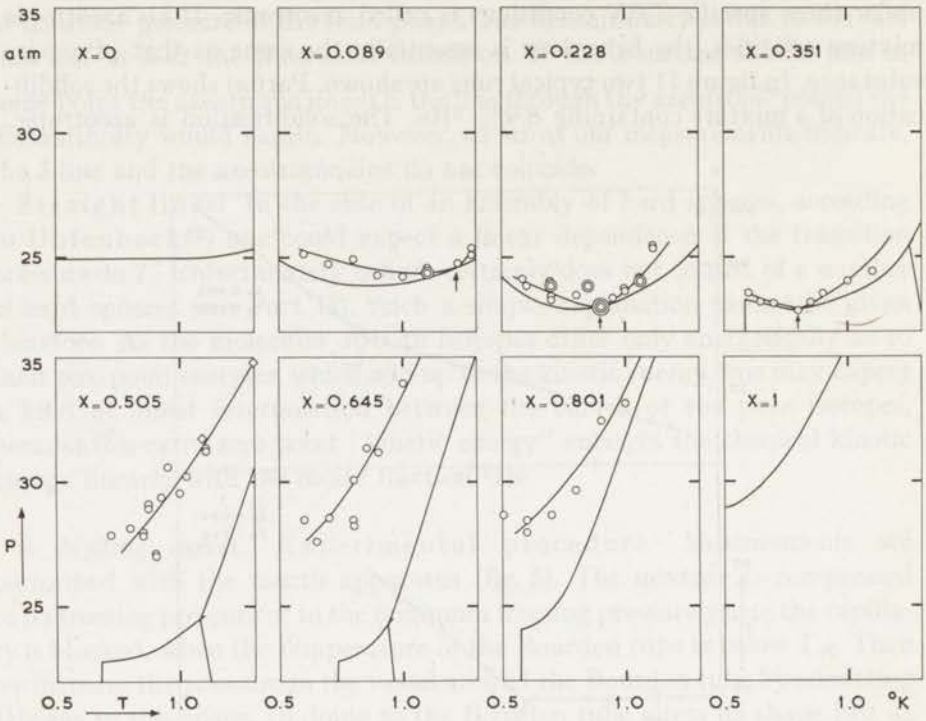

Fig. 12. Melting lines of ^{3}He–^{4}He mixtures. The arrow indicates the azetropic point.
○ points obtained with the fourth apparatus
◇ points from cooling curves
◎ etc. points that overlap.

Another source of errors in this experiment is caused by the readings of the manometer indicating the outside pressure on the Bourbon-tube, which suffered some hysteresis being not as reliable as we hoped.

It is clear from the results that the azeotropic point, which only occurs at lower concentrations, shifts to the low temperature side, when the molar fraction of ^{3}He increases. At some composition it will coincide with the onset of phase separation of the fluid. A 50.5% mixture does not show azeotropy any longer. This has important consequences for the phase diagram as will be shown later.

5. *λ-lines and minima of molar volumes.* The λ-transition of pure ^{4}He shifts towards lower temperatures if the pressure increases. The same happens if the concentration of ^{3}He increases (e.g. ref. 1). Some evidence on this shift of mixtures at higher pressures has been obtained by Fairbank and Elliot in 1958[50]). They used the second sound velocity for the λ-point detection.

The early diagram of state of helium published by Keesom and Miss

TABLE III

Measured values of the melting pressures of mixtures of ^{3}He–^{4}He

T(°K)	P(atm)	T(°K)	P(atm)	T(°K)	P(atm)	T(°K)	P(atm)
$X = 0.089$		0.700	23.88	1.100	24.40	$X = 0.645$	
		0.700	23.93	0.850	23.14	0.900	31.18
1.225	24.73	0.900	22.99	0.650	23.19	0.700	28.53
0.700	24.71	0.900	22.99			0.800	28.48
0.600	25.13	0.700	23.45			0.800	28.29
1.000	24.25	0.900	23.04	$X = 0.505$		1.000	33.98
1.280	25.10	0.600	23.85			0.850	31.37
0.900	24.29	0.587	24.13	1.000	29.53	0.650	27.57
1.280	25.38	0.950	23.38	1.025	30.24	0.750	29.91
1.100	24.59	0.850	23.85	0.800	28.12	0.600	28.48
1.100	24.40	0.850	23.86	0.720	27.87	0.800	30.06
1.100	24.40	0.700	23.26	1.090*	31.75		
0.800	24.93	0.700	23.26	1.300*	34.85	$X = 0.801$	
		0.700	23.16	1.103	31.36		
$X = 0.228$		0.900	23.04	1.103	31.32	0.600	28.46
1.115	25.34	0.700	23.85	0.900	27.14	0.600	27.98
1.115	25.36			0.900	27.06	0.700	28.66
0.800	23.48	$X = 0.351$		0.850	27.82	0.800	29.62
1.000	23.62	1.000	24.02	0.850	27.98	0.900	32.48
1.000	23.66	0.900	23.54	0.925	29.38	1.000	33.11
1.060	24.13	0.800	22.79	0.950	30.59	0.505	28.66
1.060	24.06	0.700	23.16	0.875	28.90		
1.060	24.06	0.600	23.52	0.875	29.04		

* from cooling curves with the second apparatus

Keesom, e.g. ref. 51, is known to be too simple in the vicinity of the λ-point. From the work of Lounasmaa *e.a.*[52)53)54)55)], of Atkins and of Edwards[56)], reviewed by Buckingham and Fairbank[57)], we know that in the neighbourhood of the λ-transition some thermodynamic variables show a logarithmic behaviour. The molar volume of liquid helium for instance shows a minimum at about 0.006°K above the λ-temperature T_λ. At lower temperatures the volume increases. Very close to T_λ, $(\partial V/\partial T)_P$ changes rapidly and probably has a discontinuity at T_λ. The singularity is logarithmic as to the specific heat and $(\partial P/\partial T)_V$. Recently Goldstein[58)] pointed out that a real logarithmic singularity cannot exist. Temperature differences become meaningless if they are of the order of thermal fluctuations. Obviously this is so if $|T - T_\lambda| \approx 10^{-12}$°K. In any case the change of pressure with temperature in the vicinity of the λ-point is sharp. From Lounasmaa's measurements it can be seen that the singularity is limited within 10^{-6}°K around the λ-transition. In the present experiment we watch the pressure in the Bourdon tube. The accuracy of our temperature measurement is about 10^{-3}°K. Thus we cannot get detailed information about the nature of the transition itself. A singularity at the transition however can easily be determined.

Experimental procedure. In our determinations of the λ-points a constant amount of fluid is cooled, while the pressure is recorded. If the Bourdon tube has a constant volume, the slope of the cooling curve should be

$$\delta P/\delta T = \alpha_P/\beta_T.$$

α_P is the isobaric expansion coefficient $(1/V)\ (\partial V/\partial T)_P$; β_T is the isothermal compressibility $-(1/V)(\partial V/\partial P)_T$. As the volume is not constant but a continuous function of pressure, this has to be transformed into:

$$\frac{\delta P}{\delta T} = \frac{\alpha_P}{\beta_T + (1/V)(\mathrm{d}V/\mathrm{d}P)_{\text{Bourdon}}}.$$

The derivative of the Bourdon volume with respect to P is also a continuous function of P, while no singularities of β_T in the homogeneous helium I or II regions are likely. Therefore kinks in $\delta P/\delta T$ curves occur only at that temperature where α_P shows a kink. And also $\delta P/\delta T = 0$ when $\alpha_P = 0$. In figure 13 two typical runs are shown. One represents a measurement at about 24 atm on a 22.8% mixture, the other at about 9 atm on a 64.5% mixture. From these measurements it is obvious that the negative slope of the $\delta P/\delta T$ curve exists already above T_λ. This is in agreement with the results of others on pure ^{4}He quoted in the preceding section, and of Kerr on mixtures at saturated vapour pressure[30) 31)].

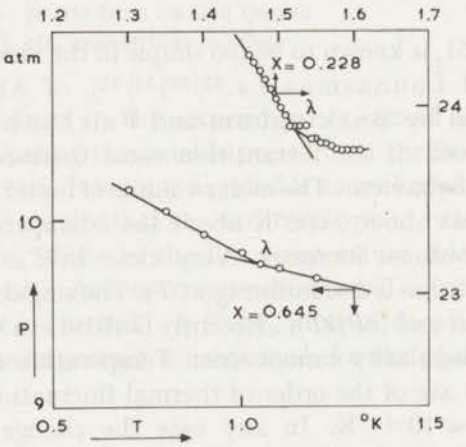

Fig. 13. Typical runs of λ-point determinations
$X = 0.228$ with mirror detection
$X = 0.645$ with ferroxcube apparatus.

Results. Measurements have been done on mixtures of the following compositions: $X = 0$; $X = 0.089$; $X = 0.228$; $X = 0.505$; $X = 0.645$. The results are listed in table IV. The values at saturated vapour pressure are

those given by Roberts and Sydoriak[43]). The measurements have been plotted in figure 9 already. The only discrepancy, which is somewhat outside the error region, is the result at the 50.5% mixture. We have no explanation for that.

TABLE IV

λ-points of mixtures of ^{3}He–^{4}He at several molar fractions of ^{3}He–^{4}He. The values at saturated vapour pressure are taken from ref. 43

$X = 0$		$X = 0.089$		$X = 0.228$		$X = 0.505$		$X = 0.645$	
P(atm)	T(°K)	P(atm)	T(°K)	P(atm)	T(°K)	P(atm)	T(°K)	P(atm)	T(°K)
SVP	2.1735	SVP	2.046	SVP	1.827	SVP	1.286	SVP	9.41
8.85	2.070	11.50	1.907	4.69	1.762	4.65	1.325	9.78	1.000
13.99	2.008	15.92	1.848	9.60	1.715	7.73	1.306	17.80	0.942
18.91	1.944	21.12	1.780	16.35	1.625	10.46	1.285	18.75	0.943
23.57	1.866	26.79	1.681	20.23	1.577	13.34	1.265		
				23.86	1.517	16.26	1.227		
				27.14	1.473	19.07	1.200		
						21.16	1.224		
						21.35	1.175		

In figure 14 series of cooling curves are plotted of a 8.9% mixture. The difference between the temperature T_M at which the molar volume minimum exists and T_λ increases with increasing pressure in accordance with the results of Lounasmaa. The very accurate volumetric experiments of Kerr[31]) prove that $T_M - T_\lambda$ increases also with increasing concentration. This effect is confirmed by us. Experiments are now in progress to obtain more detailed data concerning the λ-transition in mixtures.

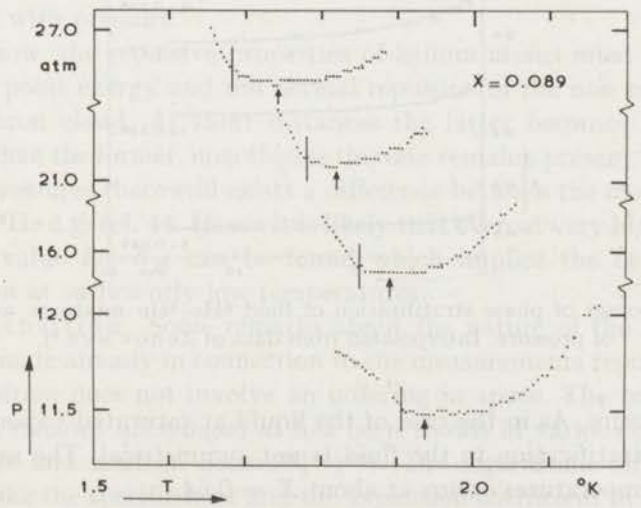

Fig. 14. Cooling curves of a fluid mixture at different pressures. Molar fraction ^{3}He is 0.089.

1. *Elements.* Stratification of the fluid. A fluid mixture of ^{3}He and ^{4}He separates into two phases below a certain temperature. This has been confirmed by many investigators for the liquid state[1]) and by Fairbank and Elliot[50]) and by Zinov'eva[6]) at higher densities. The phase separation is consistent with the observed positive heat of mixing H^E of these mixtures[32]). The attractive forces between the helium atoms are of the London-Van der Waals type, resulting in a C/r^6 attraction. (r is the distance between the centres). In general this kind of force results in a phase separation of mixtures of different molecules (e.g. ref. 59). Here we are dealing, however, with substances of which the electronic wave functions and thus the polarizability of the atoms are equal. The phase separation is generally believed to originate from other sources, such as the difference in statistics or the difference in zero point energy. The first has been treated for instance by Cohen and Van Leeuwen[76]), the second by Prigogine, Bingen, Bellemans and Simon[74]).

Zinov'eva detected the onset of phase stratification for different concentrations as a function of pressure by visual observation. We interpolated her results for the concentrations which we used in our experiments. In figure 15 the thus obtained values of the onset temperature are plotted

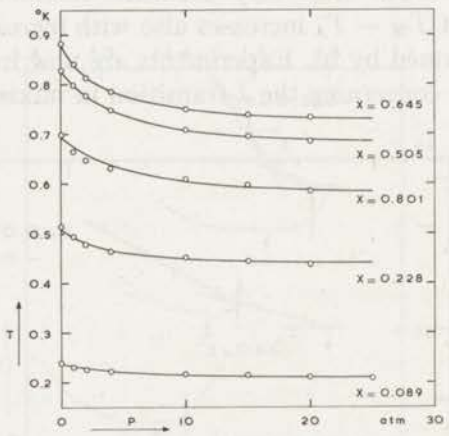

Fig. 15. The onset of phase stratification of fluid ^{3}He–^{4}He mixtures as a function of pressure. Interpolated from data of Zenov'eva [6]).

against pressure. As in the case of the liquid at saturated vapour pressure, the phase stratification in the fluid is not symmetrical. The maximum of the onset temperatures occurs at about $X = 0.64$.

The phase stratification in the solid. Specific heat measurements of solid ^{3}He–^{4}He mixtures show a strong extra contribution to the normal

heat capacity below a certain temperature[2]). This has been ascribed by the investigators to the occurrence of phase stratification in the solid. Just as in the fluid a positive heat of mixing H^E causes the separation into two phases at a temperature below a certain critical value, where the TS term of the Gibbs free energy becomes too small to be able to make the mixed state the most favourable one. Edwards, McWilliams and Daunt concluded from their measurements that the solid mixtures behave completely regularly i.e. the heat of mixing can be written as

$$H^E = X(1 - X)\, E_M$$

where $E_M/R = 0.76°K$. Recently Klemens and two of us estimated this result from a more general point of view[4]). Following the original assumption of Klemens and Maradudin[5]) about the lattice distortion around isotopic impurities, we supposed that the energy of solid helium is composed additively of the energies of individual atomic cells, and that the latter consists of a zero point energy, a lattice potential and a pressure term. The distortions of the lattices were expressed in terms of the difference in atomic volume of the two pure components and of their elastic constants assuming that the zeropoint energy varies inversely as the mass of the atom. In the same way the heat of mixing has been calculated. E_M/R was found to be 0.75°K. The mixture should be regular. The experiments of Edwards, McWilliams and Daunt were carried out at various pressures. They did not see any pressure dependency of the measured effect. We on the contrary expected a 10% decrease of the heat of mixing due to the pressure increase of 5 atm. as has been performed by them. The change may be smaller than the one predicted by us as a consequence of the change of the elastic constants of the lattices with pressure.

As we know, the repulsive properties of helium atoms must be ascribed to the zero point energy and the normal repulsion of the non penetrability of the electron cloud. At short distances the latter becomes much more important than the former, nonetheless this one remains present. So even at very high pressures there still exists a difference between the molar volumes of ^3He and ^4He e.g. ref. 44. Hence it is likely that even at very high pressures a positive value for E_M can be found which implies the occurrence of stratification at sufficiently low temperatures.

The λ-transition. Some remarks about the nature of the λ-transition have been made already in connection to the measurements reported above. The λ-transition does not involve an ordering in space. The configuration of the fluid remains unchanged as has been shown in various experiments with X rays and neutron beams[60])[61])[62]). The logarithmic singularity of properties like the specific heat and the expansion coëfficient in the vicinity of the λ-point are consistent with a treatment of the λ-phenomenon in terms of a second order transition. De Bruyn Ouboter and Beenakker[48])

investigated the thermodynamic consequences of coincidences of this kind of transitions with first order phase transformations. We did mention before the kinks in the first order transition lines at the junctions with this kind of transition. Because of the lack of change of configuration, these kinds of transitions are not the phase transitions with which the Gibbs phase rule deals*). In that sense the λ-transition does not affect the phase diagram**).

The polymorph phase transition. Three solid phases of both ^{3}He and ^{4}He are known to-day. At very high pressures the isotopes crystallise in a cubic closed packed lattice. At pressures lower than $\sim$1500 atm the structure of the solids is hexagonal close-packed (hcp). At about 140 atm ^{3}He crystallises in a body centered cubic (bcc) structure. ^{4}He exists also as a bcc solid (Vignos and Fairbank; Grilly and Mills), but only in a small pressure-temperature region along the melting line at temperatures T: $1.45 < T < 1.8$. We shall discuss the properties of the pure substances in greater detail in a later part, but we should like to mention here already that the transition between hcp and bcc solid is possibly related to a change of the sign of $\Phi_{\text{hcp}} - \Phi_{\text{bcc}}$ being the classical potential energies of the lattices. We calculated these energies in the conventional way, using the Yntema-Schneider potential[63]) and found a lower potential energy of the bcc structure at volumes greater than $\sim$20 cm^3 mole^{-1}.

Unfortunately only very little is known about the behaviour of this transition in mixtures. Vignos and Fairbank[7]) studied the velocity of sound in solid mixtures of 5%, 75% and 98% ^{3}He. From these measurements it seems that a 5% mixture just as ^{4}He has an upper and a lower triple point where hcp, bcc and fluid coexist in equilibrium. ^{3}He and the higher concentrations probably only have an upper triple point†).

Berezniak *e.a.*[19]) also studied the variation of the upper triple point with concentration. Their measurements together with those of Vignos and Fairbank indicate that the projection on the PT-plane of the line connecting the upper triple points is very nearly a straight line from the upper triple point of ^{4}He to the triple point of ^{3}He. Although nothing is known about the dimensions of the inhomogeneous region between the homogeneous hcp and bcc phases, we have to assume such a region to exist. Thus in the phase diagrams we have drawn two lines indicating the transition.

Solidification. The solidification of the mixtures as well as the soli-

---

*) Apart from this, the considerations of Goldstein about the difficulties related to the logarithmic singularity, might mean that in this special case of the λ-transition in helium, no sharp transition line exists. Following these arguments one should think about a very narrow λ-region.

**) There is for instance never an inhomogeneous region, associated with the λ-transition, where phases of different composition coexist in equilibrium.

†) Reich[64]) once mentioned that ^{3}He should have a lower triple point also. This however, has never been confirmed.

dification of the pure components takes place only at pressures greater than the saturated vapour pressure. The minimum freezing pressure of an extensive concentration region is lower than the freezing pressures of the pure components. Together with the existing minima in the PT diagram of the freezing curves of the pure components, the solidification gives rise to a peculiar type of TX phase diagram, involving a solid region surrounded completely by fluid. As we pointed out before, the minima in the freezing pressures arise from different origins as to ^{3}He, ^{4}He and mixtures. Lifshitz and Sanikidze[21]) applied the theory of dilute mixtures to a solution of ^{4}He in ^{3}He. They showed that the Pomeranchuk effect in ^{3}He should cause minima to occur in dilute solutions of ^{4}He in ^{3}He. The TX diagram at the pressure of the minimum in the melting line of a pure component near the temperature at which this minimum occurs, consists of a liquidus and a solidus touching at $T = T_M$, with the shape of a parabola determined by

$$X_{fl} = -\frac{\chi}{\chi - 1}\left\{\frac{C^0_{P,fl} - C^0_{P,sol}}{2kT_M}\right\}\frac{\Delta T^2}{T_M + \Delta T}$$

$$X_{sol} = -\frac{1}{\chi - 1}\left\{\frac{C^0_{P,fl} - C^0_{P,sol}}{2kT_M}\right\}\frac{\Delta T^2}{T_M + \Delta T}$$

$C^0_{P,sol}$ and $C^0_{P,fl}$ being the specific heat of solid and fluid of the pure solvent respectively, X_i being the molar fractions of the solute, $\Delta T = T - T_M$,

$$\chi = \exp\left(-\frac{\psi_{fl}(P_M, T_M) - \psi_{sol}(P_M, T_M)}{kT}\right)$$

ψ_i characterises the atoms of the solute in the solvent surrounding. For pressures greater than P_M, the parabolae intersect at $X = 0$. At smaller pressures they have no common point. The vertices of the parabolae are located at $T = T_M$ at

$$X_{fluid} = \frac{\chi}{\chi - 1}\,\frac{V^0_{fl} - V^0_{sol}}{kT_M}\,\Delta P$$

$$X_{sol} = \frac{1}{\chi - 1}\,\frac{V^0_{fl} - V^0_{sol}}{kT_M}\,\Delta P$$

V^0_i being the molar volume of the solvent; $\Delta P = P - P_M$.

An analogous reasoning can be held for ^{4}He, as also this component has a minimum of its own. There is however an important quantitative difference between the two parts of the TX diagram. The mixtures show a freezing pressure minimum of their own, determined by the degeneration of the entropy of mixing. The magnitude of the minimum differs very much between ^{3}He and ^{4}He. Therefore the validity of the calculations of Lifshitz

and Sanikidze will hold at the ^{3}He side in a much greater pressure-concentration region than at the ^{4}He side. The contribution to the entropy of mixing caused by 1% ^{3}He is about 0.37 Joule mol^{-1} °K^{-1}. De Bruyn Ouboter[32]) showed that a dilute liquid mixture at 0.6°K suffers a degeneration of about 1/3. The negative entropy of melting is estimated to be about 0.01 Joule mol^{-1} °K^{-1} for pure ^{4}He in this temperature region. Therefore the degeneracy of the entropy of mixing exceeds the minimum effect in pure ^{4}He already by a factor 10, when only 1% of ^{3}He is involved. Hence anomalies can be expected at concentrations lower than 1%. In our opinion the peculiar properties of the phase diagram near pure ^{4}He must be ascribed to this phenomenon.

Azeotropy. Under certain conditions the mixtures are azeotropic. This has been mentioned before in connection with the results of the melting measurements. From the freezing curves it is already obvious that azeotropy should occur. In figure 9 one can see that the mixture containing 8.9% ^{3}He freezes in a certain pressure interval at a higher temperature than mixtures of lower or higher concentration. Intersection of freezing lines in a PT-diagram implies that at some temperature and concentration:

$$(\partial P_{\mathrm{fr}}/\partial X_{\mathrm{fl}})_T = 0.$$

P_{fr} = the freezing pressure, X_{fl} = the molar fraction ^{3}He in the fluid phase. The freezing pressure of a mixture is a function of temperature and molar fraction only, hence:

$$\left(\frac{\partial P_{\mathrm{fr}}}{\partial X_{\mathrm{fl}}}\right)_T \left(\frac{\partial X_{\mathrm{fl}}}{\partial T}\right)_{P_{\mathrm{fr}}} \left(\frac{\partial T}{\partial P_{\mathrm{fr}}}\right)_{X_{\mathrm{fl}}} = -1.$$

From this relation and the measurements it follows that

$$(\partial T/\partial X_{\mathrm{fl}})_{P,\mathrm{fr}} = 0$$

under certain conditions. The TX diagram of a freezing curve at constant pressure therefore shows a maximum at that point. Apart from critical

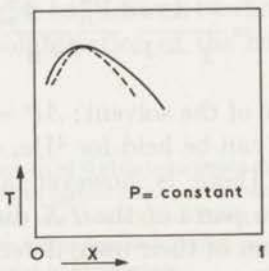

Fig. 16. TX diagram at constant pressure in the region $P \sim 25$ atm. Drawn line: freezing curve; dashed line: melting curve.

effects, which are irrelevant in connection to the phenomena under consideration, it is impossible to enter the solid region from the fluid region without passing the freezing line. Therefore the melting curve must be somewhere below this line. However, at each temperature where fluid freezes there must be a solid in equilibrium with it. This requires the melting line to coincide with the freezing curve in its maximum. Here the difference in concentration between solid and fluid $\underset{1}{\Delta} X$ vanishes. From the formulae for the slopes of the first order phase transitions in binary mixtures, given by De Bruyn Ouboter and Beenakker:

$$\left(\frac{\mathrm{d}T}{\mathrm{d}X_{i\mathrm{A}}}\right)_{P,\mathrm{a}} = \frac{-T\left(\frac{\partial^2 G_{\mathrm{A}}}{\partial X_{i\mathrm{A}}^2}\right)_{P,T} \underset{1}{\Delta} X_i}{X_{i\mathrm{B}} \underset{1}{\Delta} H_i + X_{j\mathrm{B}} \underset{1}{\Delta} H_j},$$

$$\left(\frac{\mathrm{d}P}{\mathrm{d}X_{i\mathrm{A}}}\right)_{T,\mathrm{a}} = \frac{\left(\frac{\partial^2 G_{\mathrm{A}}}{\partial X_{i\mathrm{A}}^2}\right) \underset{1}{\Delta} X_i}{X_{i\mathrm{B}} \underset{1}{\Delta} V_i + X_{j\mathrm{B}} \underset{1}{\Delta} V_j},$$

$$\left(\frac{\mathrm{d}P}{\mathrm{d}T}\right)_{X_{i\mathrm{A}},\mathrm{a}} = \frac{\underset{1}{\Delta} S - \left(\frac{\partial S_{\mathrm{A}}}{\partial X_{i\mathrm{A}}}\right) \underset{1}{\Delta} X_i}{\underset{1}{\Delta} V - \left(\frac{\partial V_{\mathrm{A}}}{\partial X_{i\mathrm{A}}}\right) \underset{1}{\Delta} X_i},$$

with T = temperature, P = pressure, X_i = the molar fraction of the i^{th} component, G = the molar Gibbs function, $\underset{1}{\Delta}$ = the difference between two quantities in the two phases in equilibrium, H_i = the partial molar enthalpy of the i^{th} component, V_i = the partial molar volume of the i^{th} component, S = the molar entropy.
The subscripts A and B denote the two phases in equilibrium, a and b denote the border lines of the two phases respectively.

It follows that when $\underset{1}{\Delta} X_i = 0$ the slope of the melting lines in the TX- and in the PX- diagram are zero. Hence the melting curves and the freezing curves are tangent to each other in the azeotropic point. In the PT diagram the solidus and liquidus are also tangent but here they need not be horizontal.

If the mixture is azeotropic, solidification takes place at constant pressure and temperature if the heat of melting is extracted and the volume change compensated. Such is the case in figure 11*a*. Azeotropic points have been found by measurements of the melting lines for 8.9%, 22.8% and 35.1% mixtures. Mixtures of higher concentrations which we used in our experiments

do not show azeotropy, because here phase stratification of the fluid occurs before the solidus and the liquidus touch.

The minima of the freezing pressures. In the diagrams at constant pressure the minima of the freezing pressure of some mixture correspond to the point where

$$(\partial T/\partial X_{\mathrm{fl}})_P = \infty,$$

except for the special point where both

$$(\partial P_{\mathrm{fr}}/\partial X)_T = 0 \quad \text{and} \quad (\partial P_{\mathrm{fr}}/\partial T)_X = 0.$$

At this point, being the absolute minimum of the freezing surface, (if this exists in this form) $(\partial T/\partial X_{\mathrm{fl}})_P$ is completely undetermined as here it is both zero (the azeotropic point) and infinite (one solid point). As it is likely from the known data that the absolute minimum of the freezing surface occurs at a common point of the freezing surface and the phase stratification surface of the fluid, both conditions have not necessarily to be fulfilled, at the absolute minimum. In that case the line connecting the azeotropic points finishes at the stratification curve at the absolute minimum.

2. *The phase diagram.* Several authors have proposed a phase diagram of the mixtures of the helium isotopes. See table I. The present one differs from all foregoing in some major and several minor aspects. As the phase diagram is very complicated we have not tried to project the three dimensional PTX diagram onto a plane surface. Instead we drew a series of TX diagrams at constant pressure and present them as a strip together with the discussion. In the various researches mixtures of different composition were used. The results of the different groups can therefore be compared in TX diagrams. As can be seen no large differences exist between the various results. The discrepancy between our earlier measurements and those of others, as mentioned by Zinov'eva[6]) does not exist, if the differences, between the various pressure units are taken into account*). The plotted data are taken from the smoothed lines through the direct measured values.

The phase review strip. In the figures we used the following symbols:

○ freezing points by Le Pair *e.a.*; this paper

● melting points by Le Pair *e.a.*; this paper

◑ lambda points by Le Pair *e.a.*; this paper

◒ three phase equilibria by Le Pair *e.a.*; this paper

△ freezing points by Lee, Weinstock, Tedrow and Lipschultz[13])[14])[15])

---

*) See part A: Temperature measurements and units.

▲ three phase equilibria, idem[16)17)]

▽ freezing points by Zinov'eva[6)]

▽ phase stratification in the fluid, idem[6)]

□ freezing points by Berezniak, Bogoyavlenskii and Esel'son[19)20)]

■ melting points by Bogoyavlenskii *e.a.*[20)]

◪ triple points, idem[20)]

× freezing points by Esel'son[8)]

◊ phase stratification in the solid by Edwards, McWilliams and Daunt[2)]

✦ melting point, idem[2)]

⊕ freezing points by Vignos and Fairbank[7)]

◕ polymorph phase transition in the solid by Vignos and Fairbank[7)]

◇ freezing points by Grilly and Mills[44)39)65)]

◈ polymorph phase transition by Grilly and Mills[44)65)]

✳ extrapolated lower melting points of ^{3}He[46)]

> temperature of the ^{4}He melting pressure minimum by Wiebes and Kramers[66)].

Figure 17. At 150 atm one freezing point of mixtures is known from Esel'son; it is situated on a straight line between the freezing points of the pure components. This should be expected according to the relatively small differences between the isotopes at high pressures. Nothing is known about the width of the solid-fluid inhomogeneous region. It should be small however according to the same argument and according to extrapolations

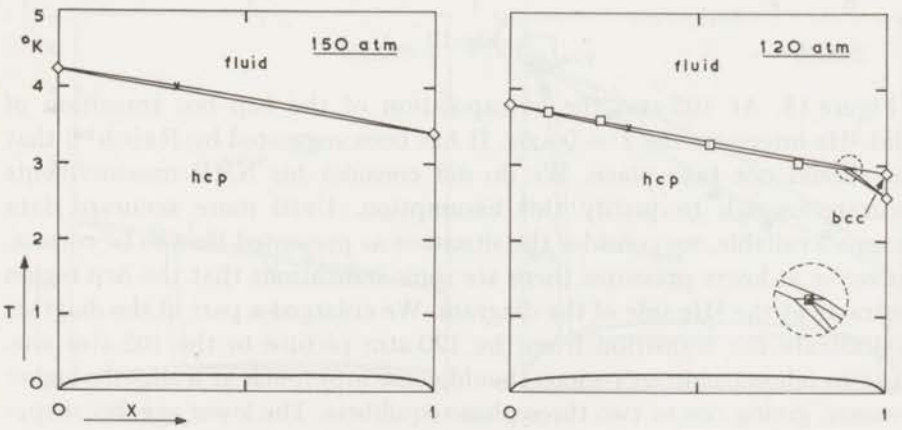

Fig. 17

from known lower pressure regions. It is known from X-ray diffraction[60)67)68)69)] that the pure solids have a hexagonal close-packed structure. A difference between the molar volumes and the internal energies of the isotopes exists. As this difference is basic in our considerations on lattice distortion and heat of mixing, we must suppose that phase separation of the solid occurs. However, in this pressure range it takes place at lower temperatures than measured by Edwards e.a. At 120 atm more information is available. Berezniak's data convince one of the correctness of the linear interpolation between ^{3}He and ^{4}He. The polymorph phase transition between bcc and hcp crystals complicates the picture. The triple point of ^{3}He is at 136.1 atm[44)]. Consequently at 120 atm a bcc region exists. Berezniak concludes from his experiments and those of Vignos and Fairbank[7)] that an almost linear projection on the PT plane of the line connecting the upper triple points of bcc–hcp-fluid exists. From this the position of the three phase equilibrium at 120 atm can be estimated to occur at $X \approx 0.9$. Probably the phase separation of the solid has a higher critical temperature than at 150 atm.

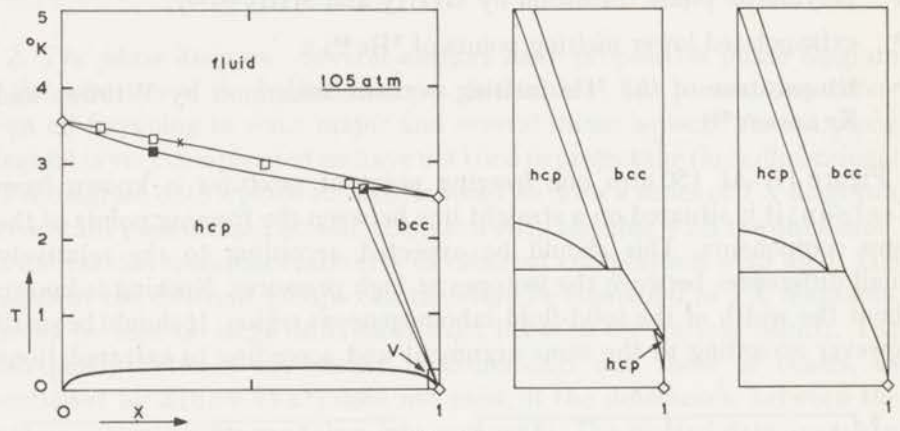

Fig. 18

Figure 18. At 105 atm the extrapolation of the hcp–bcc transition of solid ^{3}He intersects the $T = 0$ axis. It has been suggested by Reich[64)] that this should not take place. We do not consider his NMR measurements accurate enough to justify this assumption. Until more accurate data become available, we consider the situation as presented here to be correct. Moreover at lower pressures there are some indications that the hcp region contracts at the ^{4}He side of the diagram. We enlarged a part of the diagram to illustrate the transition from the 120 atm picture to the 105 atm one. The two inhomogeneous regions should come into touch at a slightly higher pressure, giving rise to two three phase equilibria. The lower one, bcc–hcp$_1$–hcp$_2$ vanishes. At this pressure one melting point has been measured by

Berezniak, providing some reality for the width of the drawn inhomogeneous region between fluid and solid.

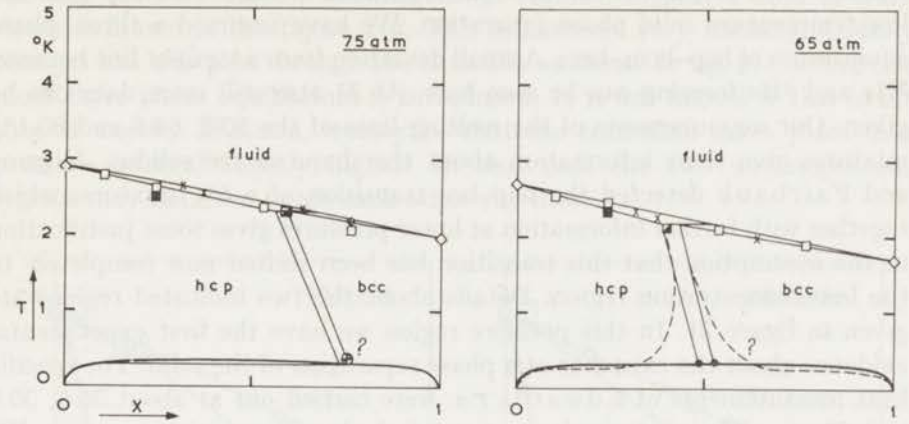

Fig. 19

Figure 19. At 75 atm more freezing points have been measured. Uncertainty arises as to the shape of the hcp–bcc transition. The sound velocity measurements of Vignos and Fairbank can be extrapolated to lower temperatures, giving a point of the transition at about 0.4°K. Hence some evidence about the transition at lower temperatures exists. Nevertheless a switch over to the ^{4}He side of the diagram is likely to behave as is drawn with a dashed line at 65 atm. If the evaluation were as has been drawn with solid lines, we should have the situation of a 4-phase equilibrium point on the top of the phase separation curve: hcp_1–hcp_2–bcc_1–bcc_2 which would be very peculiar. A behaviour as indicated by the dashed lines is therefore more likely, but as we have no data to confirm the correctness of this picture, we must leave the answer to this question open.

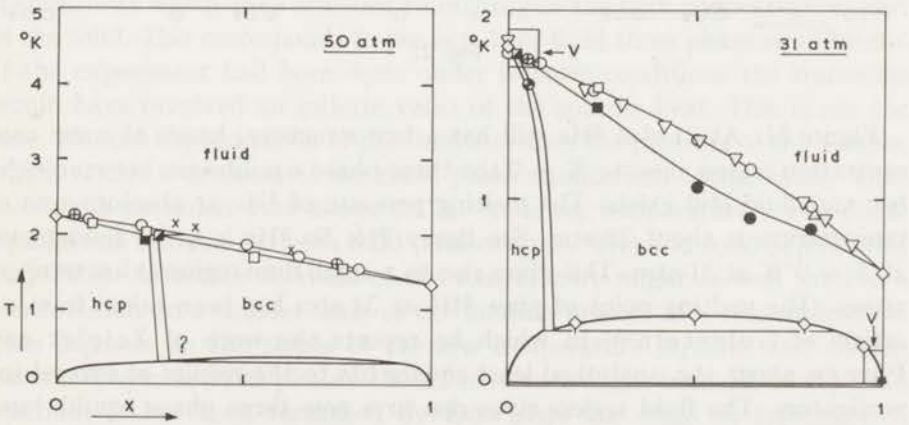

Fig. 20

Figure 20. At 50 atm. extrapolations from our freezing lines can be plotted They are in good agreement with the existing data. The same uncertainty remains with respect to the hcp–bcc transition at its connection with the low temperature solid phase separation. We have assumed a three -phase equilibrium of hcp–bcc_1–bcc_2. A small deviation from a straight line between ^{3}He and ^{4}He freezing can be seen here. At 31 atm still more data can be given. Our measurements of the melting lines of the 50.5, 64.5 and 80.1% mixtures give some information about the shape of the solidus. Vignos and Fairbank detected the hcp–bcc transition of a 5% mixture, which together with further information at lower pressures gives some justification to the assumption that this transition has been shifted now completely to the low concentration region. Details about the two indicated regions are given in figure 21. In this pressure region we have the first experimental evidence about the existence of a phase separation of the solid. The specific heat measurements of Edwards *e.a.* were carried out at about 35.8, 30.0 and 27 atm. They indicated a symmetrical phase separation to occur. We shall return to this experiment in connection with figure 22.

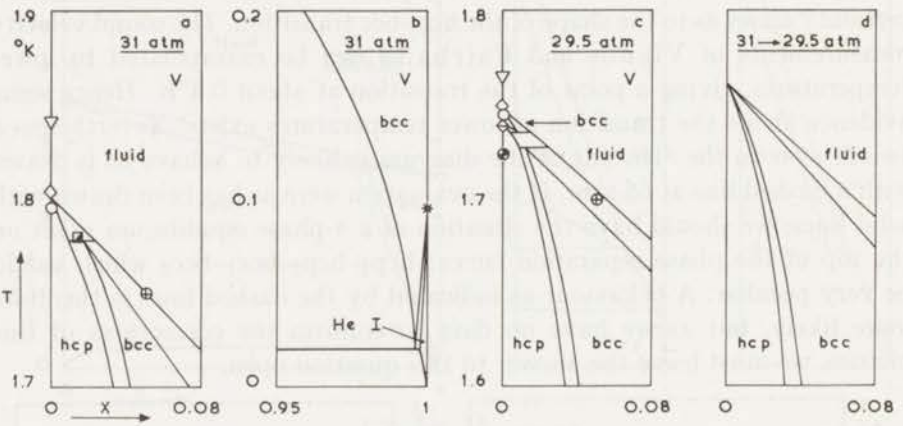

Fig. 21

Figure 21. At 31 atm ^{4}He still has a hcp structure; hence at some concentration region close to $X = 0$ the three phase equilibrium between hcp–bcc and fluid still exists. The melting pressure of ^{3}He at absolute zero of temperature is about 33 atm. See figure 21*b*. So ^{3}He is in its fluid phase at $T = 0$°K at 31 atm. This gives rise to a small fluid region at low temperatures. The melting point of pure ^{3}He at 31 atm has been taken from an article of Goldstein[46]) in which he reports the work of Zeigler and Perego about the analytical least square fits to the results of several investigators. The fluid region gives rise to a new three phase equilibrium, where hcp–bcc_2 and fluid exist at the same time. At 29.5 atm ^{4}He is known

to have a bcc solid structure between 1.7 and 1.8°K. The transition from a diagram as given before (fig. 21*a*) to this one is not known. The measurement, showing the very narrow inhomogeneous regions, suggest a kind of transition as drawn in the figure 21*d*. This is however very unlikely. Usually changes like this pass through the situation as shown in fig. 21*c*, where one more three phase equilibrium is introduced. It is not known if this is the case at exactly 29.5 atm, it may be that the transition takes place in a pressure interval slightly higher. In that case the two inhomogeneous regions may not even touch each other any more.

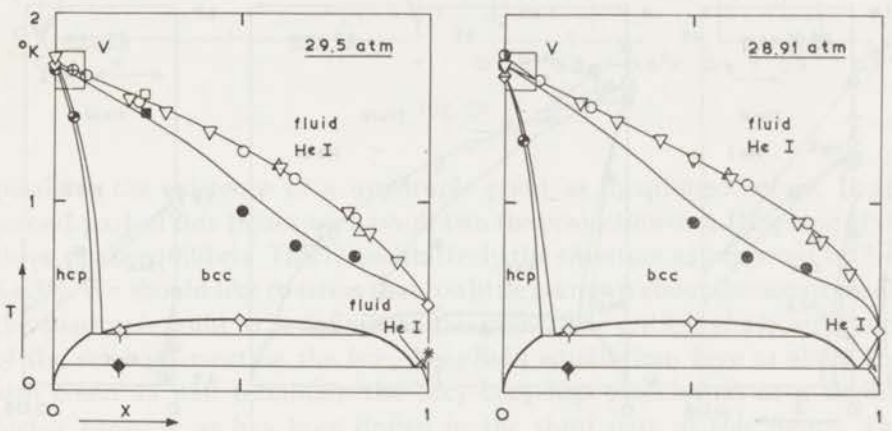

Fig. 22

Figure 22. A part of the diagram at 29.5 atm has been discussed already in connection with the details in figure 21. We should like to draw attention now to the three phase equilibrium at about 0.14°K. When cooling a 17.6% mixture at about 30 atm Edwards *e.a.* observed an increase of the specific heat which they ascribed to melting of the high concentration part of the solid. This corresponds to the hcp–bcc_2-fluid three phase equilibrium. If the experiment had been done under isobaric conditions the transition would have involved an infinite value of the specific heat. This is not the case. Instead the formation of the fluid increases the pressure of the sample, which causes a decrease of the three phase equilibrium temperature. Thus melting is extended over about 0.1°K. At lower temperature a two-phase equilibrium remains between fluid (alsmost pure ^{3}He) and solid hcp (almost pure ^{4}He). A further decrease of the temperature might as well involve a continuation on a smaller scale of the melting process as a resolidification. This depends on the slopes of the low temperature liquidus and solidus curves. A symmetrical picture should involve a slight increase of the fluid fraction. It has been remarked by Edwards *e.a.* that no indication is found about the hcp–bcc_1–bcc_2 three phase equilibrium. According to

Grilly and Mills the hcp–bcc transition of pure ^{4}He involves about $\Delta S = 0.12$ Joule mol^{-1} °K^{-1}, which implies a contribution to the internal energy at 0.1°K of about 0.012 Joule mol^{-1}. As this is about 4% of the measured value of the specific heat here, one can imagine that this small contribution over a limited temperature interval could not be seen. At 28.91 atm, where ^{3}He has its minimum melting pressure, the two fluid regions come into touch. The solidus and the liquidus according to Lifshitz and Sanikidze are tangent to each other and to the $X = 1$ axis. At low ^{3}He concentration a detail of the picture is given in the next figure.

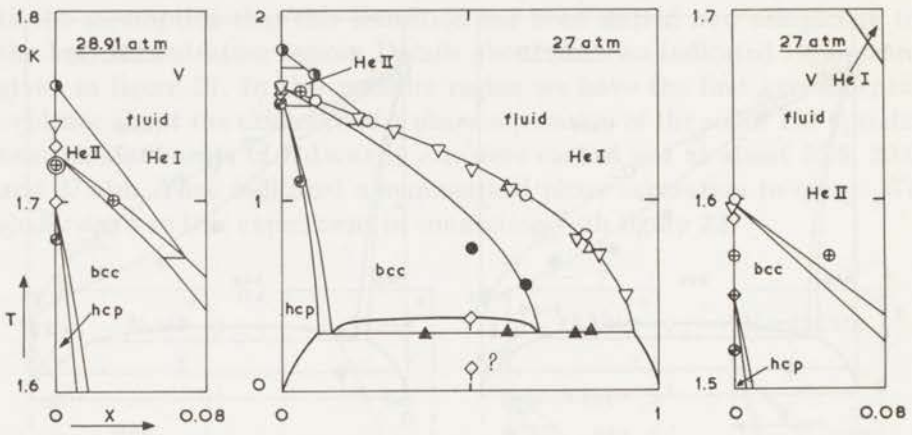

Fig. 23

Figure 23. At 28.91 atm the λ-transition separates the fluid phase into two parts as is drawn here. The first order transition lines should show an abrupt change of slope at the point of intersection. The bcc region now extends uninterrupted until the $X = 0$ axis.

At 27 atm the situation in this region does not change qualitatively. The three phase equilibrium hcp–bcc$_2$-fluid here is shifted to a higher temperature and coincides with the hcp–bcc$_1$–bcc$_2$ equilibrium, thus giving rise to a quadruple point. The existence of this point however is not absolutely certain. Edwards reports a point of the phase separation curve of the solid at 0.12°K, which is in disagreement with the diagram. As the pressure measurement in the specific heat experiment is not reliable, this could be the cause of this discrepancy. We were not able to detect a melting point of the 80.1% mixture, which indicates that the shape of the solidus of the bcc-fluid equilibrium is about as pictured here.

Figure 24. At still lower pressures (26.5 atm) the width of the solid-fluid equilibrium increases further. The 64.5% mixture probably does not exist as a homogeneous bcc solid any more. The three phase equilibria have changed now to bcc$_1$–bcc$_2$-fluid and hcp–bcc$_1$-fluid respectively. The situation corres-

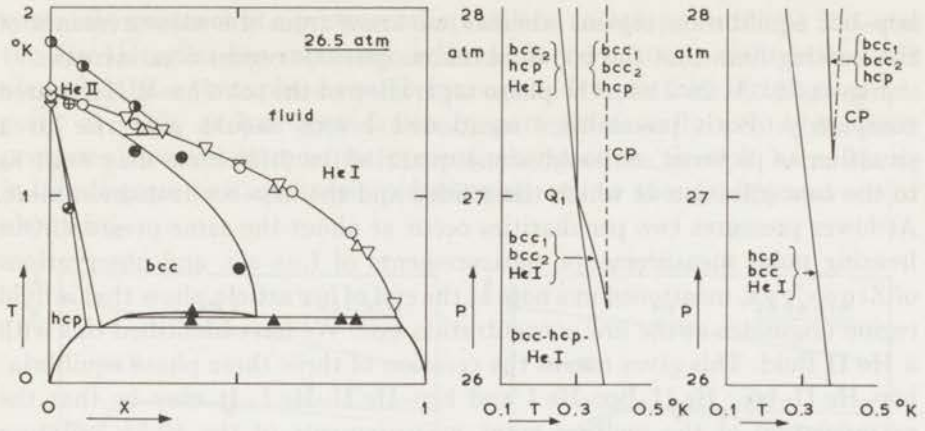

Fig. 24

ponds to the existence of a quadruple point as mentioned before. In the second part of this figure we have drawn the projection on a PT-plane of the three phase equilibria. This is qualitatively the situation as supposed by Lee *e.a.*[16]). We should like to stress that too little is known about the occurrence of the quadruple point to be definite on this point. The critical phase separation of the solid intersecting the bcc_1–bcc_2-fluid equilibrium here at about 26.4 atm could as well terminate the bcc_1–bcc_2–hcp equilibrium at a slightly higher pressure as has been drawn in the third part of this figure. This should cause the hcp–bcc inhomogeneous region to grow at low temperatures to meet the solidus before a quadruple point appears. The accuracy of the data now available is too small to make a definite choice between these two possibilities. The only reason why we have drawn the diagrams as has been done is that we do not know anything about the necessary increase of the

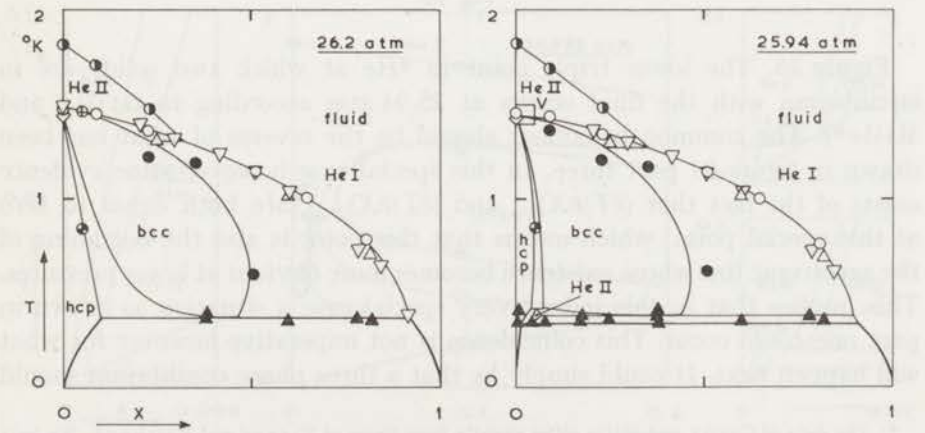

Fig. 25

hcp–bcc equilibrium region, whereas we know from the measurements of the melting lines that the bcc-fluid inhomogeneous region does increase.

Figure 25. At 26.2 atm the phase separation of the solid has dissappeared completely. Both possibilities mentioned before should give rise to a situation as pictured, although some quantitative differences may exist as to the concentration at which the solidus and the hcp–bcc transition meet. At lower pressures two peculiarities occur at about the same pressure. Our freezing point measurements, measurements of Lee *e.a.* and observations of Zinov'eva, mentioned in a note at the end of her article, show that a fluid region originates at the low concentration side. We have identified this with a He II fluid. This gives rise to the creation of three three phase equilibria: hcp–He II–bcc; He II–bcc–He I and hcp–He II–He I. It may be that the extrapolation of the melting point measurements of the 50.5% mixture cannot be justified. Therefore we did not pay too much attention to this extrapolation.

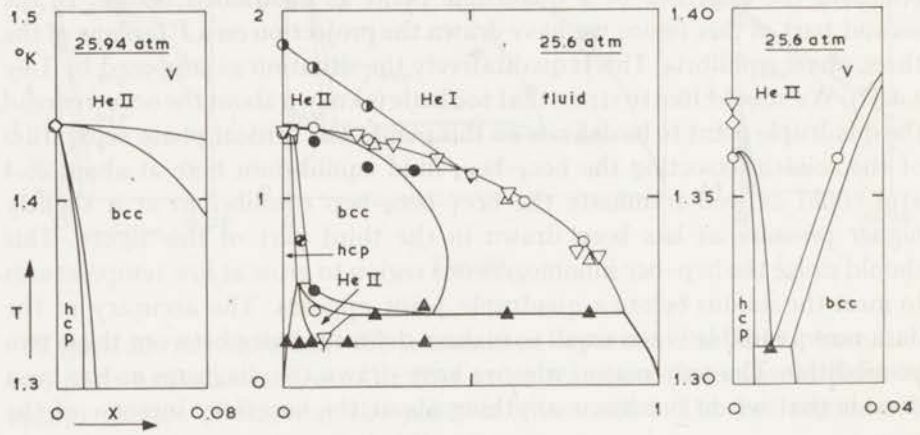

Fig. 26

Figure 26. The lower triple point in ^{4}He at which two solids are in equilibrium with the fluid occurs at 25.94 atm according to Grilly and Mills*). The common behaviour should be the reverse of what has been drawn in figure 21 part three. In this special case however some evidence exists of the fact that $(\partial T/\partial X)_{P_{tr}}$ and $)\partial T/\partial X)_{P_{melt}}$ are both equal to zero at this special point, which means that this point is also the beginning of the azeotropic line whose existence becomes more obvious at lower pressures. This implies that in this indeed very special case a situation as drawn in part one could occur. This coincidence is not imperative however for what will happen next. It could simply be that a three phase equilibrium should

*) The data of Grilly and Mills differ slightly from those of Vignos and Fairbank. We took the data of Grilly and Mills because of the particular care they paid to the pressure measurements.

come into existence at a pressure where still no azeotropy exists. At 25.6 atm the He II region has increased, whereas at very low concentrations and about 1.31°K a three phase equilibrium exists. It is not sure if the azeotropic point at 0.2% as has been drawn in part three really exists. At lower pressures however it must be present, therefore we drew it here. Hence in this diagram two azeotropic points exist: one at about 0.2% and one at about 5%.

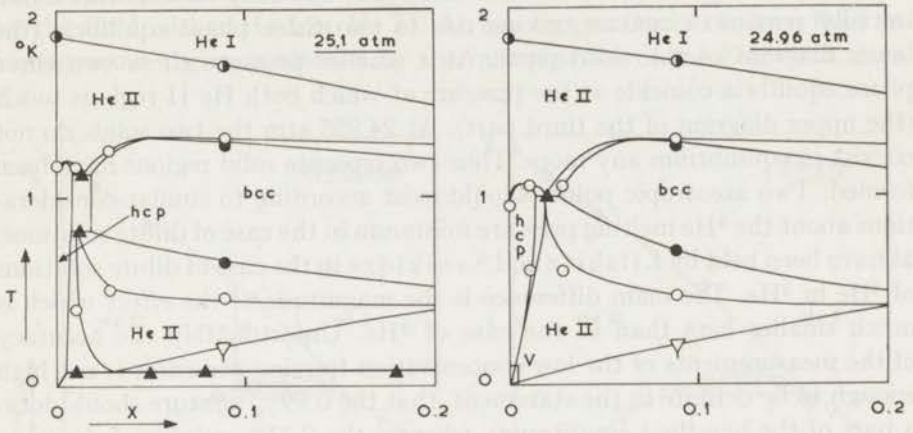

Fig. 27

Figure 27. At 25.1 atm we give only a part of the *TX* diagram showing the increase of the He II region and the decrease of the temperature region at which the two solid configurations exist in equilibrium. At 24.96 atm the two three phase equilibria between hcp–He II and bcc coincide. This pressure value is taken to be the melting pressure of pure ^{4}He at absolute zero of temperature. A detail of this diagram is given in the next picture.

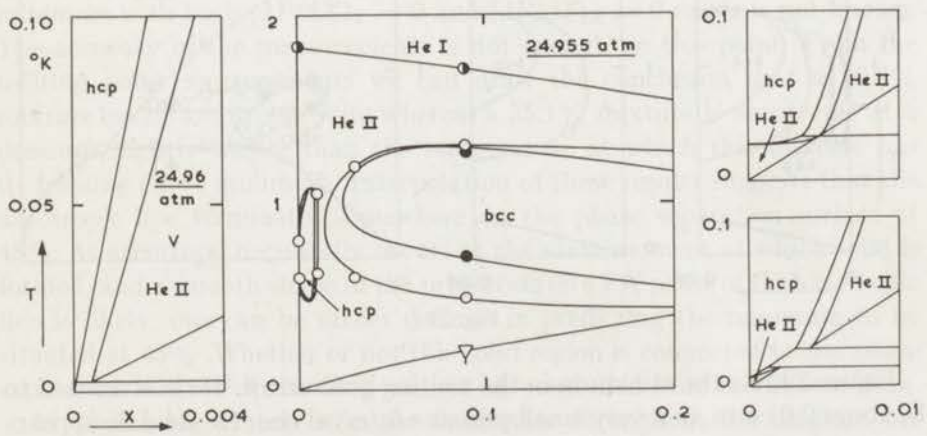

Fig. 28

Figure 28. As ^{4}He is known to have a minimum in its melting pressure also [70) 66) 71) 72)] there is some pressure which we assumed to be 24.96 atm at which ^{4}He is still completely in the solid phase at low temperatures. At a pressure $P < 24.96$ atm this is not the case. In part two the probable situation at 24.955 atm is shown. This situation results from a transition as has been drawn in the last two parts of the figure. A He II region comes into existence at low temperatures. The two inhomogeneous regions, between He II and hcp on one hand and He II and He I on the other hand, initially remain in contact, giving rise to two three phase equilibria (the lower diagram of the third part). At a smaller pressure these two three phase equilibria coincide at the pressure at which both He II regions touch (the upper diagram of the third part). At 24.955 atm the two solids do not coexist in equilibrium any more. Thus two separate solid regions have been formed. Two azeotropic points should exist according to similar considerations about the ^{4}He melting pressure minimum in the case of dilute solutions, as have been held by Lifshitz and Sanikidze in the case of dilute solutions of ^{4}He in ^{3}He. The main difference is the magnitude of the effect which is much smaller here than in the case of ^{3}He. Unfortunately the accuracy of the measurements of the low concentration freezing pressures is not high enough to be definite in the statement, that the 0.99% mixture should form a part of the hcp-fluid equilibrium, whereas the 2.77% mixture belongs to the bcc-fluid equilibrium. The uncertainty is such, that it could be, that considering the maximal error, also the 0.99% mixture could belong to the bcc-fluid equilibrium. Nevertheless a region as pictured in part two should exist, although possibly at lower concentrations.

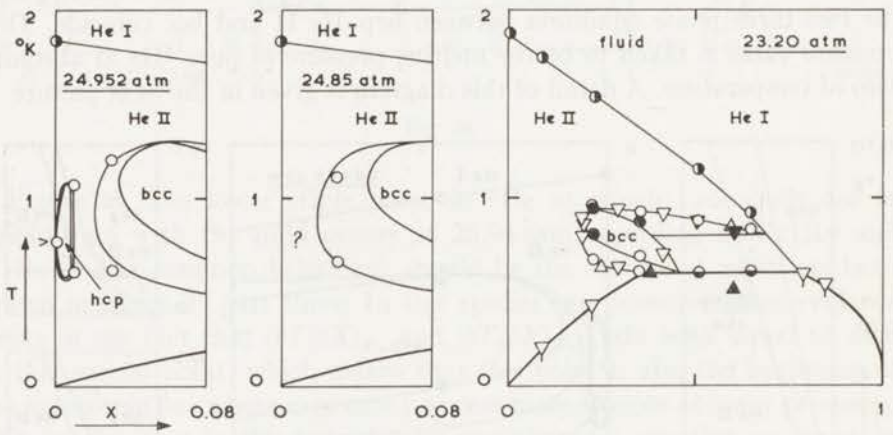

Fig. 29

Figure 29. As the minimum in the melting pressure of ^{4}He is estimated to be about 0.01 atm, in a very small pressure interval the ^{4}He solid disappears completely. The accuracy does not permit us to conclude in which way the

hcp region will disappear. As we have pictured here, the hcp region might even become a free region not connected to the $X = 0$ axis. This is the more general case. It might be however that the region would contract at $T = 0.76°K$ being the temperature at which the minimum of the melting curve of pure ^4He occurs.

At 24.85 atm the hcp region has disappeared completely and only a bcc solid continues to exist. At 23.20 atm a complete TX diagram is given with the well known fluid-solid equilibrium as a closed region surrounded by the fluid, either He I or He II. At low temperatures the two fluid inhomogeneous region is marked by the interpolation of the Zinov'eva data.

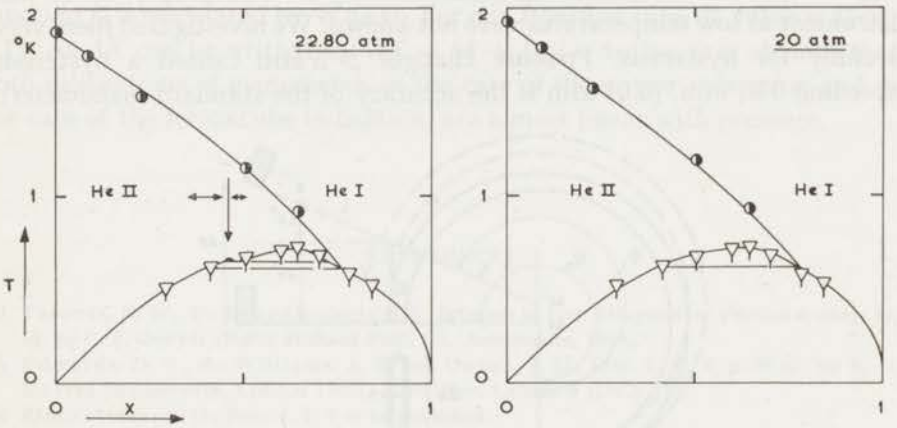

Fig. 30

Figure 30. At 22.80 atm the freezing surface of these mixtures will probably have its absolute minimum. Whether or not a kind of absolute minimum with both $(dP/dX)_T = 0$ and $(dP/dT)_X = 0$ exists is not known. The accuracy of the measurements is not enough on this point. From the melting point measurements we can draw the conclusion that a 50.5% mixture has no azeotropic point whereas a 35.1% mixture is azeotropic at a pressure slightly higher than the temperature at which this mixture has its freezing curve minimum. Interpolation of these results suggests that the azeotropic line terminates somewhere on the phase separation surface at 45%. As azeotropy necessarily occurs at the same moment at which solid is formed, and a smooth shape of the projection on a TX plane of the azeotropic line is likely, one can be rather definite in predicting the minimum to be situated at 45% .Whether or not this solid region is connected to the phase separation surface of the fluid cannot be concluded from the known data.

At 20 atm the system is in the fluid state throughout the diagram. At lower pressures the diagram does not change qualitatively any more.

In conclusion we may remark that the most simple substance demonstrates a most complex phase diagram. We believe that several characteristics in the diagram, for instance the closed solid regions, are unique. Some parts of the diagram are somewhat dubious. To clarify these points would require a very accurate and difficult research. Apart from those details we may say that the phase diagram of helium is known in this pressure range.

APPENDIX

The Bourdon tube. We used a tube, made of about 56% Cu, 26% Ni, 18% Zn*), taken from a commercial manometer. The properties of this instrument at low temperatures were not known. We investigated them very carefully for hysteresis. Pressure changes > 5 atm caused a hysteresis exceeding 0.01 atm. (0.01 atm is the accuracy of the standard manometer).

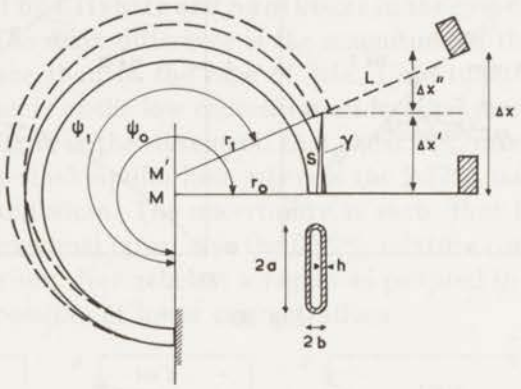

Fig. 31. The Bourdon tube. Fat lines indicate the state at zero pressure, fat dashed lines, at higher pressures.

With smaller changes we could not find any in the pressure range $0 < P < 30$ atm. At room temperature the tube is designed for pressures below 30 atm. The tube does not recover completely, when this limit is exceeded. At helium temperatures, the limiting value is about 50 atm. The applied tube, see figure 31, is flat-oval, with thin walls. We suppose that the deformations are elastic. Except for the final points of the tube, deformations, tensions and curvatures will be uniform. The length of the core does not change due to the relatively small pressures, which are involved. So $r_0\psi_0 = r_1\psi_1$ and $\Delta r/r_0 = -\Delta\psi/\psi_0$ ($\Delta r = r_1 - r_0$, $\Delta\psi = \psi_1 - \psi_0$). In the experiment with the mirror only the angle ψ is of interest. With the ferroxcube the displacement ΔX is of interest. $\Delta X = \Delta X' + \Delta X'' = S\cos\gamma + L(-\Delta\psi)$.

*) We are indebted to Mr. L. v. d. Meer, at the "Laboratorium voor Metaalkunde" at the Technological University of Delft, for the analysis.

Because $\gamma \approx 0$, $\Delta X \approx S + L \cdot (-\Delta\psi)$. Wuest[75]) calculated the properties of a Bourdon tube of this type and compared his results with experiment, finding very good agreement. He derived:

$$S = \sqrt{[1 + (2/\psi_0^2)(1 - \psi_0 \sin \psi_0 - \cos \psi_0)]}\, \psi_0 r_0\, (-\Delta\psi/\psi_0).$$

In our apparatus $\psi_0 \approx \frac{3}{2}\pi$; $r_0 = 17$ mm; $L \approx 50$ mm. The relative change of ψ can be expressed in terms of the geometric parameters of the tube, the Poisson's ratio, μ and the Young's modulus E

$$-\Delta\psi/\psi_0 = (1 - \mu^2)\, f_3(\alpha, \lambda)\, a^4 P/bh^3 E,$$

with P is the pressure; a, b and h see figure 31; $\alpha = b/a$ and $\lambda = a^2/hr_0$. The function f_3 is calculated by Wuest. For our Bourdon tube its value is about 0.11. As ΔX can be written as: $\Delta X = (A + L_0)(-\Delta\psi)/\psi_0$, it is obvious that both calibrations of manometer, in the case of the mirror indication and in the case of the ferroxcube indication, are almost linear with pressure.

REFERENCES

1) Taconis, K. W., De Bruyn Ouboter, R., Progress in Low Temperature Physics 4, chap. II, ed. by C. J. Gorter (North Holland Publ. Co., Amsterdam, 1964).
2) Edwards, D. O., Mc Williams, A. S. and Daunt, J. G., Proc. L. T. 8, p. 39 ed. by R. O. Davies (Butherwoth, London 1963), Phys. Rev. Letters **9** (1962) 195.
3) Zimmerman, G. O., Proc. L.T. 9 to be published.
4) Klemens, P. G., De Bruyn Ouboter, R. and Le Pair, C., Proc. L.T. 9 to be published; Commun. Kamerlingh Onnes Lab., Leiden, Suppl. No. 122*c*; Physica **30** (1964) 1863.
5) Klemens, P. G. and Maradudin, A. A., Phys. Rev. **123** (1961) 804.
6) Zinov'eva, K., N. Zh. eksper. teor. Fiz. **44** (1963) 1837; Soviet Physics-JETP (New York) **17** (1963) 1235.
7) Vignos, J. H. and Fairbank, H. A., Proc. L.T. 8, p. 31 ibid.
8) Esel'son, B. N. and Lazarev, B. G., D.A.N. SSSR **97** (1954) 61.
9) Le Pair, C., Taconis, K. W., De Bruyn Ouboter, R. and Das, P., Physica **28** (1962) 305.
10) Le Pair, C., Taconis, K. W., De Bruyn Ouboter, R. and Das, P., Proc. L.T. 8, p. 37 ibid.
11) Le Pair, C., Taconis, K. W., Das, P. and De Bruyn Ouboter, R., Cryogenics **3** (1963) 112.
12) Le Pair, C., Taconis, K. W., De Bruyn Ouboter, R., De Jong, E. and Pit, J., Proc. L.T. 9 to be published.
13) Weinstock, H., Lipschutz, F. P., Kellers, C. F., Tedrow, P. M. and Lee, D. M., Phys. Rev. Letters **9** (1962) 193; Proc. L.T. 8 p. 41 ibid.
14) Lee, D. M., Lipschultz, F. P. and Tedrow, P. M., Private communication 1962, following comm. Thanksgiving meeting, Am. Phys. Soc., 1962.
15) Tedrow, P. M. and Lee, D. M., Phys. Lett. **9** (1964) 130.
16) Tedrow, P. M. and Lee, D. M., Proc. L. T. 9 to be publishcd.
17) Lipschultz, F. P., Tedrow, P.M., and Lee, D. M., Proc. L. T. 9 to be published.
18) Berezniak, N. G., Bogoyavlenskii, I. V. and Esel'son, B. N.,Zh. eksper. teor. Fiz. **43** (1962) 1981; Soviet Physics-JETP (New York) **16** (1963) 1394.
19) Berezniak, N. G., Bogoyavlenskii, I. V. and Esel'son, B. N., Zh. eksper. teor. Fiz. **45** (1963) 486; Soviet Physics-JETP (New York) **18** (1964) 335.
20) Bogoyavlenskii, I. V., Berezniak, N. G. and Esel'son, B. N., Zh. eksper. teor. Fiz. **47** (1964) 480.

21) Lifshitz, J. M. and Sanikidze, D. G., Zh. eksper. teor. Fiz. **35** (1958) 1020; Soviet Physics-JETP (New York) **8** (1959) 713.
22) Zimmerman, G. O., Proc. L.T. 9 to be published.
23) Walker, E. J. and Fairbank, H. A., Phys. Rev. **118** (1960) 913.
24) Sheard, F. W. and Ziman, J. M., Phys. Rev. Letters **5** (1960) 138.
25) Callaway, J., Phys. Rev. **122** (1961) 787.
26) Bertman, B., White, C. W. and Fairbank, H. A., Proc. L.T. 9 to be published.
27) Berman, R. and Rogers, S. J., Proc. L.T. 9 to be published.
28) Garwin, R. L. and Reich, H. A., Phys. Rev. **115** (1959) 1478.
29) Lebowitz, J. L. and Rowlinson, J. S., J. chem. Phys. **41** (1964) 133.
30) Kerr, E. C., Proc. L.T. 5, p. 158, ed. J. R. Dillinger (Univ. of Wisconsin Press, Madison, 1958).
31) Kerr, E. C., Phys. Rev. Letters **12** (1964) 185.
32) De Bruyn Ouboter, R., Taconis, K. W., Le Pair, C. and Beenakker, J. J. M., Commun. Leiden No. 324*b*; Physica **26** (1960) 853.
De Bruyn Ouboter, R., Thesis, Leiden (1961).
De Bruyn Ouboter, R. and Beenakker, J. J. M., Commun. Leiden, Suppl. No. 119*a*; Physica **27** (1961) 219.
33) Roberts, T. R. and Sydoriak, S. G., Phys. Rev. **93** (1954) 1418.
34) Rosa, E. B. and Grover, F. W., Bull. Bur. Stand. **1** (1904/1905) 291.
35) Hague, B., Alternating current bridge methods 5th ed. pp. 379–386 (Sir Isaac Pitman and Sons Ltd., London, 1946).
36) Van Dijk, H., Techniques of magnetic thermometry, Commun. Leiden Suppl., No. 112*c*; Temperature, its measurement and control in science and industry II p. 199 (Reinhold Publ. Corp., New York,1955).
37) Clement, J. R. and Quinnell, E. H., Rev. sci. Inst. **23** (1952) 213.
38) Kamerlingh Onnes, H. and Van Gulik, W., Commun. Leiden, No. 184*d*; Proc. roy. Acad. Amsterdam **29** (1926) 1184.
39) Grilly, E. R., Sydoriak, S. G. and Mills, R. L., 2d Symposium on ^{3}He, ed. by J. G. Daunt (Ohio State University Press, Columbus, 1960) p. 121.
40) Baum, J. L., Brewer, D. F., Daunt, J. G. and Edwards, D. O., Phys. Rev. Letters **3** (1959) 127.
41) Vignos, J. H. and Fairbank, H. A., Phys. Rev. Letters **6** (1961) 265, **6** (1961) 646 (erratum).
42) Weinstock, B., Abraham, B. M. and Osborne, D. W., Phys. Rev. **85** (1952) 158.
43) Roberts, T. R. and Sydoriak, S. G., Proc. L.T. **5**, p. 170, ibid; Phys. Rev. **118** (1960) 901.
44) Grilly, E. R. and Mills, R. L., Ann. Phys. (New York) **8** (1959) 1.
45) Mills, R. L., Grilly, E. R. and Sydoriak, S. G., Ann. Phys. (New York) **12** (1961) 41.
46) Goldstein, L., Phys. Rev. **133** (1964) A 52.
47) Keesom, W. H., Commun. Leiden, Suppl. No. 33 (1913); Versl. kon. Acad. Wet. (1913) 701.
48) De Bruyn Ouboter, R. and Beenakker, J. J. M., Commun. Leiden, Suppl. No. 120*a*; Physica **27** (1961) 1074.
49) Uhlenbeck, G. E., Selected topics in statistical mechanics, Statistical Physics 3 chap I. Brandeis Summer Inst. 1962; Benjamin Inc. ,New York, Amsterdam, 1963).
50) Fairbank, H. A. and Elliot, S. D., Physica **24** (1958) p. S 134.
51) Keesom, W. H., Helium, chap. III (Elsevier, Amsterdam, (1942).
52) Lounasmaa, O. V. and Kojo, E., Ann. Acad Sci. Fennicae Ser A VI **36** (1959).
53) Lounasmaa, O. V. and Kaunisto, L., Ann. Acad. Sci. Fennicae Ser. A VI **59** (1960); Proc. L.T. 7 p. 535 ed. G. M. Graham and A. C. Hollis Hallet (University of Toronto Press, North Holland Publ. Cy. Amsterdam, 1961).
54) Lounasmaa, O. V., Phys. Rev. **130** (1963) 847.
55) Lounasmaa, O. V., J. chem. Phys. **33** (1960) 443.
56) Atkins, K. R. and Edwards, M. H., Phys. Rev. **97** (1955) 1429.
57) Buckingham, M. J. and Fairbank, W. M., Progress in low temperature physics, Vol. 3, chap. III, ed. C. J. Gorter (North Holland Publ. Co., Amsterdam, 1961).
58) Goldstein, L., Phys. Rev. **135** (1964) A 1471.
59) Van Arkel, A. E., Moleculen en kristallen (Van Stockum en Zn., Den Haag, 1961, 65–66).

60) Keesom, W. H., and Taconis, K. W., Physica **4** (1937) 256. Commun. Leiden No. 252*c* and 250*e*; Physica **5** (1938) 161 and 270.
Taconis, K. W., Thesis, Leiden (1938).
61) Reekie, J., Hutchinson, T. S. and Beaumont, C. F. A., Proc. phys. Soc. A **66**(1953) 409; Proc. roy. Soc. A **228** (1955) 363.
62) Hurst, D. G. and Henshaw, D. G., Phys. Rev. **100** (1955) 994; Canad. J. Phys. **33** (1955) 797.
63) Yntema, J. L. and Schneider, W. G., J. chem. Phys. **18** (1950) 641 and 646.
64) Reich, H. A., Phys. Rev. **129** (1963) 630.
65) Grilly, E. R. and Mills, R. L., Ann. Phys. (New York) **18** (1962) 250.
66) Wiebes, J. and Kramers, H. C., Phys. Letters **4** (1963) 298.
67) Schuch, A. F., Crilly, E. R. and Mills, R. L., Phys. Rev. **110** (1958) 775.
68) Schuch, A. F., Mills, R. L., Proc. L.T. 8, p. 423 ibid.; Phys. Rev. Letters **8** (1962) 469.
69) Mills, R. L. and Schuch, A. F., Phys. Rev. Letters **6** (1961) 263.
70) Goldstein, L., Phys. Rev. Letters **5** (1960) 104.
71) Le Pair, C., Taconis, K. W., De Bruyn Ouboter, R. and Das, P., Physica **29** (1963) 755.
72) Sydoriak, S. G. and Mills, R. L., Proc. L.T. 9 to be published.
73) Heer, C. V., Daunt, J. G., Phys. Rev. **81** (1951) 447.
74) Prigogine, I. and Philippot, J., Physica **18** (1952) 729; Physica **19** (1953) 227, 235 and 508.
Prigogine, I., Bingen, R. and Bellemans, A., Physica **20** (1954) 633.
Prigogine, I., The molecular theory of solutions (North Holland Publ. Cy., Amsterdam, 1958).
75) Wuest, W., VDI-Forschungsheft, **B 28** (1962) Heft 489.
76) Cohen, E. G. D., Van Leeuwen, J. M. J., Physica **26** (1960) 1171, **27** (1961) 1157.

PART II

SOME COMMENTS ON THE FLUID STATE AND THE SOLIDIFICATION OF ^{3}He AND ^{4}He AND AN EXPERIMENT ON THE MINIMUM IN THE MELTING CURVE OF ^{4}He

Synopsis

The fluid and the solid state are qualitatively discussed in terms of a random close-packing and a regular close-packing of spheres. The model is used to obtain values for the potential energies of fluid and solid. The calculation shows that the stability of the fluid phase at low temperatures cannot be ascribed, in the way London did, to the potential energies of the two phases. Experiments are reported on the melting line of ^{4}He. A minimum is found at $T \approx 0.75$°K and a pressure of about 0.008 atm below the melting pressure at $T = 0$°K. The results are compared with those of several authors.

1. *The fluid state.* At present, there does not exist a satisfactory model for the liquid condition in general; this is in contrast to gases and solids. There is also some confusion about the meaning of the word "liquid". We prefer to use it only in connection with the situation at saturated vapour pressure. At temperatures and pressures different from the equilibrium line we shall use the word fluid. So we reserve the word liquid for that typical condition where a fluid does not occupy the containing vessel with uniform density. (We neglect external forces such as gravity).

The interaction of simple molecules like those of the inert gases can be described with a spherical symmetric potential. At short distances a strong repulsive force protects against mutual penetration, whereas at greater distances the virtual dipole-dipole interaction results in a mutual attraction. If the interaction potential is known, for instance from collision experiments, or from measurements of the second virial coefficient, the potential energy of an assembly of molecules can be calculated, provided: *a* the space configuration is known and *b* the forces between the molecules can simply be added (see the next section). The interaction potential between two atoms is shown in figure 1. For helium: $\varepsilon/k \approx 10.2$°K and $\sigma \approx 2.6$ Å.

It is not possible to draw a picture as fig. 1 for a fluid as a whole, with for instance the molar volume V as an independent variable. The potential energy depends on both the interatomic distances and the space-configur-

ation. When a fluid is compressed, the molecules need not necessarily come closer, they may also slip in between each other. Hence the potential energy does not change in an uniquely determined way when the volume decreases. Only when the configuration remains unchanged in some process, we can describe the phenomena with a kind of mean atomic potential.

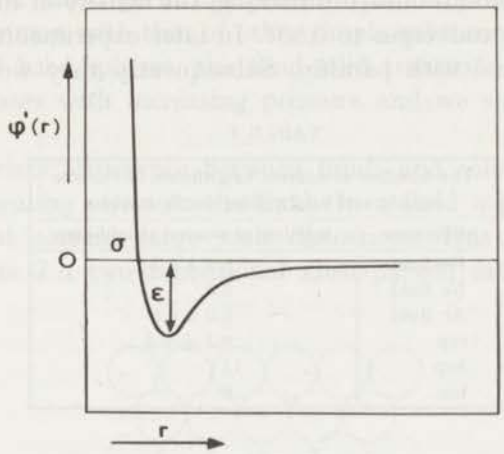

Fig. 1. Potential energy of two helium atoms: $\varphi'(r)$ as a function of the distance of the centers r.

The fluid structure. Keesom and De Smedt[1]) reported about the possibility of X-ray analysis of fluids in 1922. Since that time many investigations have been performed. Keesom and Taconis made the first analysis of the structure of liquid helium[2]), from which data about the radial distribution could be derived. More recent experiments done by Reekie, Hutchinson and Beaumont[3]) provide us with some more reliable results. From these measurements it is found that the shortest distance between two helium atoms in the liquid is about 2.3 Å. Similar experiments can be done with neutron beams. Henshaw[4]) reports a shortest separation of the atoms of 2.35 Å–2.40 Å. The number of nearest neighbours is somewhere between 8.5–9.8 atoms.

An interesting model of the liquid configuration was introduced by Bernal in 1959[5]). He stressed the importance of a geometrical model. If a number of hard spheres is packed in a regular simple cubic way, the density of the array is equal to 0.507. The density is defined as the sum of the volumes of all spheres, divided by the volume of the enveloping body. If the spheres are ordered in a hexagonal close-packing (hcp), the density is equal to 0.741. If we try to describe a fluid-solid transition by a change from a simple cubic "lattice" to a hcp lattice, the relative volume change $\Delta V/V_{\text{hcp}}$ would be equal to 0.412. This is much larger than the values $\Delta V/V_{\text{solid}}$ observed for simple substances. Bernal suggested that a random

packing of spheres could be an adequate description of the fluid. A lot of interesting experiments on the random close-packing of spheres have been done since by Bernal and coworkers[6]). Another investigator, Scott, performed an experiment in which he used thousands of steel balls[7]). Density measurements were done, in which the influence of the walls have been eliminated. After thoroughly shaking, the density of the random close-packed (rcp) balls converges to 0.637. In later experiments, after shaking, the balls were fixed with paraffin. Subsequently they were removed one

TABLE I

The number of nearest neighbours in various liquids and hard sphere configurations

substance	number of nearest neighbours
He fluid	8.5 à 9.7
Ne fluid	8.8
Ar fluid	8.0 à 8.5
rcp	9.3 ± 0.8
hcp	12
bcc	8

TABLE II

The position of maxima of the radial distribution function, relative to the position of the first maximum of several liquids and of hard sphere configurations

substance	second	third	fourth
Liquid He	1.87	2.66	3.58
Liquid Ne	1.85	2.77	3.57
Liquid Ar	1.81	2.64	3.44
rcp	1.83	2.64	3.45
hcp	1.412	1.632	1.731
bcc	1.155	1.633	1.915

TABLE III

The relative volume decrease of the fluid-solid transition of some substances at their triple points, and of helium at several pressures, and of a rcp–hcp transition of hard spheres

substance	pressure	$\frac{\Delta V}{V_{sol}}$ in %
Ne fluid-solid	triple point	15.8
Ar ,,	,, ,,	15.2
Kr ,,	,, ,,	15.8
Xe ,,	,, ,,	14.8
He ,,	30 atm	8.2
He ,,	50 ,,	6.5
He ,,	100 ,,	6.0
He ,,	1000 ,,	5.1
He ,,	3500 ,,	4.4
rcp–hcp		15.5

by one, after their position in space had been measured by means of an optical comparator. The data were supplied to a computer and the radial and angular distributions were calculated. Scott compared his results with known data for He, Ne, Ar, Kr and Xe. We have listed them in table I, II and III, if necessary completed with more data for helium. From these tables we see that although at low pressures the fluid structure of helium has much in common with that of other simple substances and that of the rcp structure of hard spheres, the fluid-solid transition is different. This difference increases with increasing pressure and we shall come back to this later.

The characteristic difference between fluids and solids is the lack of resistance to shearing stress in the fluid. In a fluid a particle can move "freely" without causing large scale distortions. This is not the case in a solid. In figure 2 a two-dimensional close-packed lattice is shown. If

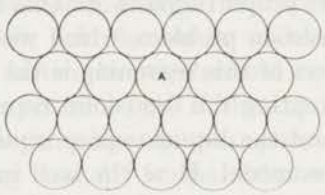

Fig. 2. Two dimensional close-packed lattice.

the elements are hard spheres, it is obvious that a displacement of molecule *A* involves a long range distortion of this lattice. Hence deformations are opposed by large energy barriers. If the molecules were hard spheres with soft skins (hsss) distortions are possible, although a certain energy gap has to be overcome. The rcp configuration shows a remarkably low resistance to shearing stress[8]). Therefore it is tempting to associate the rcp configuration with the dense fluid state. Another remarkable property of the rcp configuration is its stability. Even when some external pressure is exerted, shaking does not cause a denser packing. Thus "solidification" has not been obtained. There are three important differences between the steelball model and real molecules. *1* Friction, *2* absence of real random motion like temperature movements, *3* hard spheres. Real molecules are not hard spheres. A hsss model would probably be more appropriate. The hard sphere model does not tolerate any degree of freedom in many configurations which are not close-packed. We constructed a number of such configurations with small numbers of "molecules". In all those cases the hsss model would have permitted a change to an energetically more favourable situation. Although this seems to be the microscopic origin of the sharply defined rcp arrangement and the cause of the impossibility of configuration change when

external pressure is exerted, we did not succeed in generalising these considerations to systems with a greater number of molecules.

2. *Properties of the rcp fluid of "hsss" molecules.* As the configuration of the fluid is rather stable against volume changes, which is confirmed by X-ray experiments, we may describe the potential energy of the fluid with a molar potential of the same shape as figure 1, with the molar volume V as independent variable. The pressure of the system depends on: *1* the kinetic energy, *2* the number of particles per cm³ and *3* on $(-\mathrm{d}\Phi/\mathrm{d}V)$. Φ being the molar potential energy. For the hsss model, $(-\mathrm{d}\Phi/\mathrm{d}V)$ is not infinite. It increases rapidly with decreasing volume. Hence the pressure P increases steeply with decreasing volume. Within the rcp configuration small microscopic clusters of orderly close-packed molecules exist. The volumes of these clusters are smaller than the mean volume of that number of molecules. Therefore a molecule leaving such a cluster generally involves crossing an energy barrier proportional to P. This barrier might be the core of the fluid-solid condensation problem, which we could not solve.

One of the consequences of this reasoning is the absence of an argument for a critical point terminating the fluid-solid transition line. Solidification of a liquid by cooling and the liquid vapour equilibrium itself cannot be understood from the hsss model. Here the well in the potential energy is essential. Starting from the compressed situation a volume increase causes a sharp pressure decrease. Now we have to distinguish between $T > T_c$ and $T < T_c$ (T is the temperature of our sample and T_c the critical temperature). In the classical case if the configuration remains rcp, $T_c \approx \frac{2}{3}\Phi_0/R$, Φ_0 being the depth of the potential well. For helium this is disturbed by the influence of the zero point energy. (For ^{4}He: Φ_0 exp. $\approx$ 60 Joule mole^{-1}, $\frac{3}{2}RT_c \approx$ 65 Joule mole^{-1}, for ^{3}He these values are 21 and 41.5, respectively). Let us first consider $T < T_c$. A certain expansion would involve an increase of the potential energy of the system larger than the kinetic energy available, if the density was to remain uniform. This cannot be realised. Only a part of the molecules can escape due to configuration and energy fluctuations. This fraction depends only on T and is proportional to the volume available for the escaping atoms. A further volume increase causes an evaporation at constant temperature. It is obvious that energy has to be supplied to keep the temperature constant, because evaporation means an escape from the bound state. During this process the pressure remains constant. It is less clear that the same should occur at the fluid-solid transition discussed before. The hsss model, however, provides us with a model to understand this at least qualitatively: The configuration change implies a change of number of nearest neighbours, which involves more deformations in the skins. The larger number of deformations cooperate in such a way that the pressure remains constant. Without making predictions on the elasticity of the skin one cannot calculate the influ-

ence on the potential energy, but a fall in potential energy on solidification is likely, which implies the normal positive heat of melting*).

At $T > T_c$ the change from rcp to the incoherent unbound structure of the vapour is continuous. The molecules able to escape do not need a supply of kinetic energy. Nonetheless, energy has to be supplied to keep the temperature constant. Therefore at supercritical conditions the heat capacity C_P should increase rather strongly, dependent on the depth of the potential well in the region where the rcp structure changes into the incoherent structure. This has been confirmed by Jones and Walker[9]) for argon and by Moldover and Little[10]) for helium. According to this model the total amount of heat, supplied to a sample below and above its critical point, in order to change from rcp to incoherent structure should vary continuously.

Probably in the classical case the hard sphere and the hsss model would remain fluid at absolute zero (i.e. rcp configuration). An external pressure might be able to solidify the hsss model. If an attractive force exists things are different. With a finite kinetic energy the state depends not only on the depth of the potential well, but also on its width. Only if $\varphi(V_0 + \delta V) - -\varphi(V_0) > E_{kin}$ will the lattice be regular and resistant against shearing stress. V_0 is the volume per molecule if the rcp lattice has a minimum potential energy; φ is something like the mean potential energy per molecule; E_{kin} is the kinetic energy and δV is the volume increase of a molecule escaping from a microscopic ordered cluster. If this condition is satisfied solidification of this model takes place, when cooling down, in the same way as in the case of increasing pressure. Now a triple point occurs and the vapour pressure curve shows a kink at the triple point due to the configuration change of the bound phase.

3. *The helium case.* The radial distribution function and the number of nearest neighbours in fluid helium reminds one of a rcp configuration. The formation of a liquid however shows that the interaction between the atoms should have an attractive part. Moreover, the anomalous volume change at solidification proves that a hard sphere or a hsss model is not adequate to describe the phenomena in helium.

The attractive forces between the helium atoms are small. They are of the London-Van der Waals type. The interaction between the atoms can be obtained from experiments about scattering of helium atoms and by measurements of second virial coefficients. In order to be able to compare our results directly with those of London[11]) we based our calculations on

---

*) If a certain force K stresses a normal spring, the potential energy of the system is $\frac{1}{2}K^2/\gamma$, γ being the elasticity coefficient. If K stresses two equal springs, the potential energy is equal to $\frac{1}{4}K^2/\gamma$ or one half of the first value. As the number of nearest neighbours increases at constant P from 8.8 to 12 at the rcp–hcp transition a decrease of the potential energy is likely in the hsss model.

the same potential as used by him:

$$\varphi'(r) = \{1200\, e^{-4.82r} - 1.24\, r^{-6} - 1.89\, r^{-8}\}\, 10^{-19} \text{ Joule pair}^{-1}$$

r in Å. This form was derived by Yntema and Schneider in 1950[12]). Other potentials often used to describe the helium properties are the Lennard-Jones potential of De Boer and Michels[13]) and the Slater-Kirkwood potential[14]). Since we know from the calculations of Kihara and Koba[15]) that a quantitative change of the interatomic potential may involve qualitative differences as to the molar potential energies of several lattices, we carried out our calculations also with the Lennard-Jones potential[13]):

$$\varphi'(r) = 56.44 \left\{ \left(\frac{2.556}{r} \right)^{12} - \left(\frac{2.556}{r} \right)^{6} \right\} 10^{-23} \text{ Joule pair}^{-1}.$$

As this gave qualitatively and also to good approximation quantatively the same results, we do not mention the results thus obtained here. Assuming the additivity of the interatomic forces*), we calculated the potential energy of a hcp, a rcp and a body centered cubic (bcc) lattice, taking into account the contribution to the potential energy of one atom of all atoms within a

TABLE IV

a. The number of atoms of a rcp configuration at a distance r, within a shell of thickness Δr

random close-packed		
r distance	Δr shell thickness	n atoms in shell
0.85	0.05	0.026
0.90	0.05	0.613
0.95	0.05	1.259
1.00	0.05	1.533
1.05	0.05	1.632
1.10	0.05	1.648
1.20	0.10	2.094
1.40	0.20	2.989
1.60	0.20	4.938
1.80	0.20	9.319
1.90	0.10	6.792
2.00	0.10	7.383
2.10	0.10	6.688
2.30	0.20	13.069
2.50	0.20	17.181
2.70	0.20	22.566
3.00	0.30	38.04

b. The number of atoms at discrete distances for a hcp and a bcc lattice

hexagonal close-packed		body centered cubic	
r distance	n number of atoms	r distance	n number of atoms
1	12	1	8
1.412	6	1.155	6
1.632	2	1.633	12
1.731	18	1.915	24
1.915	12	2.000	8
2	6	2.309	6
2.235	12	2.517	24
2.380	12	2.582	24
2.449	6	2.828	24
2.516	6	3.000	32
2.582	12		
2.646	24		
2.708	6		
2.886	12		
3	12		

*) Jansen and Zimering calculated the potential energies of hcp and cubic close-packed lattices, taking into account discrepancies of the two body interactions and the effects caused by the finite size of the atoms[16]). As these effects give only differences of about 4% and our results deal with larger effects, our assumption does not put serious limitations to the validity of our conclusions.

sphere of radius $3D$. (D being the distance between nearest neighbours of that special molar volume).

For the rcp configuration we took the radial distribution function of Scott[7]) normalised for the number of 8.8 nearest neighbours. In that case the interatomic distance r is equal to $r = 1.071\ R$; $R = (V/N)^{\frac{1}{3}}$ in which V is the molar volume and N is Avogadro's number. For a hcp structure $r = 1.123\ R$ and for a bcc structure $r = 1.0911\ R$. In table IV*a* the number of atoms within a shell of thickness ΔD at a distance measured in units D are listed. Table IV*b* gives the number of atoms at discrete distances for the hcp and the bcc structure respectively. The results are shown in figure 3. The meaning of the curves are listed in the caption. The potential energy of the rcp configuration is above that of the hcp or bcc structure in the ΦV

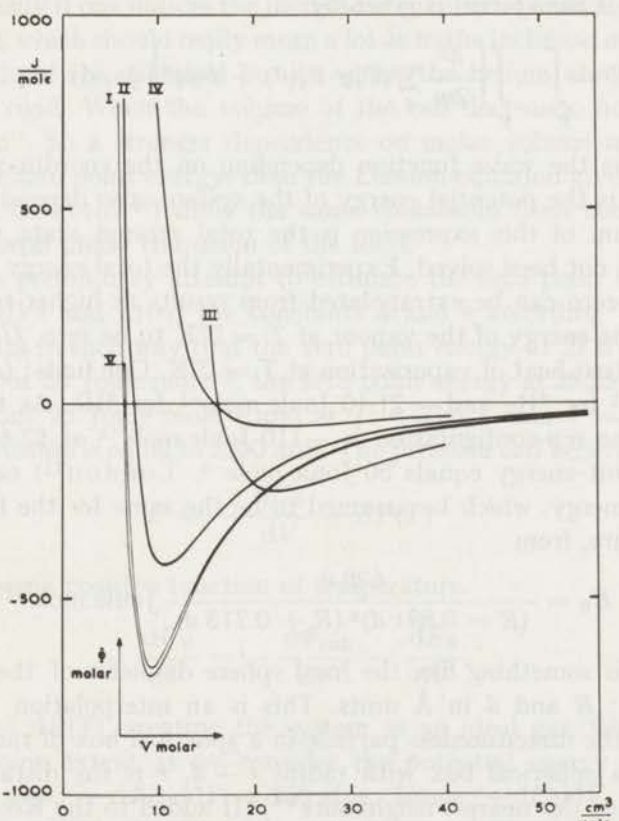

Fig. 3. The energy of helium as a function of volume
I – potential energy of a hcp lattice
II – potential energy of a rcp configuration
III – potential energy of a T_d^2 lattice
IV – total energy of the fluid, calculated by us
V – potential energy of a bcc lattice

diagram. Curve III represents the potential energy of a close-packed lattice of which only half the number of sites are occupied. It was suggested by Keesom and Taconis[2]) in order to describe the liquid structure. London used it as a basis for his calculations of the potential energy of the fluid*). The disadvantage of this model is obvious as it would involve a much too large potential energy of the fluid at a molar volume of about 10 cm³. The pressure of the sample $P > -\mathrm{d}\Phi/\mathrm{d}V$. The Keesom-Taconis potential gives: $P_{\mathrm{fl}} > > 1.45 \times 10^5$ atm at a molar volume of about 10 cm³ instead of the experimental value of about 4000 atm. The rcp model gives $P_{\mathrm{fl}} > 220$ atm, which is in better agreement. At the absolute zero of temperature the molar volumes of ^{3}He and ^{4}He are 37 and 27.6 cm³ respectively, which is much larger than the volume at which the potential energies have their minimum. The reason for this is the complete inadequacy of the classical description. The energy of the system is given by

$$E = \int_V \ldots \int_V \left\{ \frac{\hbar^2}{2m} \sum_i (\nabla_i \psi \cdot \nabla_i \psi^*) + \Phi \psi \psi^* \right\} \mathrm{d}x_i \, \mathrm{d}y_i \, \mathrm{d}z_i \ldots$$

$\psi(x_i y_i z_i \ldots)$ is the wave function depending on the coordinates of the N particles. Φ is the potential energy of the system, also depending on x_i .... The minimum of this expression is the total ground state energy. This problem has not been solved. Experimentally the total energy of the liquid at absolute zero can be extrapolated from results at higher temperatures. Assuming the energy of the vapour at $T = 0°\mathrm{K}$ to be zero, $U_0 = -L_0 \cdot L_0$ being the latent heat of vaporization at $T = 0°\mathrm{K}$. One finds: $U_0 = -59.62$ Joule mole^{-1} for ^{4}He and -21.10 Joule mole^{-1} for ^{3}He. As the potential energy of the rcp-configuration is -110 Joule mole^{-1} at 27.6 cm³ mole^{-1}, the zero point energy equals 50 Joule mole^{-1}. London[11]) calculated the zero point energy, which he assumed to be the same for the fluid and the solid structure, from

$$E_0 = \frac{628\,\mathrm{d}}{(R - 0.891\,d)^2\,(R + 0.713\,d)} \text{ Joule mole}^{-1}$$

in which d is something like the hard sphere diameter of the atoms and $R = (V/N)^{\frac{1}{3}}$; R and d in Å units. This is an interpolation between the problem of the dimensionless particle in a spherical box of radius R and a particle in a spherical box with radius $r - d$. r is the distance between the centers of the nearest neighbours**). If added to the Keesom-Taconis

*) Neither Keesom and Taconis nor London suggested that the fluid had really a crystal like structure of this type.

**) Lee, Huang and Yang calculated the energy of the ground state of a hard sphere dilute Bose gas with a pseudo potential method [76]). A volume dependency of $(1/V) + (a/V^{14})$ is found for the zero point energy. For dense systems as the present one however, the derivation does not remain valid.

potential, a total energy is found with a minimum at the right place and an energy about 16 Joule mole^{-1} lower than the measured value. If added to the hcp potential the total energy of the solid is found. The common tangent to both curves gives energy and volume of fluid and solid at the transition. London took 2.3 Å for the parameter d. Of course London realised the serious objections which can be made against this treatment. In our opinion two of the most serious disadvantages are:

1. The zero point energies of fluid and solid are taken to be the same. The cross over of $\Phi_{T_d^3}$ and Φ_{hcp} is presented as an argument for the absence of solidification of the liquid. (see ref. 11, p. 29). Our calculations show on the contrary that the potential energy of the solid, either in bcc or in hcp configuration, remains lower than that of the fluid. Hence we must conclude that the zero point energy causes the instability of the solid. This can be understood easily if one notices the increase of number of nearest neighbours from 8.8 to 12, which should really mean a lot as to the inclusion of an atom*)

2. The walls of the spherical box in which the helium atom is located are far from rigid. When the volume of the cell decreases, however, the walls "harden". So a stronger dependence on molar volume must be expected for the zero point energy, than the London-equation gives. Recently Schuch and Overton[17]) drew the same conclusion from considerations of the polymorph phase transition of the solid.

We made a preliminary attempt to estimate the zero point energy. We wrote $E_0 = a/V^b$ and fitted the constants a and b according to the experimental data in such way that the zero point energy at 27.6 cm^3 mole^{-1} should be about 50 Joule mole^{-1}, the zero point energy at 25.25 cm^3 mole^{-1} should be about 98 Joule mole^{-1} and at $T = 30.6$°K and $V = 10.15$ cm^3 mole^{-1}, the pressure is equal to 3500 atm. The pressure can be written as

$$P = -\frac{\mathrm{d}U_0}{\mathrm{d}V} + \Delta P(T)$$

where ΔP is some positive function of temperature.

$$-\frac{\mathrm{d}U_0}{\mathrm{d}V} = -\frac{\mathrm{d}\Phi_{\text{rcp}}}{\mathrm{d}V} - \frac{\mathrm{d}E_0}{\mathrm{d}V}.$$

If we estimate $\Delta P(T)$, treating the system as an ideal gas, which can be justified to some extent as we consider the potential energy separately, $\Delta P(T) \approx 250$ atm. $-\mathrm{d}\Phi_{\text{rcp}}/\mathrm{d}V \approx 200$ atm, hence $-\mathrm{d}E_0/\mathrm{d}V$ should be about 3000 atm. With these conditions an appropriate solution for E_0 is: $E_{0,\text{fluid}} = 1.154/V^3 \times 10^6$ Joule mole^{-1}, V in cm^3 mole^{-1}. With this

*) Although in the bcc lattice the number of nearest neighbours decreases to 8, we can see from table IV*b* that the number of next nearest neighbours, 6, is in very close proximity to the center if compared to the hcp lattice. It is therefore likely that the two opposing tendencies (14 versus 12 atoms against a slightly larger mean distance) cancel each other.

empirical formula and the rcp potential energy, the minimum of the $U_0 \leftrightarrow V$ curve is situated at 24 cm^3 mole^{-1}. The curves for the energy at $T = 0°$K as calculated by London and by us are drawn in figure 4. Presumably the dependency of the zero point energy of the volume is not as simple as suggested here.

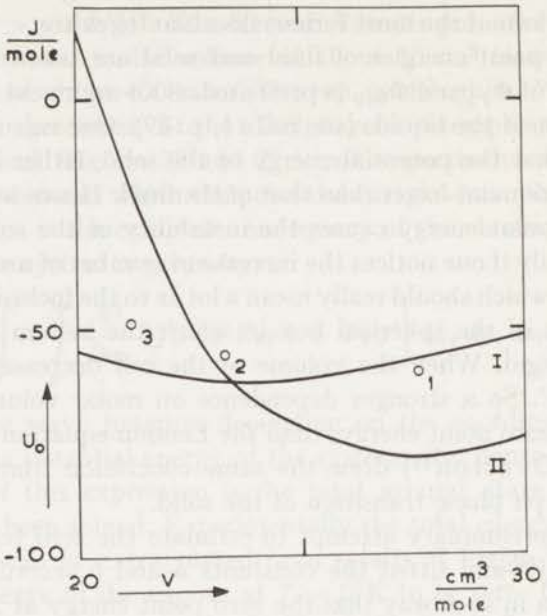

Fig. 4. The total energy of the fluid at $T = 0°$K as a function of volume.
I – our data
1 – liquid ($P = 0$) exp
2 – fluid ($P = 25$ atm) exp.
II – London's data
3 – solid ($P = 25$ atm) exp.

Therefore one should not worry too much about the fact that the experimental point for the solid lies at the wrong side of the curve. This and the wrong place of the minimum could be overcome very easily if we had chosen a slightly more complicated form for E_0.

4. *Experiments on the fluid-solid transition of* ^4He. In order to carry out experiments to get more detailed information about the fluid-solid equilibrium, we used the third apparatus described before [18]). In 1960 Goldstein predicted the existence of a minimum in the freezing pressure of ^{4}He[19]). Van den Meydenberg calculated the probable depth of the minimum to be $\Delta P \leqslant 0.04$ atm, $\Delta P = P(T = 0) - P(T = T_M)$, with $T_M < 0.8°$K. To detect this small effect, we needed the highest possible accuracy. With our apparatus differences of 0.003 atm could be seen. In order to obtain this accuracy, the experiments had to be done isothermally [46])

Procedure. Initially the Bourdon tube is filled with solid ^{4}He. This is realized by putting a fluid sample at $T \approx 2.15$°K under a pressure of about 48 atm. After cooling down to 1°K the Bourdon tube contains solid ^{4}He at about 29 atm. With aid of the ^{3}He cryostat, the temperature is lowered until about 0.5°K. Then the pressure outside the cryostat is allowed to decrease. This happens very carefully and slowly and above all continuously. When the pressure outside the cryostat becomes lower than the minimum melting pressure (about 25 atm) the gas starts escaping from the Bourdon tube and the pressure in the Bourdon tube falls very sharply. About 10 seconds before we could see any change in the tube, the temperature increases presumably because of melting in the capillary wound around the ^{3}He cryostat, to which the thermometer has been attached. The warming up can be compensated easily by increasing somewhat the pumping speed of the ^{3}He pump. The pressure of the solid decreases non uniformly in about $3\frac{1}{2}$ minutes and becomes constant at the melting pressure. The nonuniformity was expected. The solid within a long narrow vessel will not very easily transmit the pressure and the process takes place in an irreversible way. The pressure remains constant for about $\frac{1}{2}$ to 1 minute and then decreases slowly and gradually. The fluid is of course a perfect pressure transmitter. When everything has become fluid, the speed in which the ^{3}He is pumped off has to be decreased. This means that the heat leak from the ^{4}He bath

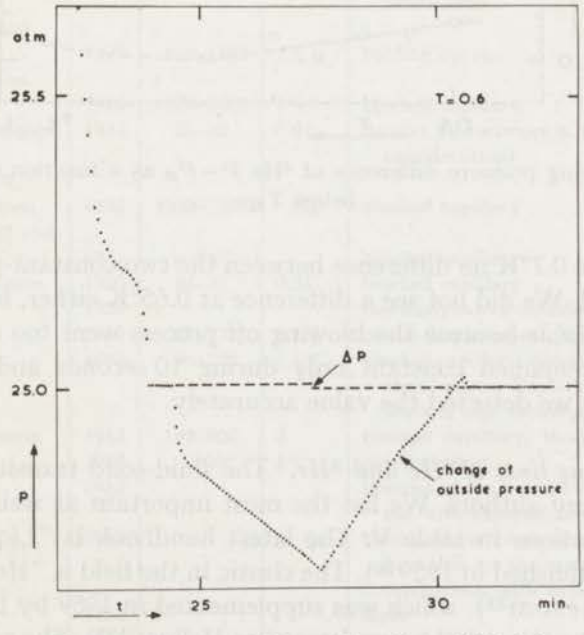

Fig. 5. Typical run of a measurement of the melting line of ^{4}He below the temperature at which this line has a minimum.

to the low temperature part of the apparatus through the 24 cm long, 0.18 mm i.d. capillary of stainless steel, filled with He II is much smaller than the heat produced during the melting process. When it is certain that the sample is in the fluid phase, the pressure outside the cryostat is raised and the process is reversed. Now the pressure within the Bourdon tube increases uniformly and at a certain moment drops about 0.015 atm and remains constant. Then the difference between the two constant pressures is known. The first one gives the melting pressure at that particular temperature; the last one – the blocked capillary result – gives the minimum freezing pressure. Hence ΔP is known. A typical run as described here is shown in figure 5. Calculations of the jump occurring each time the pressure is increased and solidification sets in, show that the volume contraction of freezing in the capillary is large enough to compensate for the extra number of moles supplied to the Bourdon tube. Actually only 0.1 of the total length of the capillary within the vacuum jacket needs to be filled with these extra moles to compensate for the effect of overpressurizing. So the solid block in the capillary extends to about 2.4 cm. Results are shown in

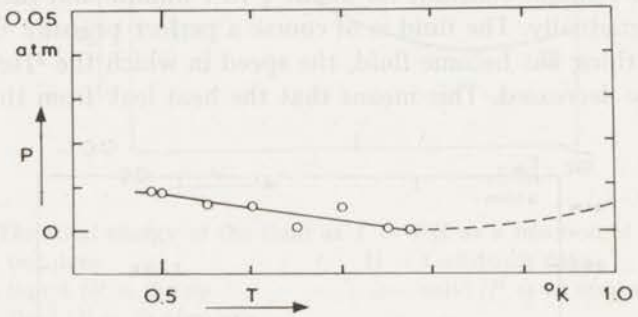

Fig. 6. The melting pressure difference of ^{4}He $P - P_M$ as a function of temperature below T_M.

figure 6. Above 0.7°K no difference between the two constant-pressure-lines could be found. We did not see a difference at 0.65°K either, but this result is not very reliable because the blowing off process went too quickly here; the pressure remained constant only during 10 seconds and we are not quite sure that we detected the value accurately.

5. *The melting lines of ^{4}He and ^{3}He.* The fluid-solid transition has been studied by many authors. We list the most important as well as the most recent contributions in table V. The latest handbook is "Liquid Helium" by Atkins, published in 1959[20]). The classic in the field is "Helium" by the late W. H. Keesom[21]), which was supplemented in 1959 by Lifshitz and Andronikashvili with "A supplement to Helium"[22]). The phase diagram of both isotopes is shown qualitatively in figure 7. The diagram has no

ordinary triple point. Both isotopes exist in two known solid configurations in the pressure range up till a few hundred atmospheres: bcc and hcp. The properties of the polymorph phase transition have been investigated by several authors[40][38][43]. The λ transition in the ^{4}He fluid has been discussed in the previous part[18]. Both melting lines show a minimum. This property is very peculiar as it involves a larger degree of disorder in the solid than in the liquid. In ^{4}He this minimum is so small, that it is not to be seen in the figure; but see fig. 6. The history of our knowledge on this point shows a parallel. In both cases the theoretical prediction came first: Pomeranchuk (^{3}He) and Goldstein (^{4}He). Next the experimental confirmation by detection of a negative heat of melting[55] and [45] and than a direct determination:[56] and [46]. ^{3}He has a nuclear spin because of the odd number of particles in the nucleus. The random distribution of these spins contributes $R \ln 2$ to the total entropy. At temperatures at which kT becomes of the same order of magnitude as the magnetic dipole-dipole interaction, spin

TABLE V *a*

Contributions to the knowledge of the fluid-solid equilibrium of ^{4}He

author	year	pressure range atm	estimated accuracy atm	method used, theoretical considerations and typical aspects	ref.
Keesom	1926	25–140	0.1	blocked capillary, theoretical considerations	21
Simon, Ruhemann and Edwards	1929	800–1800	1%	heating curve	23
Simon, Ruhemenn and Edwards	1929	1800–5500	1%	blocked capillary	24
Keesom and Keesom	1933	26–30	0.01	density measurements, theoretical considerations	21
Holland, Huggill, Jones and Simon	1950	4000–7500	100	blocked capillary	25
Holland, Huggill and Jones	1951	> 5000		blocked capillary	26
Simon and Swenson	1950	25–27	0.01	blocked capillary	27
Swenson	1950			thermodynamic considerations	28
Swenson	1952	27–130	0.1%	piston displacement, theory	29
Swenson	1953	26–130	0.1%	blocked capillary, detailed discussion about piston displacement and blocked cap. techniques	30
Dugdale and Simon	1953	140–800	3	blocked capillary, thermodynamics	31
Robinson	1953	9000	5%	moving pellet	32
De Boer	1952			theories of the liquid state, comparison with experiment	33
Fisher	1954			theory, deriviation of theoretical formulae for the melting line, comparison with experiment	34
Salter	1954			idem	35
Domb	1957			theory, difference of internal energy of ^{3}He and ^{4}He	36

TABLE V *a* (*continued*)

author	year	pressure range atm	estimated accuracy atm	method used, theoretical considerations and typical aspects	ref.
Domb and Dugdale	1957			review article from which part of table is taken, extensive theoretical considerations	37
Grilly and Mills	1959	35–3500	0.05%	blocked capillary, volume of melting etc.	38
Lounasmaa	1960			theory, thermodynamics	39
Goldstein	1960			theory, thermodynamics, prediction of minimum in melting curve	19
Vignos and Fairbank	1961	25–33	0.01	velocity of sound, new solid phase	40
Langer	1961	14000	200	piston displacement	41
Van den Meydenberg	1961			theory, depth of the minimum	42
Grilly and Mills	1962			*PVT* relations and polymorph phase transition	43
Goldstein	1962			theory, thermodynamics calculation of depth of minimum	44
Wiebes and Kramers	1963			heat capacity measurements, indirect verification of existense of melting pressure minimum	45
Le Pair, Taconis, De Bruyn Ouboter and Das	1963			direct pressure measurement, verification of existence of melting pressure minimum	46
Sydoriak and Mills	1964			heat capacity idem, indirect	47
Zimmerman	1964			heat capacity measurements idem, indirect	48

alignment will occur. Pomeranchuk estimated the transition temperature for the solid to be about 10^{-7}°K. The fluid structure, although being more open than the solid structure, has a shorter mean atomic distance than the solid. This effect is small, it amounts to about 3% in ^{3}He. It should involve a transition at $T < 10^{-6}$°K. Specific heat measurements, however, together with heat of vaporization data show that the entropy of the liquid falls below $R \ln 2$ at about 0.5°K. At higher pressures this happens at slightly lower temperatures. At the melting pressure it happens at $T = 0.33$°K. This must be attributed to strong exchange effects in the fluid, which do not occur in the solid because of its long range ordering. (In the fluid density fluctuations of microscopic size are larger and more frequent). As the slope of the fluid-solid transition line is determined by the Clausius-Clapeyron equation $\mathrm{d}P/\mathrm{d}T = (S_{\mathrm{fl}} - S_{\mathrm{sol}})/(V_{\mathrm{fl}} - V_{\mathrm{sol}}) = \overset{1}{\Delta}S/\overset{1}{\Delta}V$ and $\overset{1}{\Delta}V$ is not affected within the first order approximation by the spins, the change of sign of $\overset{1}{\Delta}S$ preserves the slope of the transition curve. At very low temperatures $\overset{1}{\Delta}S$ should become zero again, according to Nernst's heat theorem. According to Goldstein, who reported the work of Zeigler and Perego[68]) about the least square fits to an analytical function of all known data, the

TABLE V *b*

Contributions to the knowledge of the fluid-solid equilibrium of ^{3}He					
author	year	temperature °K	accuracy atm	method and typical aspects	ref.
Pomeranchuk	1950			theory, prediction of minimum	49
Osborne, Abraham and Weinstock	1951	1.02–1.51	0.1	blocked capillary	50
Daunt	1952			review article; discussion of exp. results	51
Osborne, Weinstock and Abraham	1952	0.16–1.51	0.1	blocked capillary; no minimum	52
Roberts and Sydoriak	1954			heat capacity; disadvantage blocked capillary technique	53
Mills and Grilly	1955	1.3–30.0	0.05%	blocked capillary; comparison with Simon melting equation	54
Domb	1957			theory	36
Walters and Fairbank	1957	< 0.5		heat capacity; indirect conformation of the existence of a minimum	55
Domb and Dugdale	1957			review article	37
Baum, Brewer, Daunt and Edwards	1959	0.12–0.7	0.2–0.01	strain gauge; minimum directly	56
Goldstein	1959			theory; thermodynamics	57
Grilly and Mills	1959	> 1.3		volumetric; solid-solid transition	38
Grilly, Sydoriak and Mills	1960	0.3–0.5	0.02	volumetric; minimum directly	58
Edwards, Baum, Brewer, Daunt and Mc Williams	1960	0.12–0.7		specific heat; strain gauge	59
Peshkov and Zinov'eva	1959			review article	60
Sydoriak, Mills and Grilly	1960	> 0.3		extension of [58]; thermodynamical considerations	61
Bernardes and Primakoff	1960			theory	62
Anderson, Reese and Wheatley	1961	> 0.03		magnetic properties	63
Mills, Grilly and Sydoriak	1961	0.3–1.2		extension of [61]	64
Edwards, Mc Williams and Daunt	1962	> 0.1		heat capacity	65
Goldstein and Mills	1962			theory; thermodynamics	66
Anderson, Reese and Wheatley	1963	0.03			67
Goldstein	1964	0.02		theory; extensive article; comparison with experiments	68

melting pressure of ^{3}He at $T = 0°\mathrm{K}$ should be:

$$P_0 < P_{0,02} + R \ln 2/\Delta V \times 0.02 \approx 33.87 \text{ atm.}$$
$$1$$

^{4}He has no spin contribution to its entropy. At low temperatures only

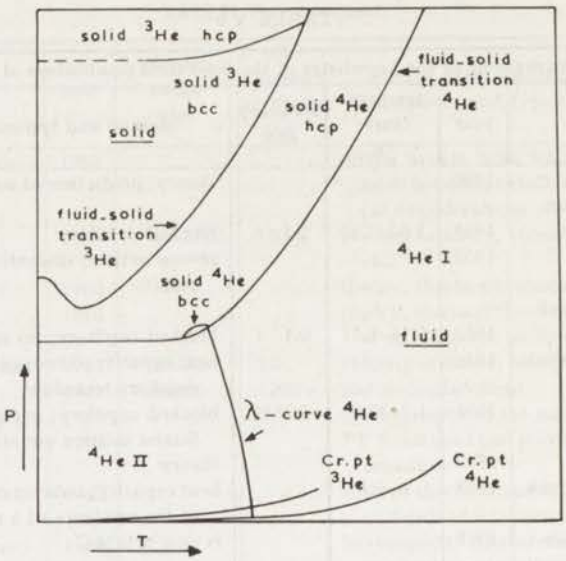

Fig. 7. *PT* diagram of ³He and ⁴He. Below are the liquid lines, ending at the critical points. Other lines are discussed in the text.

configurational and collective motion contributions to the entropy of both fluid and solid are left. Only very recently the first information about the entropy of fluid and solid below 1°K has been collected[69]). The data have not yet been used in calculations about the transition. Goldstein launched the idea about a possible minimum. He estimated it to be about 0.052 atm below the pressure at $T = 0$°K[44]). Van den Meydenberg, however, estimated it to be smaller than 0.04 atm[42]). The idea that underlies the phenomenon is the fact that in solid helium longitudinal and transversal wave propagation is possible. In the fluid only longitudinal phonons exist. So in the region where phonons are the only excitations, the entropy of the solid may exceed that of the fluid, even when the sound velocity is larger in the solid. Wiebes and Kramers found a negative heat of melting below 0.76°K. They estimated the depth of the minimum to be about 0.008 atm[45]). Our measurements confirmed this result[46]). Uncertainties in our measurements are: *1* The complete dependency on the block in the capillary. If this occurs too close to the Bourdon tube, the measured effect is too small. *2* The possibility of hysteresis of the Bourdon tube, this possibility was discussed with Mills and Sydoriak in private comments on mutual work. We refer to the appendix of part I about the properties of the Bourdon tube[18]). The complete absence of even the least effect above 0.7°K strengthens our belief in the validity of the absence of an appreciable hysteresis. Sydoriak and Mills investigated also the minimum of ⁴He[47]), Their measurements suggested an effect of 0.027 atm at $T = 0.6$°K and the minimum occurring at 0.875°K.

Zimmerman[48]) states in the program of the 9th conference on Low Temperature Physics, p. 32: "Using the Clapeyron equation, the average slope of the melting curve of pure ^{4}He between 0.145 and 0.6°K was computed to be 0.008 atm °K^{-1}. This result is in good agreement with Le Pair *e.a.* and Wiebes *e.a.* and somewhat smaller than that calculated by Goldstein". In his address to the conference he declares: "By inserting the specific heat data of Atkins and Stasior[70]) and the change in volume upon solidification data of Swenson[28]), one obtains for an average slope between the two above mentioned temperatures: $dP/dT = -0.2$ atm °K^{-1}. This value is greater than the determination of the negative slope in the melting curve of Le Pair *e.a.* and Wiebes and Kramers and gives a change in pressure between the minimum and 0°K greater by a factor of two than that calculated by Goldstein when added to the change in pressure reported by Sydoriak and Mills". This shows above all how delicate the question is. Tests on the properties of our Bourdon tube as mentioned before (ref. 18, appendix), although not sufficient to claim absolute certainty, improve our faith as to the reliability of our measurements. So until better information on heat capacities etc. become available, we trust our results to be correct*). It might be that the deformation energies of the Bourdon tube used by Sydoriak and Mills are responsible for the discrepancy. We have evidence from the measuring technique of Fokkens *e.a.*[71]) that deformation of metals produces a considerable amount of heat at low temperatures. The slope of the Los Alamos curve below T_M is about 5 times steeper than ours. If the heat contribution from the tube would be 4 times the heat of melting effect, this would cause the difference. Above T_M the relative influence of this effect decreases rapidly with about T^3. Above T_M the positive heat of melting will soon exceed the Bourdon contribution. The result would be a too steep slope below T_M and a too flat slope above. This is in agreement also with some other peculiarities reported by Sydoriak and Mills**).

6. *Concluding remarks.* From the foregoing sections it is clear that neither for ^{3}He nor for ^{4}He the Nernst-condition: $dP/dT = 0$ at sufficiently low temperatures, has been confirmed experimentally. The existence of the minimum in the melting line of pure ^{4}He has become sufficiently certain, although serious discrepancies exist about the order of magnitude of the results between the various experimentalists.

The calculation of the potential energy of the fluid based on the rcp configuration indicates that the non-existence of the solid in equilibrium with the bound fluid phase cannot be ascribed to the potential energies, but must be due to differences of the zero point energies.

*) Wiebes also still believes his observation of the value of T_M to be correct.

**) Up till now the discussion between the LAS and the KOL groups is not closed. We are indebted to Dr. Sydoriak and Dr. Mills for sending us preprints and private comments about their work.

In our calculation of Φ we took into account contributions to the potential energy of the atoms by atoms within a sphere of radius three times the atomic distances. Contributions from further atoms as well as manybody forces and deviations from the central force model are negligible compared to the effects studied here. The potential well found in this way is about 100 Joule mole^{-1} deeper than that calculated by London from the same interatomic potential, taking into account only nearest and next nearest neighbours. Only a small difference exists between Φ_{hcp} and Φ_{bcc} and a cross over at $\sim$20 cm^3 mole^{-1} occurs. The effect is very small and without more detailed knowledge about the zero point energy and the limitations of the two body interaction assumption no conclusions may be drawn as to the bcc–hcp transition, which occurs at about that molar volume.

As far as higher temperatures are concerned, one is inclined to pay more attention to the classical hard sphere model. Uhlenbeck even goes as far as calling the solidification of helium an argument in favour of the probable phase transition of a hard sphere assembly[72]). We are a little bit reluctant on this point, because it might be that a hard sphere model is stable against transitions caused by pressure. On the other hand the deviation from the hard sphere model is obvious and becomes even more so at large pressures. The

TABLE VI

Data about ^{3}He and ^{4}He along the melting line, taken from Grilly and Mills[38]).

P atm	T °K		V_{fl} cm^3 mole^{-1}		V_{sol} cm^3 mole^{-1}		S Joule mole^{-1} °K^{-1}		dP/dT Joule cm^{-3} °K^{-1}	
	^{4}He	^{3}He	^{4}He	^{3}He	^{4}He	^{3}He	^{4}He	^{3}He	^{4}He	^{3}He
30	1.793	0.517	22.349	25.807	20.683	24.619	3.605	1.273	2.192	1.071
50	2.332	1.332	20.857	23.700	19.581	22.663	5.025	3.528	3.940	3.405
100	3.418	2.490	19.023	20.894	17.941	20.055	5.665	4.345	5.230	5.180
1000	14.049	13.297	12.919	13.342	12.299	12.764	7.110	6.675	11.45	11.54
3500	31.110	30.533	10.077	10.355	9.650	9.939	7.630	7.280	17.82	17.53

large compressibility of the fluid for instance is not due to a gradual configuration change but to a decrease of the interatomic distances. In table VI some data about both isotopes are listed. We see that even the hcp arrangement shows a very large compressibility. At high temperatures, Uhlenbeck argues that the transition line for hard spheres should be straight. Along the line the Gibbs functions of both phases are equal:

$$U_{fl} - TS_{fl} + PV_{fl} = U_{sol} - TS_{sol} + PV_{sol}.$$

Because hard spheres have only kinetic energies, $U_{sol} = U_{fl}$. The entropies depend only on configuration, not on T, so we have:

$$\frac{P}{T} = \frac{S_{fl} - S_{sol}}{V_{fl} - V_{sol}} = \text{constant}.$$

Hence the melting pressure is simply proportional to T. From table VI it is clear that this does not hold in the helium case. dP/dT changes considerably even at pressures up to 700 times the critical pressure. The melting pressure at high temperatures can be described by a Simon equation [73]), with constants according to Domb and Dugdale [37]):

$$\frac{P}{17.23} = \left(\frac{T}{1.0179}\right)^{1.5554} - 1.$$

This formula covers even the result of Langer [41]) at 13950 atm. As we see, no indication of a linear behaviour at all. Helium has to be considered as a soft sphere assembly, which explains the anomaly in the value of $\Delta V/V_{sol}$ for this substance. More detailed calculations should be made about the hcp-cubic closed packed transition at very high pressures [74]) [37]), using Jansen's theory [16]). Recently more reliable data about the total energy of fluid and solid have become available [69]) [75]). We intend to use these in further calculations, to obtain a better picture of the volume dependency of the zero point energy.

REFERENCES

1) Keesom, W. H. and De Smedt, J., Proc. roy. Acad. Amsterdam **25** (1923) 118; **26** (1923) 112.
2) Keesom, W. H. and Taconis, K. W., Physica **4** (1937) 256; Commun. Kamerlingh Onnes Lab., Leiden No. 252*c*; Physica **5** (1938) 270.
Taconis, K. W., Thesis, Leiden (1938).
3) Reekie, J., Hutchinson, T. S. and Beaumont, C. F. A., Proc. Phys. Soc. **A 66** (1953) 409. Proc. roy Soc. **228** (1955) 363.
4) Henshaw, D. G., Phys. Rev. **119** (1960) 9; **105** (1957) 976, **111** (1958) 976.
5) Bernal, J. D., Nature **183** (1959) 141.
6) Bernal, J. D., Proc. roy. Soc. **A 280** (1964) 299.
7) Scott, G. D., Nature **188** (1960) 908; **194** (1962) 956; Scott, G. D. and Mader, D. L., Nature **201** (1963) 382.
8) Scott, G. D. Charlesworth, A. M. and Mak, M. K., J. chem. Phys. **40** (1964) 611.
9) Jones, G. O. and Walker, P. A., Proc. phys. Soc. (London) **B 69** (1956) 1348.
10) Moldover, M. and Little, W. A., Proc. L.T. 9, Columbus, Ohio, 1964, to be published.
11) London, F., Superfluids II (John Wiley and Sons, New York 1954) p. 21.
12) Yntema, J. L. and Schneider, W. G., J. chem. Phys. **18** (1950) 641, 646.
13) De Boer, J. and Michels, A., Physica **5** (1938) 945, **6** (1939) 409.
De Boer, J., Progress in Low Temperature Physics I ed. by C. J. Gorter (North-Holland Publ. Cy., Amsterdam 1955).
14) Slater, J. G. and Kirkwood, J. G., Phys. Rev. **37** (1931) 682.
15) Kihara, T. and Koba, S., J. phys. Soc. Japan **7** (1952) 348.
16) Jansen, L. and Zimering, S., Phys. Letters **4** (1963) 91–98,
Jansen, L., Phys. Rev. **135** (1964) **A** 1292.
17) Schuch, A. F. and Overton, W. C., Proc. L.T. 9, Columbus, Ohio, 1964, to be published.
18) Le Pair, C., Taconis, K. W., De Bruyn Ouboter, R., Das, P. and De Jong, E., Commun. Leiden No. 343*a*; Physica **31** (1965) 764.
19) Goldstein, L., Phys. Rev. Letters **5** (1960) 104.
20) Atkins, K. R., Liquid Helium (Cambridge University Press, 1959).
21) Keesom, W. H., Helium (Elsevier, Amsterdam, 1942).

22) Lifschitz, E. M. and Andronikashvili, E. L., A supplement to "Helium" (translated from Russian, Consultants Bureau Inc. N.Y., 1959).
23) Simon, F., Ruhemann, M. and Edwards, W. A. M., Z. phys. Chem. **B 2** (1929) 340.
24) Simon, F., Ruhemann, M. and Edwards, W. A. M., Z. phys. Chem. **B 6** (1929) 62.
25) Holland, F. A., Huggill, J. A. W., Jones, G. O. and Simon, F. E., Nature **165** (1950) 147.
26) Holland, F. A., Huggill, J. A. W. and Jones, G. O., Proc. roy. Soc. **A 207** (1951) 268.
27) Simon, F. E. and Swenson, C. A., Nature **165** (1950) 829.
28) Swenson, C. A., Phys. Rev. **79** (1950) 626.
29) Swenson, C. A., Phys. Rev. **86** (1952) 870.
30) Swenson, C. A., Phys Rev. **89** (1953) 538.
31) Dugdale, J. S. and Simon, F. E., Proc. roy. Soc. **A 218** (1953) 291.
32) Robinson, D. W., Thesis, Oxford (1952).
33) De Boer, J., Proc. roy. Soc. **A 215** (1952) 4.
34) Fisher, I. Z., Zh eksper. teor. Fiz. (USSR) **28** (1955) 171, 437 and 447.
35) Salter, L., Phil. Mag. **45** (1954) 369.
36) Domb, C., Proc. phys. Soc. (London) **70B** (1957) 150.
37) Domb, C. and Dugdale, J. S., Progress in Low Temperature Physics II edited by C. J. Gorter (North Holland Publ. Cy., Amsterdam, 1957).
38) Grilly, E. R. and Mills, R. L., Ann. Phys. (N.Y.) **8** (1959) 1.
39) Lounasmaa, O. V., J. chem. Phys. **33** (1960) 443.
40) Vignos, J. H. and Fairbank, H. A., Phys. Rev. Letters **6** (1961) 265; **6** (1961) 646 (erratum).
41) Langer, D. W. J., J. Phys. Chem. Solids **21** (1961) 122.
42) Van den Meydenberg, C. J. N., Thesis, Leiden (1961).
43) Grilly, E. R. and Mills, R. L., Ann. Phys. (N.Y.) **18** (1962) 250.
44) Goldstein, L., Phys. Rev. **128** (1962) 1520.
45) Wiebes, J. and Kramers, H. C., Phys. Letters **4** (1963) 298.
46) Le Pair, C., Taconis, K. W., De Bruyn Ouboter, R. and Das, P., Physica **29** (1963) 755.
47) Sydoriak, S. G. and Mills, R. L., Proc. L.T. 9, Columbus, Ohio, 1964, to be published.
48) Zimmerman, G. O., Proc. L.T. 9, Columbus, Ohio, 1964, to be published.
49) Pomeranchuk, I., Zh. eksper. teor. Fiz. (USSR) **20** (1950) 919.
50) Osborne, D. W., Abraham, B. M. and Weinstock, B., Phys. Rev. **82** (1951) 263.
51) Daunt, J. G., Adv. Phys. **1** (1952) 209.
52) Weinstock, B. Abraham, B. M. and Osborne, D. W., Phys. Rev. **85** (1952) 158.
53) Roberts, T. R. and Sydoriak, S. G., Phys. Rev. **93** (1954) 1418.
54) Mills, R. L. and Grilly, E. R., Phys. Rev. **99** (1955) 480.
55) Walters, G. K. and Fairbank, W. M., Bull. Am. phys. Soc. **2** (1957) 183.
56) Baum, J. L., Brewer, D. F., Daunt, J. G. and Edwards, D. O., Phys. Rev. Letters **3** (1959) 127.
57) Goldstein, L., Ann. Phys. (N.Y.) **8** (1959) 390.
58) Grilly, E. R., Sydoriak, S. G. and Mills, R. L., 2d Symposium on liq. and sol. ^{3}He (Ohio State Univ. Press) p. 121, publ. by J. G. Daunt (1960).
59) Edwards, D. O., Baum, J. L., Brewer, D. F., Daunt, J. G. and McWilliams, A. S., 2d symposium on liquid and solid ^{3}He, p. 126, ibid.
60) Peshkov, V. P. and Zinov'eva, K. N., Rep. on Progr. in Phys. **22** (1959) 504.
61) Sydoriak, S. G., Mills, R. L. and Grilly, E. R., Phys. Rev. Letters **4** (1960) 495.
62) Bernardes, N. and Primakoff, H., Phys. Rev. **119** (1960) 968.
63) Anderson, A. C., Reese, W. and Wheatly, J. C., Phys. Rev. Letters **7** (1961) 366.
64) Mills, R. L., Grilly, E. R. and Sydoriak, S. G., Ann. Phys. (N.Y.) **12** (1961) 41.
65) Edwards, D. O., McWilliams, A. S. and Daunt, J. G., Phys. Letters **1** (1962) 101.
66) Goldstein, L. and Mills, R. L., Phys. Rev. **128** (1962) 2479.
67) Anderson, A. C., Reese, W. and Wheatley, J. C., Phys. Rev. **130** (1963) 1644.
68) Goldstein, L., Phys. Rev. **133** (1964) A 52.
69) Wiebes, J., private communication (Jan. '65), to be published.
70) Atkins, K. R. and Stasior R. A., Canad. J. Phys. **31** (1953) 1156.
71) Fokkens, K., Taconis, K. W. and De Bruyn Ouboter, R., Proc. L.T. 8, p. 34, ed. by R. O. Davies (Butterworths, London, 1963).

Fokkens, K., Vermeer, Miss W., Taconis, K. W. and De Bruyn Ouboter, R., Commun. Leiden No. 341*a*; Physica **30** (1964) 2153.
72) Uhlenbeck, G. E., Statistical Physics 3. Ch. 1 (Brandeis Summer Inst. 1962; Benjamin Inc., New York, Amsterdam, 1963).
73) Simon, F. and Glatzel, G., Z. anorg. Chem. **178** (1929) 309.
74) Schuch, A. F. and Mills, R. L., Proc. L.T. 8 p. 423, ibid; Phys. Rev. Letters **8** (1962) 469.
75) Dugdale, J. S. and Franck, J. P., Phil. Trans. roy. Soc. London Ser. **A** No. 1076 Vol. **257** (1964) 1.
76) Lee, T. D., Huang, K. and Yang, C. N., Phys. Rev. **106** (1957) 1135.

SAMENVATTING

In dit proefschrift worden een aantal experimenten beschreven over de phase overgangen van helium bij drukken van enkele tientallen atmosferen. Onderzocht werden zowel mengsels van ^{3}He en ^{4}He, als puur ^{4}He. Bij het onderzoek werd gebruik gemaakt van een Bourdon veer, die in het lage temperatuur gebied fungeerde als manometer. Dit maakte het mogelijk, drukken te meten, zelfs als door het optreden van minima in de stolkrommes de toevoer capillairen door vast helium waren geblokkeerd. Voor de druk-aanwijzing werd achtereenvolgens een spiegelaflezing en een electro-magnetische methode gebruikt. De apparatuur en de meetresultaten zijn beschreven in deel I A. Bij vaste samenstelling vertonen de stol- en smeltlijnen van de mengsels een minimum in het PT-diagram, dat qualitatief kan worden verklaard. De apparatuur maakte het ons tevens mogelijk om singulariteiten in de Volume-Temperatuur relatie van vloeibare mengsels te vinden; aan de hand waarvan de λ-overgangen van de mengsels als een functie van de druk konden worden vastgesteld. Tevens kon worden bevestigd dat bij de ontmoeting van een tweede en eerste orde overgangslijn de laatste een knik vertoont.

In deel I B is, gebruik makend van de gevonden resultaten en van de gegevens van anderen een phase diagram van helium geconstrueerd. Daarbij is rekening gehouden met de ontmenging in de vloeistof en de vaste stof, met de structuur verandering van de vaste stof, met de vast-vloeistof overgang en met de daar soms bij optredende azeotropie. Hoewel nog niet alle gebieden van het diagram met voldoende zekerheid bekend zijn, kan toch worden gezegd, dat het gecompliceerde phase diagram zijn meeste geheimen heeft prijsgegeven.

In deel II zijn wat beschouwingen gewijd aan het tot op heden onopgeloste probleem betreffende de struktuur van een ideale vloeistof. Gebruik makend van een model van een willekeurige stapeling van harde bollen – dat een door meetresultaten verrassend gerechtvaardigd beeld van de fluide toestand geeft – zijn berekeningen over de energie van de pure componenten bij het absolute nulpunt uitgevoerd. De resultaten van dit werk, die afwijken van hetgeen eerder door anderen werd gevonden, konden kwalitatief worden verklaard. Hiertoe moest voor de vaste stof een grotere nulpuntsenergie dan voor de vloeistof worden aangenomen.

Tot slot zijn in het tweede deel ook de resultaten gegeven van gevoelige metingen aan de stollijn van ^{4}He beneden 1°K. Op grond van het phonon-energie spectrum zowel in de vaste- als in de vloeistof was hier een weinig geprononceerd minimum voorspeld. De vermelde resultaten bevestigen dit vermoeden.

STUDIEOVERZICHT

Op verzoek van de faculteit der wiskunde en natuurwetenschappen volgen hier enkele gegevens over het verloop van mijn studie.

Na het behalen van het einddiploma HBS-B aan de Gemeentelijke HBS, thans Rembrandt Lyceum, te Leiden, begon ik in 1953 mijn studie aan de Leidse Universiteit. In 1957 legde ik het candidaatsexamen natuur- en wiskunde (A') af.

Mijn practische opleiding kreeg ik op het Kamerlingh Onnes Laboratorium in de groep onder leiding van Prof. dr K. W. Taconis. Aanvankelijk assisteerde ik dr C. J. N. van den Meydenberg bij zijn experimenten aan de filmsnelheid van mengsels ^3He en ^4He. Vervolgens werkte ik samen met dr R. de Bruyn Ouboter aan de meting van de soortelijke warmte van deze mengsels. In 1960 legde ik het doctoraalexamen, hoofdvak experimentele natuurkunde, af. De doorvoor vereiste tentamens in de theoretische natuurkunde werden afgenomen door Prof. dr S. R. de Groot en Prof. dr P. Mazur.

In 1961 werd begonnen met de onderzoekingen over de stoleigenschappen van ^3He–^4He mengsels, die in dit proefschrift zijn beschreven. Achtereenvolgens werd ik daarin bijgestaan door de heren drs. K. Fokkens, drs. P. Das, P. Guthman, J. Walter, H. Alblas, A. C. de Vroomen, E. de Jong en J. Pit. Grote steun heb ik gehad van dr R. de Bruyn Ouboter. De constructie van de verschillende apparaten is tot stand gekomen in nauw overleg met de heer E. S. Prins, technisch ambtenaar.

In samenwerking met drs. B. van Laar ontwikkelde en beproefde ik een methode voor de bepaling van de concentratie van helium mengsels met behulp van thermische neutronen. De experimenten werden gedaan in het Reactor Centrum Nederland.

Sinds 1961 heb ik als hoofdassistent in de rang van wetenschappelijk ambtenaar leiding gegeven aan het natuurkunde practicum voor praecandidaten in de biologie.

Met gevoelens van dankbaarheid vermeld ik hier ook de hulp en de medewerking die ik ontvangen heb van de technische staf van het Laboratorium, in het bijzonder van mijn vader en de heren A. Ouwerkerk, L. Neuteboom, K. I. Mechelse en J. Turenhout.

De dames E. S. E. Groen-Plesman en J. A. van Zijl ben ik erkentelijk voor het typen van het manuscript en de heer W. F. Tegelaar voor de zorg waarmee hij de tekeningen heeft vervaardigd.

STELLINGEN

1

Uhlenbeck ontleende aan de stolling van helium een argument voor het bestaan van een "fluid-solid" overgang in een systeem van harde bollen. Dit argument is niet steekhoudend.

Uhlenbeck, Statistical Physics 3, pp. 47, 48.

2

Thermodiffusie kan veelal met succes worden gebruikt voor de contrôle op de zuiverheid van een gas. De methode is bijzonder waardevol, indien het aantal verontreinigingen groter dan één is.

3

Het is bedenkelijk de metingen van Pickard en Simon aan de soortelijke warmte van ^{4}He als argument voor de T^3-afhankelijkheid hiervan te gebruiken.

Lane, Superfluid Physics, p. 81.

4

De instabiliteit van de dichtste bolstapeling van helium bij lage temperaturen en drukken mag niet aan de potentiële energie van het systeem worden toegeschreven, zoals door London werd gedaan.

Dit proefschrift, part II.

5

De struktuur van vloeistoffen van eenatomige moleculen vertoont grote overeenkomst met de resultaten van modelproeven over de lukraak stapeling van harde bollen. Hieruit mag echter niet worden geconcludeerd, dat de onderlinge aantrekking tussen de moleculen de struktuur van een vloeistof niet in belangrijke mate beïnvloedt.

Zie: Bernal, Proc. Roy, Soc. A **280** (1964) p. 321.

6

Het is misleidend om de periodieke variatie van de kritische stroom als functie van de omvatte magnetische flux, zoals gemeten en beschreven door Mercereau c.s., op te vatten als een interferentie verschijnsel, volkomen analoog aan dat van het experiment*) m.b.v. electronenstralen door twee spleten.

Advertentie Ford Motor Company, Sc. Am. sept. 1964,
Mercereau c.s., Phys. Rev. Letters **12** (1964) 159,
*) Möllenstadt, Phys. Blätt. **18** (1962) 299,
*) Chambers, Phys. Rev. Letters **5** (1960) 3.

7

De experimentele contrôle door Sitnikov van Van Vleck's theorie over de soortelijke warmte van een spin-systeem in paramagnetische zouten is van generlei waarde.

Sov. Phys. Solid State **4** (1963) 2592.

8

Phasescheiding in mengsels van ^{3}He en ^{4}He is niet noodzakelijk een gevolg van de derde hoofdwet van de thermodynamica, zoals o.a. door Mendelssohn wordt beweerd.

Mendelssohn, M & B Laboratory Bull. Vol. IV No. 4.

9

Ten onrechte concludeert Chance dat de beslissende informatie over het al of niet cyclische karakter van een fotochemische reactie wordt verkregen uit experimenten, waarbij de snelheid van de licht- en donkerreacties van slechts één tussenproduct wordt gemeten.

Chance, Bacterial Photosynthesis (1963) p. 369.

10

In zijn verslag van de experimentele verificatie van het uitsluitingsbeginsel bij levende spinnen verzuimt Tretzel belangrijke directe uitkomsten van zijn meetresultaten te geven. Dit is te betreuren, omdat daardoor een inconsistentie in zijn cijfers niet kan worden opgehelderd en zijn conclusies statistisch niet zijn na te gaan.

Zeits. für Morph. u. Ökol. d. Tiere **44** (1955/56) 43.

11

Er bestaan aanwijzingen dat bij de politieke overwegingen die aan de strategische beslissing over het al of niet oprichten van een Multilaterale Kernmacht voorafgingen, niet voldoende rekening gehouden werd met de terugkoppeling op de politieke verhouding tussen Oost en West.

12

De effectiviteit van de "geweldloze actie" zou vermoedelijk aanzienlijk kunnen worden verhoogd door gebruik te maken van psychologische gevoeligheden van de mens, zoals die o.a. ook bij de reclame worden toegepast.

C. le Pair, 29 juni 1965.